virtual

Open access
virtual testing protocols
for enhanced
road user safety

Current and future accident and impact scenarios for pedestrians and cyclists

WP Number: 4

WP Title: Vulnerable Road User Protection

Deliverable D4.1

This project has received funding from the European Union's Horizon 2020 research and innovation programme under grant agreement No 768960.

Current and future accident and impact scenarios for pedestrians and cyclists

Work Package 4, Deliverable 4.1.

Please Refer to this Report as Follows:
Klug, Corina; Leo, Christoph; Schachner, Martin; Rizzi, Maria; Grumert, Ellen; Davidse, Ragnhild; Heinzl, Philipp; Iancovici, Sava; Wågström, Linus; Lindman, Magdalena; Thomson, Robert; Linder, Astrid (2020). Current and future accident and impact scenarios for pedestrians and cyclists, Deliverable 4.1. of the H2020 project VIRTUAL.

Project details:	
Project start date: Duration: Project name:	01/06/2018 48 months Open access virtual testing protocols for enhanced road user safety – VIRTUAL
Coordinator:	Astrid Linder, Adj Prof, PhD – Research Director Traffic Safety Swedish National Road and Transport Research Institute (VTI) Regnbågsgatan 1, 417 55 Gothenburg, Sweden
	This project has received funding from the European Union Horizon 2020 Research and Innovation Programme under Grant Agreement No. 768960.

Deliverable details:	
Version: Dissemination level: Due date: Submission date: Online location:	Final PU (Public) 31/07/2019 31/03/2020 -

Lead Contractor for this Deliverable:
VTI, TU Graz

Report Author(s):	Corina Klug, Christoph Leo, Martin Schachner (TU Graz) Ellen Grumert, Maria Rizzi, Astrid Linder (VTI) Philipp Heinzl (Siemens) Ragnhild Davidse (SWOV) Sava Iancovici, Linus Wågstöm, Magdalena Lindman, (Volvo)
Reviewer:	Robert Thomson (Chalmers), Sweden

Legal Disclaimer

All information in this document is provided "as is" and no guarantee or warranty is given that the information is fit for any particular purpose. The user, therefore, uses the information at its sole risk and liability. For the avoidance of all doubts, the European Commission and INEA has no liability in respect of this document, which is merely representing the authors' view.
© 2018 by VIRTUAL Consortium

Revision History

Date	Version	Reviewer	Description
26.11.2019	Preliminary draft 1	Corina Klug	First draft
02.03.2020	Draft 2	All Co-Authors	First consolidated draft
10.3.2020	Draft 3	Corina Klug	Draft for internal review
21.03.2020	Draft 4	Robert Thomson	Content Review
27.03.2020	Draft 5	Elisabet Agar	Language Review
27.03.2020	Draft 6	Corina Klug	Consolidate and revise based on reviews
29.03.2020	Draft 7	Ingrid Skogsmo	Quality Review
30.03.2020	Draft 8	Elisabet Agar	Language Review
31.03.2020	Final	Astrid Linder	

Table of Contents

1 Introduction 4

1.1 Terminology 4
1.2 Objectives 4
1.3 Scope 6

2 Current Accident and Impact Scenarios 7

2.1 Method 7
2.1.1 Data Sources 7
2.1.2 Collected Data 13
2.1.3 Parameter Describing Injured VRUs and Relevant Body Regions 20
2.1.4 Current Probability of Specific VRU Accident Scenarios 21
2.2 Results 24
2.2.1 Injured VRUs 24
2.2.2 Relevant Injuries 26
2.2.3 Probability of Specific Accident Scenarios 32

3 Future Accident and Impact Scenarios 52

3.1 Method 52
3.1.1 VIRTUAL VRU Pre-crash Tool 53
3.1.2 Conceptual AEB System 61
3.1.3 Simulation Matrix 61
3.1.4 Data Analysis 66
3.2 Results 68
3.2.1 Future Pedestrian - Car Accident Scenarios 68
3.2.2 Future Cyclist - Car Accident Scenarios 73
3.2.3 Future Pedestrian - Tram Accident Scenarios 77

4 Discussion 80

5 Outlook and the Next Steps 82

6 References 83

Appendix 89

Symbols and Abbreviations

Symbol/ Abbreviation	Description	Units
m	Vehicle mass	kg
A	Vehicle cross section area	m^2
l	Wheelbase	m
l_r	Distance CoG to rear axle	m
c_A	Drag coefficient	$-$
g	Gravity	m/s^2
ρ	Air density	kg/m^3
μ	Friction coefficient	$-$
t	Simulation time	s
$p = (x, y)$	Agent position at time t	m
$v = (v_x, v_y)$	Longitudinal and lateral velocity at time t	m/s
$a = (a_x, a_y)$	Longitudinal and lateral acceleration at time t	m/s^2
ψ	Yaw angle at time t	rad
$T_{look-aheed}$	Look-ahead time	s
$d_{look-aheed}$	Look-ahead distance	m
$p_p = (x_p, y_p)$	Predicted agent position for time $t + T_{look-aheed}$	m
$\hat{p} = (\hat{x}, \hat{y})$	Target agent position at time t	m
δ	Wheel angle	rad
δ_f	Required front wheel angle	rad
t_{c_1}	Tyre coefficient 1	$1/N$
t_{c_2}	Tyre coefficient 2	$-$
c_r, c_f	Cornering stiffness	N
W_r, W_f	Vertical axle load (rear, front)	N
κ	Curvature of the current driving radius	m^{-1}
κ_{req}	Required curvature	m^{-1}
AAP	Accident Analysis and Prevention	
ADAS	Advanced Driver Assistance Systems	
AEB	Autonomous Emergency Braking	
AIS	Abbreviated Injury Scale	
AsPeCSS	Assessment methodologies for forward looking Integrated Pedestrian and further extension to Cyclists Safety	
BMI	Body Mass Index	
CARE	Community Database of Accidents on the Roads in Europe	
CaDas	Common Accident Data Set	

CEDATU	Central Database for In-Depth Accident Study
DaCoTA	Data Collection Transfer & Analysis
DALY	Disability Adjusted Life Year
EES	Energy Equivalent Speed
GIDAS	German In-Depth Accident Study
GOFT	Goodness of Fit
ICD	International Classification of Diseases
IGLAD	Initiative for the Global Harmonisation of Accident Data
IRTAD	International Traffic Safety Data and Analysis Group
ISS	Injury Severity Score
HBM	Human Body Model
LBZ	National Basic Registration Hospital Care (Landelijke Basisregistratie Ziekenhuiszorg)
LMR	National Medical Registration
MAIS	Maximum Abbreviated Injury Scale
NASS	National Automotive Sampling System
PMI	Permanent Medical Impairment
PROSPECT	Proactive Safety for Pedestrians and Cyclists
RAIDS	Road Accident In-Depth Study
RPMI	Risk of Permanent Medical Impairment
SEV	Small Electric Vehicles
STRADA	Swedish Traffic Accident Data Acquisition
TTC	Time to Collision
YoR	Years of Recording
V_CAD	Volvo Cars Cyclist Accident Database
V_PAD	Volvo Cars Pedestrian Accident Database
VRU	Vulnerable Road User
VT	Virtual Testing
WP	Work Package

Executive Summary

An extensive accident analysis of three Vulnerable Road User (VRU) use cases was performed: pedestrian – car, cyclist – car, pedestrian - tram. Both, in-depth databases as well as national statistics were used by different partners to derive current accident scenarios. To summarise the results from the different data sources accessible by the partners of this task, a comparable methodology, applicable for the different sources was defined. In total, more than 4 Million accidents involving pedestrians or cyclists and cars or trams were available for further analysis.

Injuries of pedestrians and cyclists were analysed in detail to derive requirements for the Human Body Models (HBMs) in WP2 and the assessment procedures developed in WP1 of the VIRTUAL project. Some significant differences between males and females were identified (i.e., higher share of lower extremity injuries for female cyclists compared to males) which should be investigated by means of simulations in future steps of this project.

Due to the unavailability of comprehensive data of tram - pedestrian accidents, only basic analyses were performed.

Accident probabilities were derived for different accident scenarios consisting of the probability of a specific type of conflict situation and the probability of the initial speed of the involved vehicles and VRUs for cars.

The probability for a specific type of conflict situation was derived by applying Iterative Proportional Fitting (IPF). The conflict situation clusters associated with the occurrence of the most accidents are "car straight on, cyclist crossing" and "car straight on, pedestrians crossing". The probability of conflict situations involving cars going straight and cyclists crossing from the right or left, is together above 50% independent of injury severity (slight, severe and fatal) and database. A similar pattern was observed for pedestrians associated with the cluster "car straight on, pedestrian crossing". The probability of conflict situations involving pedestrians crossing from the left or right, together account for above 64% among all severities held on all analysed databases. The overall probability is very low for certain clusters and some types of conflict situations were not actually present in any of the analysed datasets. It remains unclear if this is due to unclear coding or if the conflict situations are not relevant in the field. Furthermore, probabilities for accident parameters for each type of conflict situation were derived for the car accidents. Weibull distributions were fitted to the available data to reduce the available data to two parameters and to estimate the overall distributions from the available samples.

The newly developed VIRTUAL Pre-crash Tool was applied to derive future accident scenarios and relevant impact conditions for vehicles equipped with an Autonomous Emergency Braking (AEB) system. All conflict situations were modelled on one generic road geometry.

The simulated conceptual AEB system (sensor range of 80m and angle of 60°) showed the potential for avoiding the majority of straight crossing scenarios, with the avoidance rate increasing for lower severities. The number of pedestrian - car conflicts, have been reduced by 93% (slight), 76% (severe) and 61% (fatal). For the cyclist - car conflicts the numbers have been reduced by 58% (slight), 65% (severe) and 31% (fatal). The collision velocities for the remaining cases, were drastically reduced compared to the baseline for all considered use-cases.

To allow users to derive "future remaining accident scenarios" and finally establish an overall injury probability, the VT catalogue including underlying probabilities, will be used in conjunction with the Pre-crash Tool for the integrated assessment framework developed as the next step within WP4 of the VIRTUAL project.

1 Introduction

1.1 Terminology

For consistency in terms of terminology, the consortium has agreed on common definitions that are used throughout the report:

- **Vulnerable Road Users** (VRUs): Defined as (virtually) unprotected road users, who have to rely heavily on partner-protection of the vehicles in case of a collision (Wegman *et al.*, 2008). Only pedestrians and cyclists are considered within WP4 of the VIRTUAL project, although motorcyclists and wheelchair users are often also associated with this group.

- **Conflict Situations:** Rough description of the participants intention (e.g. pedestrian crossing from the right and vehicle driving straight).

- **Accident Parameters:** Parameters necessary for describing the boundary conditions of an accident (e.g., Initial Velocities, Road Conditions, Weather Conditions, Collision Velocities, etc.,)

- **Accident Scenario:** Specification of a conflict situation and all accident parameters. It therefore includes a detailed description of the environment (e.g., street width, lightning conditions, weather conditions, visual obstructions) as well as the velocity profile and trajectory of road users. The term is used for actual (and not potential) accidents (i.e., collisions between vehicle and VRU).

- **Virtual Testing Scenario**: Detailed description of the environment (e.g., street width, lightning condition, weather condition, visual obstructions) as well as the velocity profile and trajectory of road users. Together with the motion profile and the environment parameters, a single conflict situation can lead to a variety of possible VT scenarios. The term is used for scenarios that are used as a Baseline for the assessment. Hence not all VT scenarios will lead to accidents and impact scenarios in the treatment simulations.

- **Baseline:** Baseline simulations are based on the original VT scenarios. Active safety systems have not been considered (w/o AEB).

- **Treatment:** Treatment is applied based on the Baseline. AEB systems have been considered (with AEB). In treatment simulations described in this report, vehicle models are equipped with generic virtual AEB systems.

- **Impact Scenario:** Describes the boundary conditions of the VRU impact (i.e., collision) relative to the vehicle.

- **Future Scenarios:** Refers to predicted accident and impact scenarios which cannot be directly derived from accident databases. In particular, VIRTUAL focuses on predicting the effect of AEB systems, mandatory in passenger cars from 2024 (European Parliament and European Council, 2019).

1.2 Objectives

In the year 2016, 47% of all road fatalities in Europe affecting the lives of VRUs (European Commission, 2018), amounted to 11,925 fatalities. Besides other strategies, car manufactures and governments are

expecting that the introduction and market penetration of new active safety systems, such as AEB and emergency evasion, respectively, will significantly change the overall number of pedestrian accidents (Hummel *et al.*, 2011; Chen *et al.*, 2015; Strandroth *et al.*, 2016; Vertal and Steffan, 2016; Luttenberger *et al.*, 2014; Detwiller and Gabler, 2017; Lindman *et al.*, 2010; Isaksson-Hellman and Lindman, 2019). However, the studies also conclude that it will not be possible to avoid all VRU accidents.

In case of unavoidable accidents, the impact configuration will be significantly affected, due to active safety systems influencing the relative velocity, between VRUs and vehicles (Gruber *et al.*, 2019). Therefore, developing an integrated assessment procedure, considering the ratio of avoided cases as well as the effect on unavoidable cases, is anticipated within VIRTUAL.

Pedestrian AEB Systems are already assessed in current Euro NCAP assessments and have therefore gained increasing importance in the last few years. From 2024 onwards they will become mandatory. Hence, the distribution of crash configurations of VRU accidents is predicted to change in the near future. Consequently, new priorities of crash configurations will have to be considered in crash performance testing since simply analysing contemporary accidents will not suffice. Hence, it is also necessary to predict how the priorities will change due to the continued implementation of crash avoiding safety systems, such as AEB. This Deliverable introduces and applies a new methodology to derive these future accident scenarios.

A common approach to determine testing scenarios involves using reconstructed real-world accidents. Each conflict scenario is represented in a detailed, explicit way, comprising trajectories of all accident participants based on evidence collected in case records. The use of reconstructed accident scenarios is a fundamental method for the evaluation of safety systems. However, they also represent the extremes of possible scenarios, which are determined and influenced by many different parameters that may not be present in a sampled accident. An attempt to tackle this issue is applying the stochastic determination of conflict situations. Such approaches attempt to determine potential conflict scenarios by objectively analysing the variation of "possible" influencing factors.

By means of virtual pre-crash simulation, the effectiveness of active safety systems (such as AEB) can be assessed on a variety of generic or real-world conflict scenarios (Jeppsson *et al.*, 2018; Erik *et al.*, 2010; Page *et al.*, 2015; Barrow *et al.*, 2018; Roth *et al.*, 2018; TRL *et al.*, 2018; Lindman *et al.*, 2010).

The aim of Task 4.1. is to identify the relevance of different conflict situations as well as the relevance of different parameters (for specific conflict situations). Based on these analyses, we will finally be able to derive representative VT scenarios, in which the integrated safety systems addressing VRUs can be assessed. This means that by using real life crash data from different databases, we can weigh the VT scenarios according to their relevance. By using this approach, the potential of an integrated safety system can be derived and used to estimate how the relevance of different conflict situations and scenarios would change due to a higher market penetration of enhanced safety systems.

A hybrid approach is applied to determine a catalogue of potential conflict scenarios for this particular virtual pre-crash simulation and to derive future impact scenarios (i.e., impact locations and relative velocities among accident participants). Potential factors that influence scenarios are retrieved from accidents and combined with possible conflict scenarios (based on motion patterns) to derive future accident and impact scenarios.

Three different vehicle - VRU use cases are under investigation in WP4 of the VIRTUAL project:

1. Conflict situations between cars and pedestrians
2. Conflict situations between cars and bicycles
3. Conflict situations between trams and pedestrians

1.3 Scope

This deliverable describes current accident scenarios derived from multiple accident databases. Based on these analyses, VT scenarios have been defined as shown in Figure 1-1. By means of virtual pre-crash simulations, expected changes to current scenarios due to AEB systems were analysed to estimate which impact scenarios will be relevant in future.

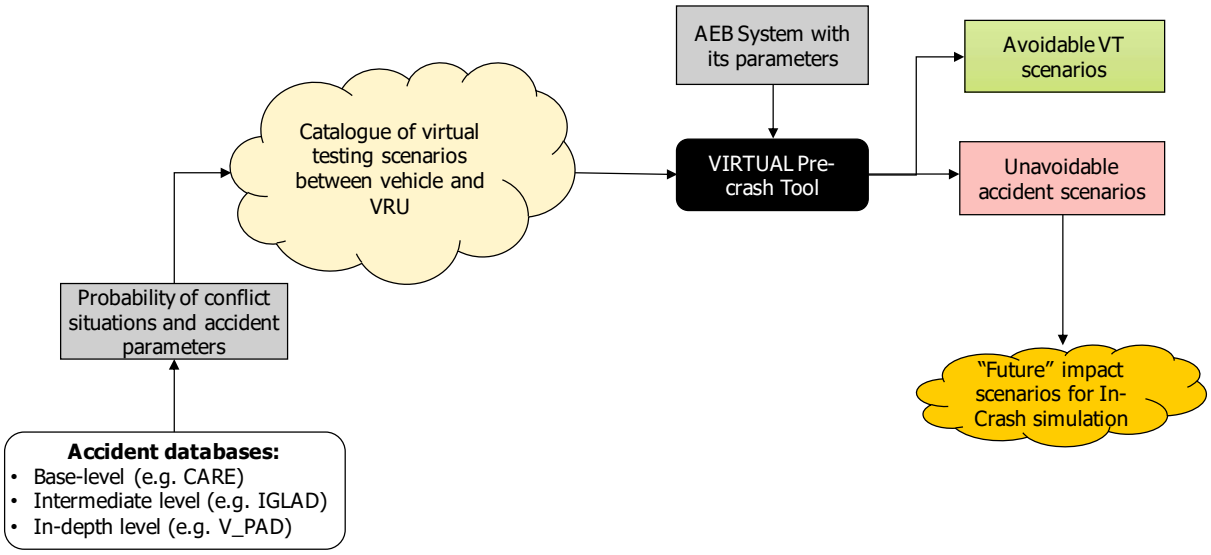

Figure 1-1 Approach to predict future vehicle - VRU accident scenarios

2 Current Accident and Impact Scenarios

Accident databases are profoundly valuable for analysing the relevance of conflict situations and accident parameters, as well as to identify the most relevant injuries for different road user groups. Databases of different levels of detail are available to answer different research questions. The differences between each level are discussed in (Thomas *et al.*, 2003) with an overview outlined in Section 2.1.1.

The number of cases held on the base level databases (national statistics) collected from a significant number of traffic accidents is high, although the level of information is low. In-depth accident (in-depth level) studies provides a high degree of detailed information, however the number of accidents is lower. While national statistics (base level) are present in nearly all countries worldwide, in-depth accident studies are not available for many countries. A single accident database addressing all the information needs of policy makers, car manufacturers, etc., does not exist, and therefore it is necessary to combine the sources. (Thomas *et al.*, 2003)

2.1 Method

To derive current and future accident scenarios, data from many different sources were used by the involved partners on different levels: Base Level, Intermediate and In-Depth.

Templates were developed and completed by partners using their specific data sources. Finally, the data were consolidated to derive European-wide probabilities for:

- Accident Severities
- Conflict Situations
- Motion Parameters
- Environment Parameters
- VRU Parameters

2.1.1 Data Sources

Databases of different levels of detail and coverage were made available by partners and used within WP4 of VIRTUAL. An overview of the applied data sources is given in Table 2-1. The last column YoR refers to the year of recording that will be used within the VIRTUAL project. The applied databases are described within the following section in more detail, structured according to each level type.

Table 2-1: Descriptions of accident databases and the samples used as data sources for accident analysis of pedestrian and bicyclists.

Database Name	Country	Level	Sample description	YoR	Analysed by
CARE	Europe	Base Level	European database that includes all national road statistics for 26 European countries. Included variables and values are standardised according to the Common Accident Data Set (CaDaS).	2000-2017	SWOV
CEDATU	Austria	In-Depth	National Austrian database, random accidents including at least one injured road user, for which access to the court file is given.	2003-2018	TU Graz
GIDAS	Germany	In-Depth	Accidents from the area around Hannover and Dresden selected according to a statistical sampling process.	2008-2017	Volvo
IGLAD	Inter-national	Inter-mediate Level	Summary of samples originating from in-depth data of 11 countries worldwide, of which 7 European countries.	2007-2016	TU Graz
Linked police and hospital data (NL)	Nether-lands	Base Level	All accidents in which a pedestrian or cyclist collided with a passenger car, registered by the police in the Netherlands that could be linked to hospital data.	2000-2014	SWOV
SaferWheels	European	In-Depth	A representative sample of all bicycle-car accidents that occurred in the sampling region, 6 European countries, not necessarily injurious. Included countries: France, Greece, Italy, Netherlands, Poland, and the UK.	2015-2017	SWOV
Statistic Austria UDM	Austria	Base Level	Austrian National Statistics; only including analysis of accidents between trams and pedestrians.	2002-2017	TU Graz
STRADA ped/cyc-passenger car	Sweden	Base Level	All recorded accidents in Sweden involving a VRU in conflict with a passenger car and reported by both the police and an emergency hospital department.	2017-2018	VTI
Tram	European	Intermediate	Description of European tram-accidents with varying levels of detail.	2004-2012	Siemens
Tram	Austria	Base Level	Austrian National Statistics; only including analysis of accidents between trams and pedestrians.	2010-2017	TU Graz
Tram	Germany	Base Level	Federal Office of Statistics, Police headquarters of Baden-Würtemberg, Nidersachsen, Brandenburg-West, Mittelfranken, Bayern, Berlin and Saarland; accidents between trams and pedestrians	2010-2017	Siemens
Tram	Latvia	Base Level	CSSD, Road Traffic Safety Directorate; accidents between trams and pedestrians	2010-2017	Siemens
Tram	Switzerland	Base Level	Federal Office for Transport; accidents between trams and pedestrians	2010-2017	Siemens
V_CAD	Sweden	In-Depth	Bicycle Accidents with Volvo cars, reported to an insurance company.	2005-2014	Volvo
V_PAD	Sweden	In-Depth	Pedestrian accidents with Volvo cars, reported to an insurance company.	2000-2017	Volvo

2.1.1.1 Base Level Databases

Base level or macroscopic databases are characterised by holding a large amount of data, which are not very detailed. The main scope of macroscopic databases is to give an overview and identify trends in accident characteristics, for example, following the trends of the number of fatalities or severely injured in different road user groups. For this purpose, accident characteristics such as which road user groups were involved, where and when the accident occurred, and classification into general conflict situations, is necessary. These databases allow us to access a large amount of data from which shortcomings can be identified (i.e., in terms of crash causation) on a more general level. Specific details such as information on vehicle kinematics and road user behaviour are not held in such databases.

In Europe, national statistics are available for every country, thereby allowing for cross national comparison of certain parameters. At the base level, the most comprehensive aggregated database in the EU is the Community Road Accident Database (CARE), which contains police-reported crashes from all EU member states (Verma et al., 2017). The International Traffic Safety Data and Analysis Group (IRTAD) is another example, which includes accident statistics from more than 70 member organisations from about 40 countries worldwide (OECD, 2019).

The **CARE** database provides road accident data on road accidents resulting in death or injury since 1991, comprising detailed data on individual accidents as collected by the Member States (Verma et al., 2017). Thirty-one European countries have been supplying data on traffic crashes for a number of years. Most of the older Member States have been supplying data since 1991. New Member States who joined the EU in recent years often lack available data or only hold data from recent years. The CARE database contains the number of casualties and several accident characteristics such as time of the accident, location, circumstances, accident severity, and characteristics of the road users who sustained injuries (injury severity, age, mode of transport, road user type, gender). Although accident data for each country were collected by the police, there are substantial differences in the way these data were collected. Therefore, the variables and values included in the CARE database are standardised according to the Common Accident Data Set (CADaS).

The Swedish Traffic Accident Data Acquisition (**STRADA**) database with national coverage contains information related to road traffic accidents collected from emergency care hospitals and police reports. In Sweden, a road traffic accident is defined as "a crash that occurs in traffic on a road, involving at least one vehicle in motion and involving at least one personal injury" (Mattsson and Ungerbäck, 2013). The police are obliged by law (Swedish Government Offices, 1965) to report all road accidents that involve at least one personal injury in accordance with the definition of a road traffic accident previously stated. To date, reporting to STRADA is voluntary for emergency care hospitals, and the information can only be reported with the consent of the injured person (Ds 2016:20, 2016). The information provided by the police includes information of the accident location and other circumstances, for example date and time of accident, weather and road conditions, and posted speed limit. The hospital data collection started in 2003 and have gradually increased to national coverage. In 2013, all but two emergency care hospitals reported to STRADA and since 2016, all emergency care hospitals are included, making data on injuries considered representative on a national level. Hospital reports normally include a number of parameters regarding accident circumstances (i.e., a brief description of the accident, accident type and location of the accident), as well as personal information about the patient (age, gender, use of protective equipment, etc.) and full diagnosis classified according to the

2005 Abbreviated Injury Scale (AIS) (AAAM, 2005) and the International Classification of Disease (ICD-10-SE) (National Board of Health and Welfare, 2010). A unique aspect of the STRADA database is that police and hospital reports can be matched. The contribution has been stable for police reports, but as the number of hospitals reporting to STRADA has increased, the contribution of hospital data has varied across different years, but in recent years around 30% of accidents in STRADA include both police and hospital reports (Yamazaki, 2018). Matching police and hospital reports for the same accident is of particular value in accident analysis as it allows connecting important accident circumstances (provided by the police) with details on injuries sustained in the accident (provided by the hospital). This connection is crucial for understanding how various accident circumstances will impact injuries, which is the goal of virtual testing.

Linked police and hospital data from the Netherlands: All road traffic accidents in the Netherlands that are recorded by the police are included in the national road accident registration (BRON). BRON contains a large number of characteristics of each accident and driver as well as any involved casualties. The accident location is linked to the National Roads Register (NWB). Vehicle information is added based on the vehicle registration, and data is available from 1976. BRON contains 90% of all fatal road accidents. For accidents of lesser severity, and accidents in which no motorised vehicles were involved (i.e., single bicycle accidents), BRON is less comprehensive. Comparing or linking with other files, facilitates estimating the actual number of casualties (SWOV, 2016). Police assessment of accident severity is not always accurate. Therefore, the Dutch Institute for Road Safety Research (SWOV) supplements BRON data with data from the National Basic Register Hospital Care (LBZ), which was previously known as the National Medical Register (LMR). This results in more reliable information of the actual severity of injuries sustained in traffic accidents. In LBZ, injuries are registered according to ICD9 or ICD10, the latter since 2012. SWOV recodes these injuries into AIS90-codes using the software programme ICDmap90 (SWOV, 2016). The data provided to VIRTUAL contain the number of injuries in the Netherlands in 2000-2014 per AIS code according to AIS90 (using recode from ICD9/ICD10). For 2000-2011, only injuries of patients reported in both police registration and hospital data were included, and only when road user type (pedestrian or cyclist) and opponent (car) were (almost) identical in both databases. In more recent years (2012-2014), hospitals have been using ICD10-coding which provides more extensive information on road user type and opponent. Therefore, for this particular period, injuries only registered by hospitals have also been included. Since passenger cars and light goods vehicles are in the same category in ICD10, it cannot be guaranteed that all opponents were passenger cars.

The tram dataset consists of a combination of National Statistics from Austria, Switzerland, Latvia as well as regional parts of Germany (police headquarters of Baden-Würtemberg, Niedersachsen, Brandenburg-West, Mittelfranken, Bayern, Berlin and Saarland). The dataset derived within a master thesis (Klager, 2019) in total contains 6,254 tram accidents including 7,460 injured/killed individuals, for the period from 2010 to 2017. Although exact accident parameters are lacking in particular, certain inputs such as age/gender distribution, are still exploitable and highlight relevant tram - VRU accident scenarios.

2.1.1.2 Intermediate Level Databases

Because of the absence of a European or even worldwide funding framework, the Initiative of Global Harmonisation of Accident Database **(IGLAD)** was initiated (Ockel *et al.*, 2012; Bakker *et al.*, 2014):

The attempt of IGLAD is to harmonise the available datasets and build upon existing databases rather than creating a completely new harmonised regular data collection. The number of cases and the level of information in IGLAD is somewhere between the base level and the in-depth level (intermediate level). Active and passive safety information as well as sketches of accidents are included for all cases in the database. Therefore, integrated safety measures can be analysed by combining the active and passive safety variables in the analysis. (Bakker *et al.*, 2017).

IGLAD contains the accident data from 11 different countries (Germany, Spain, Czech Republic, Italy, Australia, India, USA, France, Sweden, Austria and China). Due to the different data collection methods and templates used, a harmonised data scheme is necessary to combine the different datasets into one single database in order to be able to analyse non-aggregated data. At the moment, 93 accident parameters are available in IGLAD. A definition of those parameters can be found in the official codebook. The distribution of accidents is compared with national statistics. Some of the data is biased, so this should be considered by comparing variables available in national statistics. (Bakker *et al.*, 2017).

Tram accident analyses started with data collected by European tram network services with varying levels of detail, available at Siemens Mobility. Additionally, another European-wide data inquiry was carried out within the scope of a recent master thesis (Klager, 2019) which lead to comprehensive intermediate-level data collection for tram accidents.

2.1.1.3 In-Depth Databases

In-depth level, or microscopic databases, are characterised by a much smaller number of cases, while the level of detail is high for each case. In-depth databases hold information of the whole accident, including parameters of the pre-crash, crash and post-crash phase. The parameters are gained from accident investigation teams on the spot (e.g., GIDAS, RAIDS) or retrospectively using judicial court information (e.g., CEDATU) consisting of accident reports, hospital reports and accident reconstructions. The sample sizes in single in-depth accident databases quickly diminish when the research questions become very specific (Klug *et al.*, 2015; Li *et al.*, 2017). Therefore, it can be challenging to draw significant conclusions using a single database. Harmonised in-depth data collection is not currently ongoing for Europe, although some initiatives have been initiated in the past (Ross *et al.*, 1998; del Pozo de Dios *et al.*, 2013; Lenard *et al.*, 2006; Morris *et al.*, 2018). A first step towards harmonised data collection of accidents in Europe was initiated within the EC funded project Standardisation of Accident and Injury Registration Systems (STAIRS), in which a harmonised protocol/methodology for data collection as a basic framework for crash injury studies was developed. However, the STAIRS protocol only included variables to passive safety research questions, as they were most important at that time. (Ross *et al.*, 1998). The STAIRS protocol was applied in the project Pan-European Co-ordinated Accident and Injury Databases (PENDANT), in which passenger car accidents were collected and analysed in different European countries. The STAIRS protocol was enhanced and extended with some active safety variables. (Morris and Thomas, 2003).

Additional active safety variables were included in the subsequent project SafetyNet, where the structure for a European fatal accident database was also established (Morris *et al.*, 2010). The attempts of establishing a European-scale accident data collection was further investigated in the EC funded DaCoTa project (Thomas *et al.*, 2013). The DaCoTa data protocol contains about 1,500 variables and is capable of analysing active, passive, and integrated safety research questions. In spite of all these efforts, a funding mechanism to support continuous accident investigation across Europe is yet to be established. However, there are several ongoing national in-depth accident collection activities such as the German GIDAS (Brunner *et al.*, 2003), Austrian CEDATU (Tomasch and Steffan, 2006a), American NASS (NHTSA, 2018), Crash Investigation Sampling System (NHTSA, 2017) and UK-wide RAIDS project (Department of Transport, 2013). The data from in-depth databases have been used in the past to retrospectively evaluate the effects of safety regulations and Euro NCAP ratings (Zander *et al.*, 2015; Pastor, 2013;

Strandroth *et al.*, 2011; Li *et al.*, 2018), for example, or different vehicle geometries (Li *et al.*, 2017) on the injuries observed in the field. Other parameters that have been analysed by means of retrospective accident statistics is the relationship between VRU age, collision speed and fatality/injury risk (Rosén and Sander, 2009; Wisch *et al.*, 2017; Otte *et al.*, 2012; Li *et al.*, 2017; Piantini *et al.*, 2017). Partners of the VIRTUAL project have access to four different in-depth databases:

The German In-Depth Accident Study (**GIDAS**) is a German in-depth database which holds accident data from the area around Hannover and Dresden. The GIDAS database includes information of environmental conditions, road design, traffic control, accident details and cause of the accident, accident information such as driving and collision speed, delta-v and EES, degree of deformation, vehicle deformation, impact contact points for passengers or pedestrians, technical vehicle data, information relating to the individuals involved, such as weight, height and medical information (injuries, treatment, etc.). For each accident the dataset contains 500 to 3,000 parameters. Accidents are selected according to a statistical sampling process. Only accidents involving at least one injured person are recorded. Weighting factors are calculated based on comparison with national German statistics to avoid bias in the database. (Brunner *et al.*, 2003).

The Central Database for In-Depth Accident Study (**CEDATU**) is an in-depth database provided by the Vehicle Safety Institute at Graz University of Technology in Austria and currently covers approximately 3,300 cases. The database includes a detailed description of accidents in Austria. Accidents with at least one injured road user are included, for which access to the court file is granted. The dataset contains accidents with fatal, serious and slight injuries. Detailed accident parameters, such as collision velocities and pre-crash trajectories are derived from accident reconstructions. Each accident case contains a set of approximately 350 core parameters. Accident parameters such as accident type, accident site, road users, etc., can be used to extrapolate findings to the national level. (Tomasch and Steffan, 2006b; Tomasch *et al.*, 2008).

Volvo Cars Cyclist Accident Database (**V_CAD**) and Volvo Cars Pedestrian Accident Database (**V_PAD**) contains extensive information on car - cyclist/pedestrian accidents in Sweden including information of a total of 126 variables with regard to pre-crash scenario, crash, car, driver and the cyclist/pedestrian. The information about the cyclist and pedestrian accidents are provided by the insurance company Volvia (IF P&C Insurances) to Volvo's Traffic Accident Research Team and stored in the V_CAD/V_PAD databases. All new Volvo passenger cars in Sweden are insured with Volvia for at least three years, and since drivers in Sweden are obligated to report cyclist and pedestrian accidents according to the terms of their insurance, comprehensive coverage is assured. Therefore, as the information on accidents is provided based on insurance claims, the data is an important complement to the accidents reported in STRADA, which is solely based on police and hospital records. For example, (Isaksson-Hellman and Werneke, 2017) performed a study based on IF P&C Insurances data and found that only 50% of bicycle - car accidents reported to the insurance company were covered by police reports in STRADA. The information considered by the accident investigators at Volvo's Traffic Accident Research Team, have been collected from several sources; vehicle claims reports, cyclist/pedestrian claims reports, police reports and from interviews with involved parties and other eyewitnesses. Vehicle reports contain information of the course of events from the driver's perspective as well as estimated speed at impact, traffic environment (often described in a sketch), VRU impact points, car damage, driver distraction elements and a description of injuries sustained. Further, medical records and/or autopsy reports for those involved is collected by informed consent and coded according to the AIS by a physician. Vehicle specification data were used to add additional car information, such as equipment and optional safety systems. Map data provide further information of the accident scene, such as road geometry and roadside objects. Conflict Situations were coded and based on the accident investigator's compilation of all information of the pre-crash phase, each case was digitalised in order to provide vehicle paths in relation to vehicle velocities and to the surroundings in a numerical format. The databases are further described in Lindman *et al.* (2011) and Lindman *et al.* (2015).

The **SaferWheels study** is a European project conducted in the years 2014 to 2017 with the aim to investigate accident causation for traffic accidents involving powered two-wheelers and bicycles in the European Union. In-depth accident investigations were carried out for 500 accidents of which 95 were bicycle - car accidents. These accident investigations were carried out by six teams in France, Greece, Italy, the Netherlands, Poland and the UK, to give a representative view of such accidents in Europe. In the selection of which accidents to include in the study, utmost care was taken to achieve a random selection procedure (Morris *et al.*, 2018). Most cyclist accidents were collected in the Netherlands, Poland and the UK. The data collection system used was derived from the DaCoTA project and involved approximately 1,500 variables (or fields) per case that would potentially be available for collection during an accident investigation. It was mandatory for all teams to collect a set of core variables for each case, including collection of additional variables where possible. However, it was recognised that no single accident case would ever comprise all of the variables stated in the data collection protocol. A brief description of the type of variables included in each category relevant to bicycle - car accidents is given in brackets by way of examples (Morris *et al.*, 2018):

2.1.2 Collected Data

2.1.2.1 **Injury Coding**

Different injury coding systems applies for different data sources:

- In national, or base level accident databases, injury severity is often expressed as "slightly injured", "severely injured", or "fatally injured" per accident. This information is not based on objective severity scales such as Abbreviated Injury Scale (AIS).

- In-depth crash databases include injury diagnoses from medical reports and the AIS scale, a globally used predictive scale that mainly focuses on initial survival, is generally used. The AIS scale classifies injuries by body region and injury severity (based on the risk of not surviving a specific injury) on a 1-6-point ordinal scale, where 1=minimum and 6=maximum. Each sustained injury is classified separately, while multiple injuries will be classified according to the Maximum AIS (MAIS), which represents the highest injury severity classification assigned to an individual (AAAM, 2005). Further, the Injury Severity Score (ISS) and the New Injury Severity Score (NISS) scales are based on AIS, and address the risk related to multi trauma (Baker *et al.*, 1974; Samin and Civil, 1999).

- In hospital data (that can be linked to some national statistics), the international classification of diseases and health problems (ICD) is most commonly used to describe injury diagnoses (WHO, 2010).

<u>Assessing long-term impact from injuries</u>

The assessment of long-term impact from injuries is a crucial addition with regard to understanding the impact injuries that advance beyond initial survival, also reflected in previously mentioned injury classification systems, such as AIS.

A method for assessing the long-term injury impact, Risk of Permanent Medical Impairment (RPMI), was developed by the Swedish insurance company Folksam. RPMI estimates the risk of long-term impairment based on loss of physical and/or mental function. RPMI was developed to estimate the risk of patients sustaining a certain level of Permanent Medical Impairment (PMI), based on the diagnosed injury location and severity (according to AIS) as well as criteria specified by Swedish insurance companies (Malm *et al.*, 2008; Försäkringsförbundet, 2004). RPMI is based on approximately 35,000 diagnoses of 20,000 injured car occupants who have reported an injury to the insurance company. The injured car occupants were followed for at least five years to assess the risk of permanent medical impairment for different body regions and AIS severity levels.

Besides RPMI, other scales that estimate long-term impact from injuries exist. The Functional Capacity Index (FCI) is a consensus-based score assigned to AIS injuries and reflects the degree of functional capacity one year after injury (MacKenzie et al., 1996). Similar to the RPMI, the FCI is a predictive scale, however, they differ in that the RPMI is predictive based on an actual assigned degree of medical impairment, while the FCI is predictive based on an expert panel's estimation of functional capacity. Also, the RPMI is based on permanent medical impairment which is assigned after at least 3-5 years, while the FCI is estimated at 12 months post injury.

Based on the comparison of the RPMI and FCI, the advantage of RPMI is that it is based on an actual outcome and the follow-up period is more extensive. It was decided to include RPMI analysis based on STRADA data to facilitate estimating the long-term impact of injuries among cyclists and pedestrians.

The risk was derived from risk matrices from Malm et al. (2008) based on the location and severity of the injury for 1%+ and 10%+ RPMI. The risk matrices for 1% and 10% level of impairment are shown in Table 2-2. For reference, an AIS 2 injury to an upper extremity gives a 35% risk of a 1% or more medical impairment (RPMI 1+) but only a 3% risk of a 10% or more medical impairment (RPMI 10+).

Table 2-2: Risk of Permanent Medical Impairment of at least 1% impairment (left side) and at least 10% impairment (right side). Source: Malm et al. (2008).

RPMI 1+						RPMI 10+					
Body region	AIS 1	AIS 2	AIS 3	AIS 4	AIS 5	Body region	AIS 1	AIS 2	AIS 3	AIS 4	AIS 5
Head	8.0%	15%	50%	80%	100%	Head	2,5%	8%	35%	75%	100%
Cervical spine	16.7%	61%	80%	100%	100%	Cervical spine	2,5%	10%	30%	100%	100%
Face	5.8%	28%	80%	80%	n.a.	Face	0,4%	6%	60%	60%	n.a.
Upper extremity	17.4%	35%	85%	100%	n.a.	Upper extremity	0,3%	3%	15%	100%	n.a.
Lower extremity	17.6%	50%	60%	60%	100%	Lower extremity	0,0%	3%	10%	40%	100%
Thorax	2.6%	4.0%	4%	30%	20%	Thorax	0,0%	0%	0%	15%	15%
Thoracic spine	4.9%	45%	90%	100%	100%	Thoracic spine	0,0%	7%	20%	100%	100%
Abdomen	0%	2.4%	10%	20%	20%	Abdomen	0,0%	0%	5%	5%	5%
Lumbar spine	5.7%	55%	70%	100%	100%	Lumbar spine	0,1%	6%	6%	100%	100%
External (skin)	1.7%	20%	50%	50%	100%	External (skin)	0%	0%	50%	50%	100%

The predicted number of impaired individuals or impairing injuries is the accumulated risk for all individuals or each body region. Accumulating the risk for each body region facilitates analysis of the distribution of predicted impairing injuries in a population of injured. When accumulating the risk, the impaired individuals or impairing injuries are referred to as PMI individuals or PMI injuries. In this Deliverable, the predicted PMI injuries are calculated based on data from STRADA.

2.1.2.2 Conflict Situations

To describe accidents between pedestrians and passenger cars or cyclists and passenger cars or trams it is necessary to provide a harmonised coding system of conflict situations. Most of the databases adhere to their own data scheme for coding and classifying accidents, which are often difficult to compare. For example, in the CADAS classification in CARE, information required for the detailed classification used by Lindman et al. (2011, 2015), are often missing. They introduced a clustering of conflict situations for car - pedestrian and car - cyclist accidents, that differs from other classifications as the classification of conflict situations is based on the moving patterns of the pedestrian, cyclist, and the car. Parameters such as visual obstruction or light conditions are excluded from the conflict situation description although they are collected as accident parameters. An overview of the above mentioned conflict situations is given below in Figure 2-1 and Figure 2-2.

The conflict situations identified by Lindman et al. (2011, 2015) differ from the situations applied in previous projects where motion pattern and environments were not tested separately (Wisch *et al.*, 2017; Aparicio *et al.*, 2017; Luttenberger *et al.*, 2013; Wisch *et al.*, 2013).

SCPPL	SCPPR	SCPPLSD	SCPPLOD	SCPPRSD
Straight Crossing Path, Pedestrian from Left	Straight Crossing Path, Pedestrian from Right	Straight Crossing Path, Pedestrian from Left, initially from Same Direction	Straight Crossing Path, Pedestrian from Left, initially from Opposite Direction	Straight Crossing Path, Pedestrian from Right, initially from Same Direction
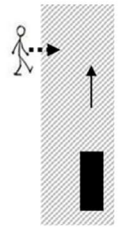	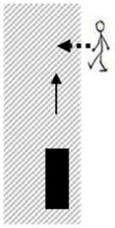	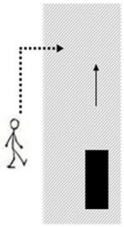	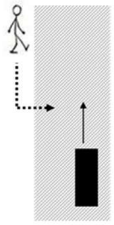	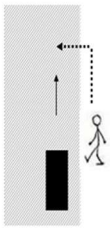
SCPPROD	**LT/SD**	**RT/SD**	**LT/SDLD**	**RT/SDRD**
Straight Crossing Path, Pedestrian from Right, initially from Opposite Direction	Left Turn, Pedestrian from Same Direction	Right Turn, Pedestrian from Same Direction	Left Turn, Pedestrian from Same Direction, initially from Left Direction	Right Turn, Pedestrian from Same Direction, initially from Right Direction
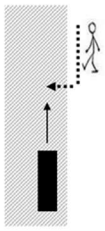	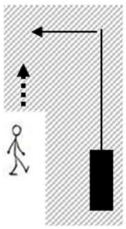	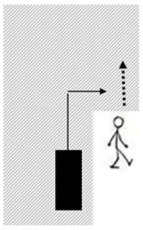	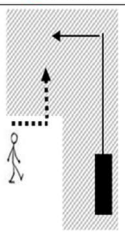	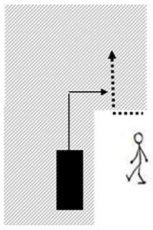
LT/OD	**RT/OD**	**LT/ODLD**	**LT/ODRD**	**RT/ODLD**
Left Turn, Pedestrian from Opposite Direction	Right Turn, Pedestrian from Opposite Direction	Left Turn, Pedestrian from Opposite Direction, initially from Left Direction	Left Turn, Pedestrian from Opposite Direction, initially from Right Direction	Right Turn, Pedestrian from Opposite Direction, initially from Left Direction
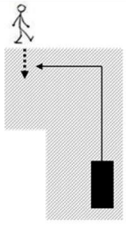	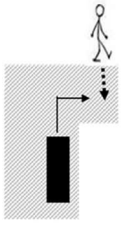	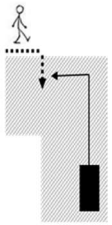	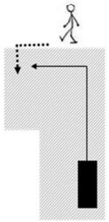	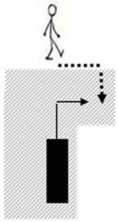
RT/ODRD	**SD**	**Oncoming**	**Reversing**	**Unspecified**
Right Turn, Pedestrian from Opposite Direction, initially from Right Direction	Straight, Pedestrian Same Direction	Straight, Pedestrian Oncoming	Car Reversing accident	
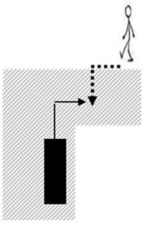	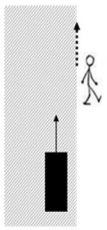	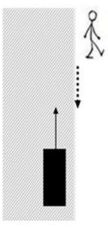	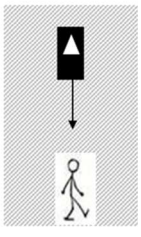	

Figure 2-1 Definitions of vehicle-pedestrian moving patterns (Lindman *et al.*, 2011).

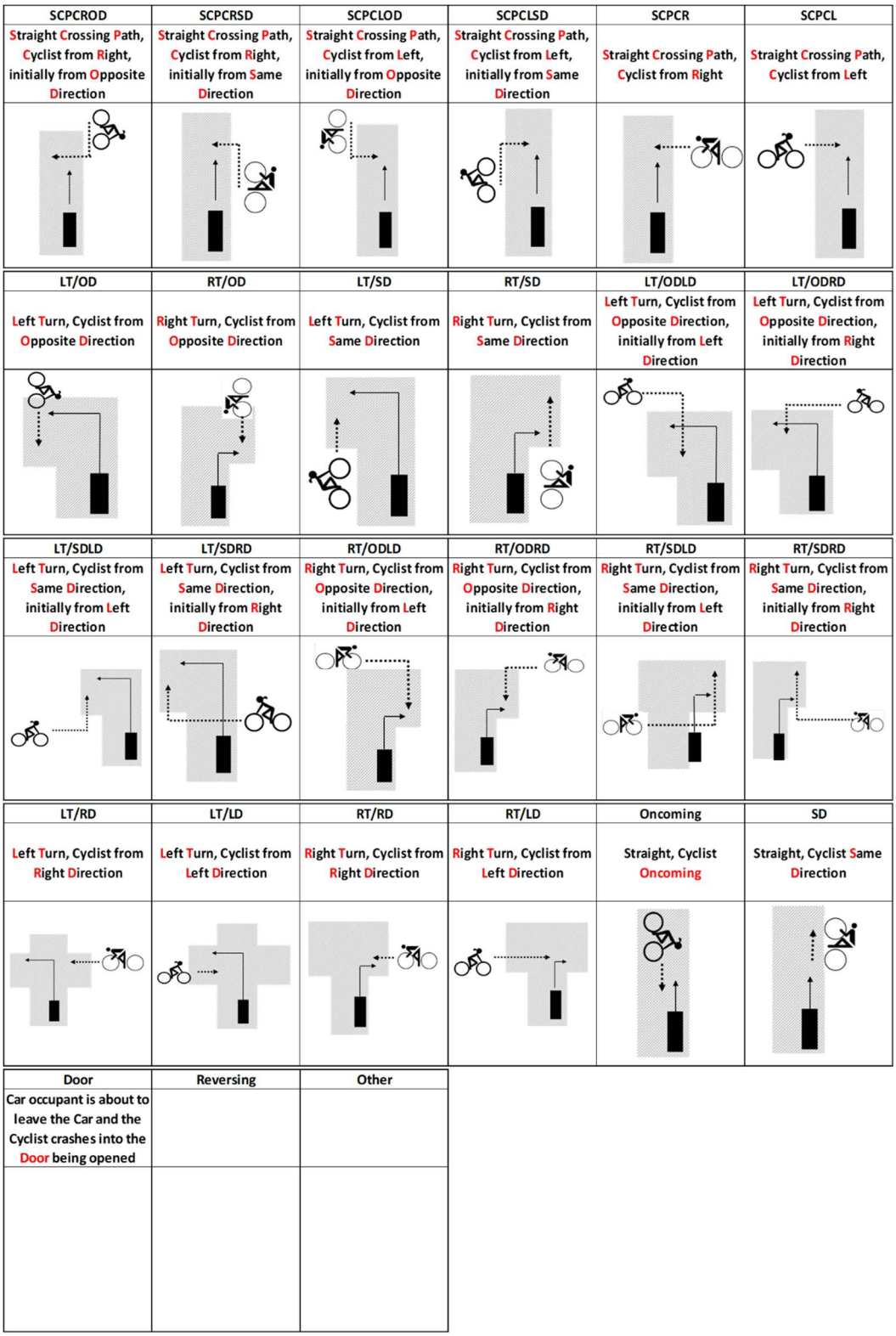

Figure 2-2 Definitions of vehicle-cyclist moving patterns (Lindman *et al.*, 2015).

It has been decided within VIRTUAL to use the conflict situation clustering, based on the motion patterns (Lindman *et al.*, 2011; Lindman *et al.*, 2015) shown in Figure 2-1 and Figure 2-2. This clustering is based on moving patterns of the conflict partners, and therefore appropriate for the assessment of active safety measures. Furthermore, the clustering represents a good compromise between level of detail and applicability. However, the level of detail of some of the databases scheduled for Task 4.1 were not sufficient for classifying according to the original classification and, therefore, the conflict situations were further gathered into Conflict Situation Groups. The conflict situations are shown in Figures 7 and 8 illustrating the Conflict Situation Groups by colour coding.

The detailed clustering originally consisted of 20 different conflict situations for pedestrians and 27 for cyclists. These conflict situations were further grouped into fewer clusters, six for pedestrians and nine for cyclists, to enable the use of data from national statistics and macroscopic databases, as well. Thus the amount of conflict situation input options for national comparison in VIRTUAL will be more comprehensive compared with previous projects, trying to find a compromise between detailed and rough classification.

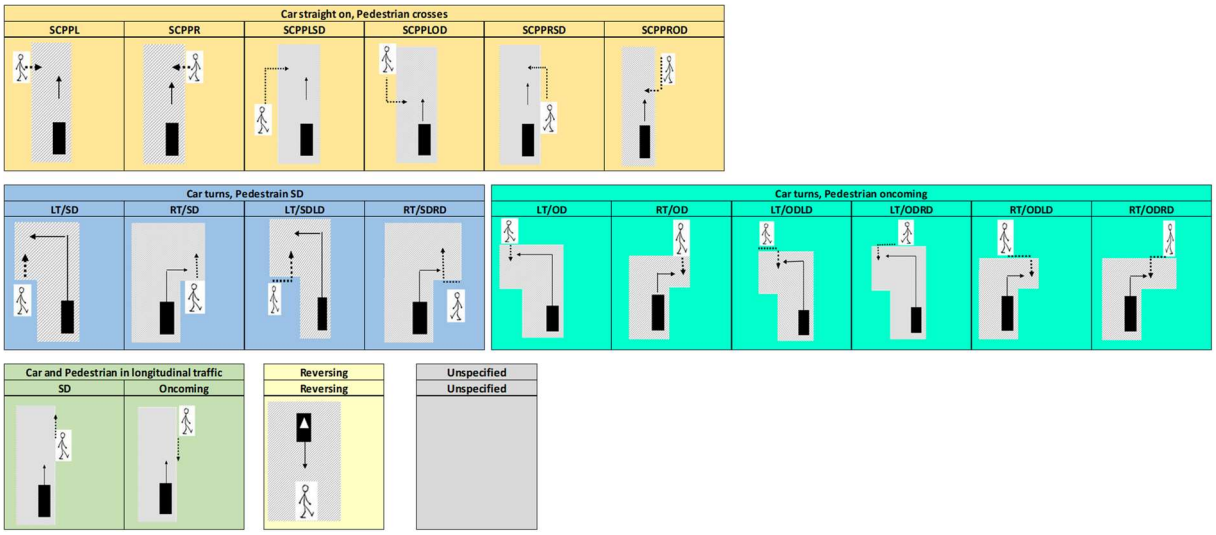

Figure 2-3 Clustering of VIRTUAL conflict situations for vehicle - pedestrians.

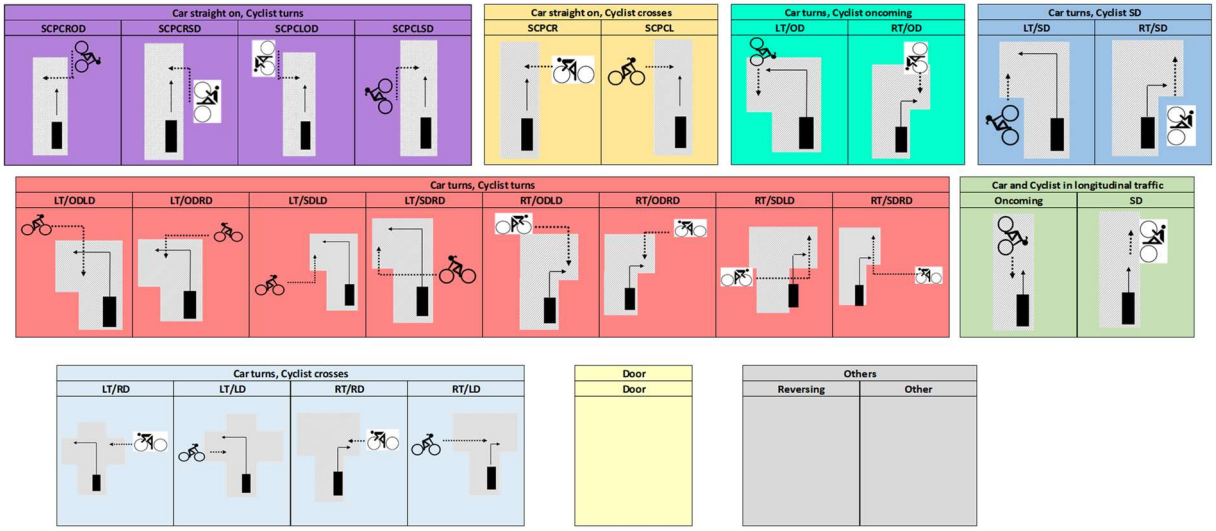

Figure 2-4 Clustering of VIRTUAL conflict situations for vehicle - cyclists.

2.1.2.3 Accident Parameters

To establish the VIRTUAL testing scenarios as well as describing future accident scenarios, relevant parameters are needed for each of the conflict situations. The consortium has agreed on a set of accident parameters considered relevant for describing the scenarios, listed in Table 2-3 below. These parameters were considered important to determine the input parameters for the pre-crash simulation. For example, necessary parameters for the in-crash simulation include initial speed and braking deceleration. Parameters such as age, Body Mass Index (BMI), gender and height are important to scale the HBM for the in-crash simulation. Parameters such as light and weather conditions, as well as visual obstructions are important for the assessment of the effectiveness of active safety systems.

Table 2-3 List of accident parameters.

Parameter	from	to	resolution	Unit / parameters
Accident Location	-	-	-	Motorway, rural, urban
Age VRU	0	100	1	[years]
BMI VRU	0	50	1	[kg/m^2]
Braking Deceleration	0	1	0.01	[g]
Collision Speed Vehicle t0	0	100	1	[km/h]
Collision Speed VRU t0	0	100	1	[km/h]
Daytime	00:00	24:00	00:15	[h:min]
Gender VRU	-	-	-	Male, female
Height VRU	0	200	1	[cm]
Injured Body Regions VRU	1	9	1	Head, face, neck, thorax, abdomen, spine, upper extremity, lower extremity, unspecified
Road Conditions	-	-	-	Dry, glazed frost, slippery, wet, other
Visual Obstructions	-	-	-	Non, static, dynamic
Initial Speed Vehicle(v0)	0	100	1	[km/h]
Initial Speed VRU(v0)	0	100	1	[km/h]
Weather Conditions	-	-	-	Bright, cloudy, rain, storm, snow, fog, other
Weight VRU	0	200	1	[kg]
Year	2000	2018	1	[year]
Light Conditions	-	-	-	Darkness, dawn/twilight, daylight, artificial light
Deceleration Distance	0	100	1	[m]
Road Situation	-	-	-	Foot path, cycle/rambling path, other
Speed Limits	0	150	1	[km/h]

All parameters above the upper threshold were summarised in an additional category (i.e., 100+ for initial vehicle speed).

2.1.3 Parameter Describing Injured VRUs and Relevant Body Regions

Data from STRADA and from the Dutch Institute for Road Safety Research (SWOV) were analysed to identify injuries in pedestrian and cyclist - passenger - car collisions in detail, including full AIS codes of the injuries for analysis. For STRADA, only data on accidents including both police and hospital information that occurred from 2016 to 2018 were included in the data sample. This information was available for 1,311 injured persons involved in 1,272 pedestrian - passenger car collisions; these individuals sustained 3,198 injuries to which 442 different AIS2005 codes were assigned. Similar data were available in STRADA for 1,932 cyclists with a total of 3,840 injuries, covering 365 different AIS2005 codes.

Data from the Netherlands included cases from 2000 to 2014. For 2000-2011, only the injuries of patients included in both police registration and hospital data were assessed, as hospital data alone (ICD-9-CM) did not include detailed information on the road users involved. In more recent years (2012-2014), hospitals have used ICD-10 coding methods, providing more information. Therefore, injuries

only registered at hospitals for these years were also included. However, since they belong to the same category, it was not possible to separate passenger cars and light goods vehicles for that period. Injuries in ICD-9-CM and ICD-10 were mapped to AIS © 1990 (ICDmap90) (Johns Hopkins University 1998), and subsequently converted to AIS © 2005 Update 2008 using the AIS Crosswalk. This allowed the compilation of a dataset of 15,650 cyclists with a total of 29,515 injuries and 269 different AIS codes. Data from the Netherlands had to date only been used to analyse injuries of cyclists in detail. As this data is also available for pedestrians, a detailed analysis of the Dutch data will be performed.

2.1.4 Current Probability of Specific VRU Accident Scenarios

The probability of a specific accident scenario is defined as the probability of a specific severity, type of conflict situation and related accident parameters, such as speed. The probabilities are outlined in the probability tree in Figure 2-5 and will later be used for the weighting of scenarios according to their estimated relevance.

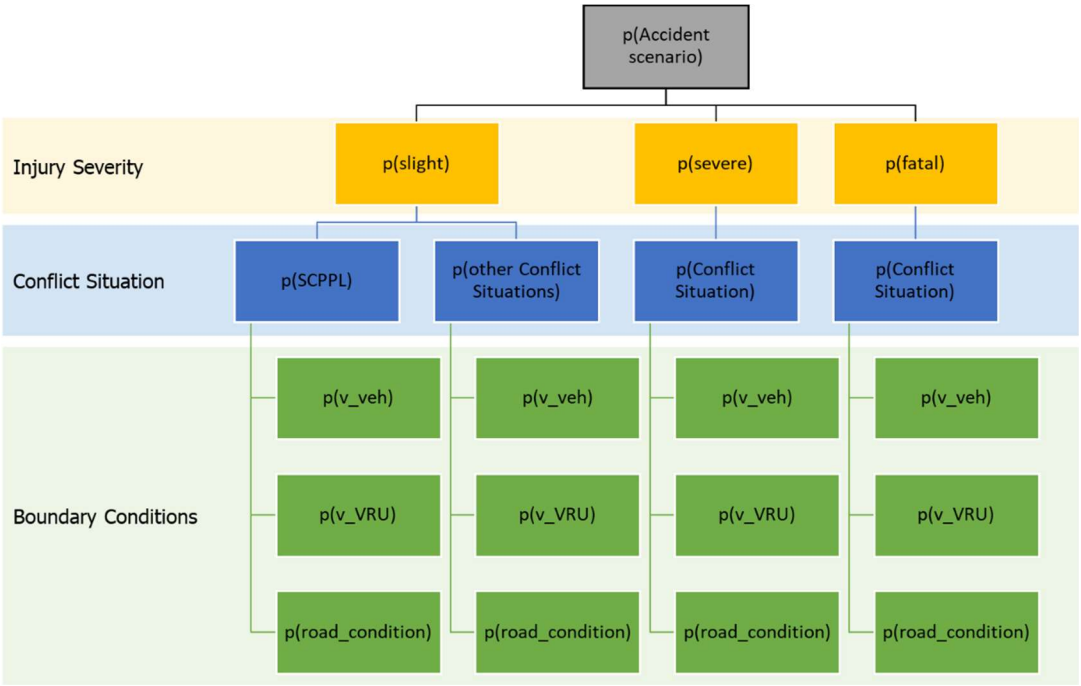

Figure 2-5 Probability tree describing the probability of a specific accident scenario.

2.1.4.1 Analysis of the Probability of Specific Types of Conflict Situations

The Iterative Proportional Fitting (IPF) method is used to derive the probabilities of injury severity, and the probability of a specific conflict situation, in each cluster of conflict situations. The method has been proposed by Deming and Stephan (1940) as a method to estimate cell probabilities in a contingency table when the rows and column sums are known, displaying information from two or more datasets. It has since been used in many different disciplines and several articles have covered different aspects and usages of IPF, for example, see Norman (1999) for an overview of different application areas. The method has also been used to estimate the amount of traffic counts at specific locations in relation to weather condition, day of week, vehicle type, etc. (Evers and Santapaola, 2007), origin-destination matrices (McCord et. al., 2010), synthetic populations used for simulating flows of individuals in a traffic system (Frick, 2003) and for finding country-specific multidimensional distributions of accident parameters (Niebuhr et. al., 2013, Kreiss et. al. 2015).

An iterative process is used to update the cells in a contingency table until the column and row sums agree with the observed column and row sums (as much as possible). The resulting table consists of a joint probability distribution of the expected values (or maximum likelihood estimates) for each cell. Hence, by combining two or more accident databases consisting of the number of injuries categorised into injury severity (i.e., slight, severe and fatal or number of injuries belonging to a conflict situation within one Conflict Situation Group), an estimate of the probability of slight, severe, and fatal injury or a probability of a specific conflict situation within a cluster can be estimated.

A necessary assumption is that the categorisation of slight severe and fatal injuries as well as the categorisation of specific conflict situations are independent of database (the division of each injury and conflict situation are equally divided for the different databases). Had this not been the case, significant deviation between observations and estimations would be found, which can be interpreted as a need for unique probabilities for each of the databases.

Figure 2-6 illustrates the IPF procedure using data from three databases (V_PAD, GIDAS and CEDATU) for one of the pedestrian conflict situation clusters including three conflict situations (*SD, oncoming and details unknown*). The data from the three databases are organised as a contingency table according to Figure 2-6. The goal is to find an estimated contingency table such that the probability of *SD, oncoming and details unknown* are the same for all databases. If the resulting estimated contingency table is close enough to the observed contingency table, it would be safe to assume the databases are independent and that the estimated probabilities can be used for databases with a similar structure, although the categorisation of accidents (only into clusters of conflict situations) will not be detailed.

The specific conflict situation probabilities can be calculated following identification of the expected number of accidents in the slight, severe and fatal injury categories, including a specific conflict situation within each cluster.

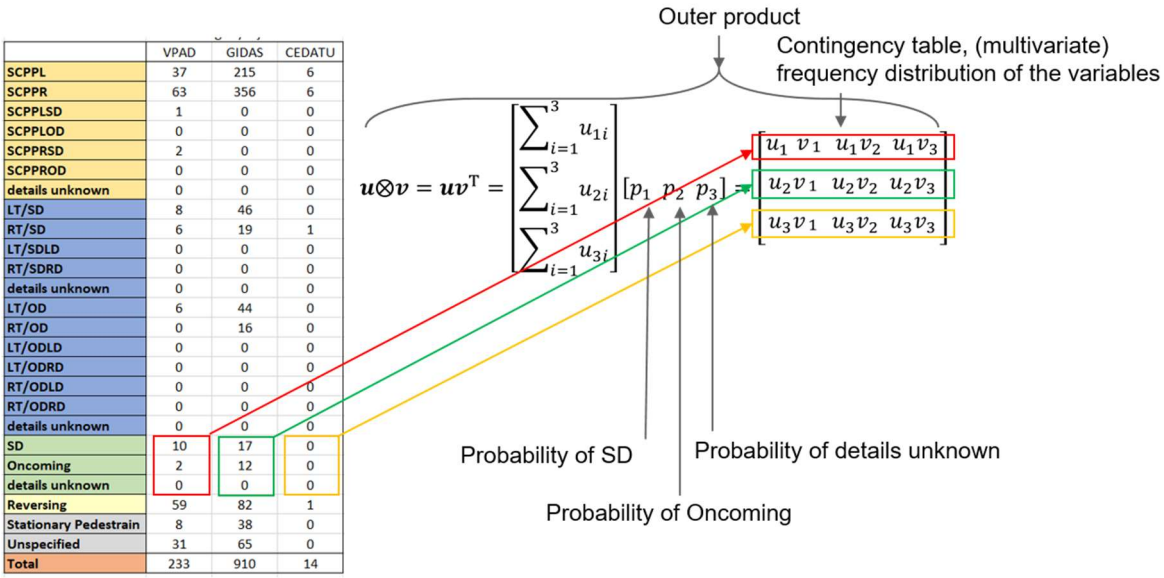

	VPAD	GIDAS	CEDATU
SCPPL	37	215	6
SCPPR	63	356	6
SCPPLSD	1	0	0
SCPPLOD	0	0	0
SCPPRSD	2	0	0
SCPPROD	0	0	0
details unknown	0	0	0
LT/SD	8	46	0
RT/SD	6	19	1
LT/SDLD	0	0	0
RT/SDRD	0	0	0
details unknown	0	0	0
LT/OD	6	44	0
RT/OD	0	16	0
LT/ODLD	0	0	0
LT/ODRD	0	0	0
RT/ODLD	0	0	0
RT/ODRD	0	0	0
details unknown	0	0	0
SD	10	17	0
Oncoming	2	12	0
details unknown	0	0	0
Reversing	59	82	1
Stationary Pedestrain	8	38	0
Unspecified	31	65	0
Total	233	910	14

Figure 2-6: Outline of the Iterative Proportional Fitting algorithm.

In the example above the resulting estimated contingency table and the corresponding probabilities result in Equation 2-1.

$$\boldsymbol{u}\otimes\boldsymbol{v} = \begin{bmatrix}12\\29\\0\end{bmatrix}[0.66\ 0.34\ 0] = \begin{bmatrix}7.92 & 4.08 & 0\\19.14 & 9.86 & 0\\0 & 0 & 0\end{bmatrix}. \quad \text{2-1}$$

The resulting estimated contingency table is comparable with the observed contingency table (see Figure 2-6), although small deviations occur. This may be an indication of the databases not being independent (i.e., the probabilities might differ between the databases if the deviations are too large). However, given the small number of accidents the results are uncertain, making it challenging to guarantee they are independent. Hence, the larger number of observations within a conflict situation cluster, the more certain are the resulting probabilities and that the databases are independent of each other.

The algorithm is outlined in Appendix A.1. For a detailed description of the IPF method, the mathematical procedure and its corresponding properties, see Fienberg (1970), Bishop et. al. (1975) and Norman (1999).

2.1.4.2 Probability of Accident Parameters

For the probability analysis of the motion sequence parameters, particularly the initial velocities of the vehicle and the VRU, the data of GIDAS, VOLVO (V_PAD and V_CAD) and CEDATU have been summarised for each conflict situation. As data from GIDAS and CEDATU are also included in the IGLAD, and data and accidents must not be double counted, data from IGLAD was not used for the probability analysis of the accident parameters. The next step involved the Shapiro–Wilk test (Shapiro and Wilk, 1965), applied for the data sample to establish if the data distribution was normal. The test revealed that significant amounts of available data are atypical. The decision not to use a normal distribution was also made because the sample data are not symmetric to the centre (mean and median values are not the same). The software package R (R Core Team, 2019) was used to consider other distributions which are more appropriate to describe the skewed data. With the help of the Goodness of Fit (GoFt) package (González-Estrada and Villaseñor, 2018) it is possible to analyse the GoFt for probability functions such as Gamma, Log Normal and Weibull. The parameters for the different distributions are determined for the detailed conflict situations, as they are of more interest for the pre-crash simulations. Moreover, the data was categorised according into slight, severe and fatal injury severities. Following a number of tests, it was decided that the Weibull distribution should be used, as it seems most suitable for the sample data. The Weibull probability density function f(x) and the Weibull cumulative distribution function F(x) are described below in Equation 2-2 and 2-3 , where λ is the scale and k is the shape factor:

$$f(x) = \frac{k}{\lambda} * \left(\frac{x}{\lambda}\right)^{k-1} * e^{-\left(\frac{x}{\lambda}\right)^{k}} \quad \text{2-2}$$

$$F(x) = 1 - e^{-\left(\frac{x}{\lambda}\right)^{k}} \quad \text{2-3}$$

By determining the scale and shape factor it is possible to fit the Weibull distribution to a given data sample. As two parameters are required to fit the distribution, only conflict situations where more than two data samples (accidents) are available are used. This was the case for 11 detailed cyclist situations with slight injuries, three detailed situations with severe injuries, and four detailed situations with fatal injuries to the cyclists. For pedestrians, six detailed situations with slight injuries, two with severe injuries, and two with fatally injured pedestrians were suitable for Weibull distribution.

To test if the data is statistically significant, we have assumed a null hypothesis H_0. As we want to test if it is possible to describe the accident sample data by a Weibull distribution our null hypothesis can be formulated as:

H_0: The accident sample data does not significantly differ from a Weibull distribution.

To check if the null hypothesis is applicable the p-value and the significant level α are compared to each other. If p>α, H_0 cannot be rejected, it is safe to assume that the accident sample data is not significantly different to a Weibull distribution. A significance level of 5% was used. The p-value of the fitted Weibull distribution was thereby calculated with the statistical software R (R Core Team, 2019) and obtained by Monte Carlo simulation (González-Estrada and Villaseñor, 2018).

As initial speeds of the road users were not available for tram accidents, these particular analyses were only performed for car accidents. For estimating the probability of road friction, relative frequencies based on the combined in-depth dataset for cars, based on statistics from Austria (Statistics Austria) for tram accidents, were derived.

2.2 Results

In total, more than 4 Million accident cases were available for further analysis (Table 2-4). Exemplary results will be outlined in this section. Results have been partly published already (Leo *et al.*, 2019b; Leo *et al.*, 2019a; Linder *et al.*, 2020), and further manuscripts have been prepared and will be submitted once the paper describing the Pre-crash Tool (Schachner *et al.*, 2020) is published, providing the reference for further WP4 analysis.

Table 2-4 Number of Cases in different Databases for Pedestrians and Cyclists.

Database	Pedestrian	Cyclist
	[#]	[#]
CARE	2260354	1822415
CEDATU	232	57
GIDAS	156	117
IGLAD	430	300
SaferWheels	-	95
STRADA	631	1048
Tram	2366	-
VOLVO	481	316

2.2.1 Injured VRUs

2.2.1.1 Pedestrian and Cyclist - Car Accidents

The age and gender distribution of casualties reported in the CARE database are shown in Figure 2-7-Figure 2-10. Regarding pedestrians, 45% of the severely injured and 34 % of the fatally injured, were females. Of the cyclists, 33% of the severely injured and 20% of the fatally injured were females. Both datasets presented a number of injured road users only reported as seriously or slightly injured, prohibiting assigning a particular injury to the data. The injury severity was related to the average age of the injured VRUs, at 35 years for slightly injured, 41 years for severely and 53 for fatally injured

pedestrians. A similar trend was observed for cyclists where the average age was 35 years for slightly injured, 42 years for severely injured and 54 years for fatally injured cyclists.

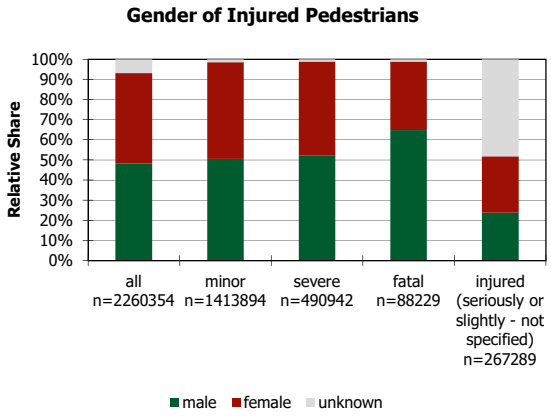

Figure 2-7: Gender of injured pedestrians (based on CARE).

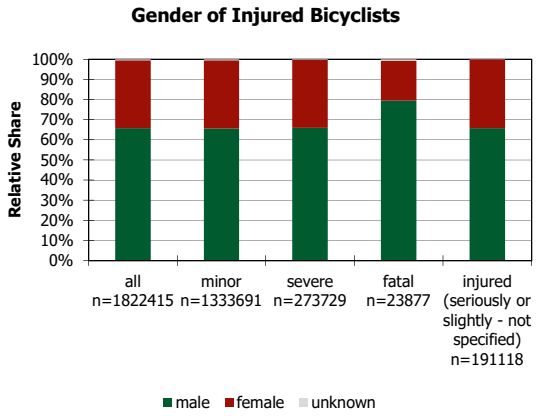

Figure 2-8: Gender of injured cyclists (based on CARE).

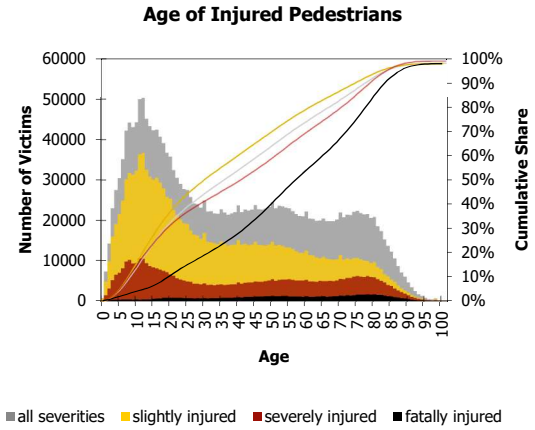

Figure 2-9: Age of injured pedestrians (based on CARE).

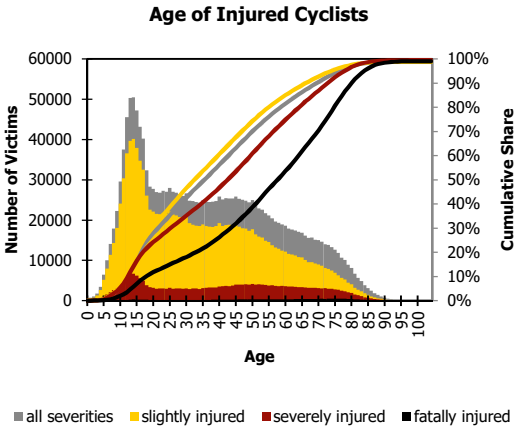

Figure 2-10: Age of injured cyclists (based on CARE).

Table 2-5 shows the average height and weight of injured adult (age 18+) pedestrians and cyclists analysed from IGLAD cases for all injury severities. Average values were derived for cases from the European IGLAD dataset only.

Table 2-5: Height and weight of adult (age 18+) injured pedestrians and cyclists from the European IGLAD database.

	Female		Male	
	Pedestrian	**Cyclist**	**Pedestrian**	**Cyclist**
Number of adult victims	61	57	44	87
Mean height of adults [cm]	164.9	166.9	175.1	179.9
Mean weight of adults [kg]	66.8	66.6	79.9	80.3

2.2.1.2 Pedestrian - Tram Accidents

Some exemplary results of a tram accident data analysis from Austria, Germany, Switzerland and Latvia for the years 2010 to 2017, are presented in Figure 2-11 and Figure 2-12. The majority of the tram accident cases did not reveal the gender of those injured, categorised under unspecified in the table below. When specified, it can be seen that females more often receive severe injuries than males. The opposite trend applies for fatal injuries, whether this is the true trend remains unconfirmed due to the large number of unspecified cases.

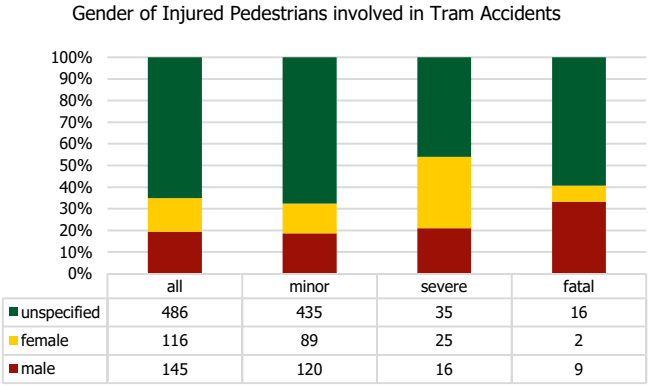

	all	minor	severe	fatal
unspecified	486	435	35	16
female	116	89	25	2
male	145	120	16	9

Figure 2-11 Gender of Injured Pedestrians involved in Tram Accidents.

By analysing the age of pedestrians involved in accidents with trams it can be seen that younger pedestrians seem to be involved in this particular type of accident more often. Most of the tram accidents occurred on dry roads.

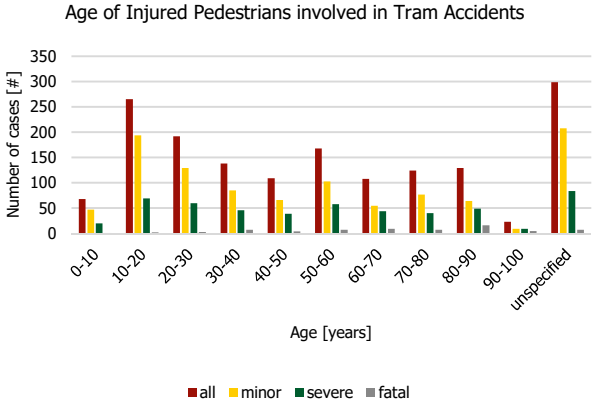

Figure 2-12 Age of Injured Pedestrians involved in Tram Accidents.

For more information on tram accidents and the analysed data, please refer to (Klager, 2019).

2.2.2 Relevant Injuries

2.2.2.1 Relevant Body Regions for Pedestrian and Cyclist Injuries in Car Accidents

The analysis of STRADA data showed certain differences when comparing AIS 2 and AIS 3+ with PMI 1+ (impairing injuries) and PMI 10+ injuries (severe impairing injuries). For example, Figure 2-13 show that AIS 3+ pedestrian injuries to the thorax were common, however, these injuries were not common

when looking at the long-term impact according to PMI 1+ and PMI 10+ injuries. On the other hand, lower extremity injuries are most common among both AIS 2 and AIS 3+, as well as PMI 1+ injuries. Further, Figure 2-13 illustrates that almost half of all severe impairing injuries (PMI 10+) were head injuries. The injury distributions were similar for male and female pedestrians.

Certain dissimilarities between men and women were shown for cyclists. Figure 2-14 shows that lower extremity injuries were common, however, the pattern shows that overall, women tended to sustain a higher proportion of lower extremity injuries. The pattern is the same for head injuries, as well, where women presented a higher proportion of severe (AIS 3+ and predicted PMI 10+) head injuries.

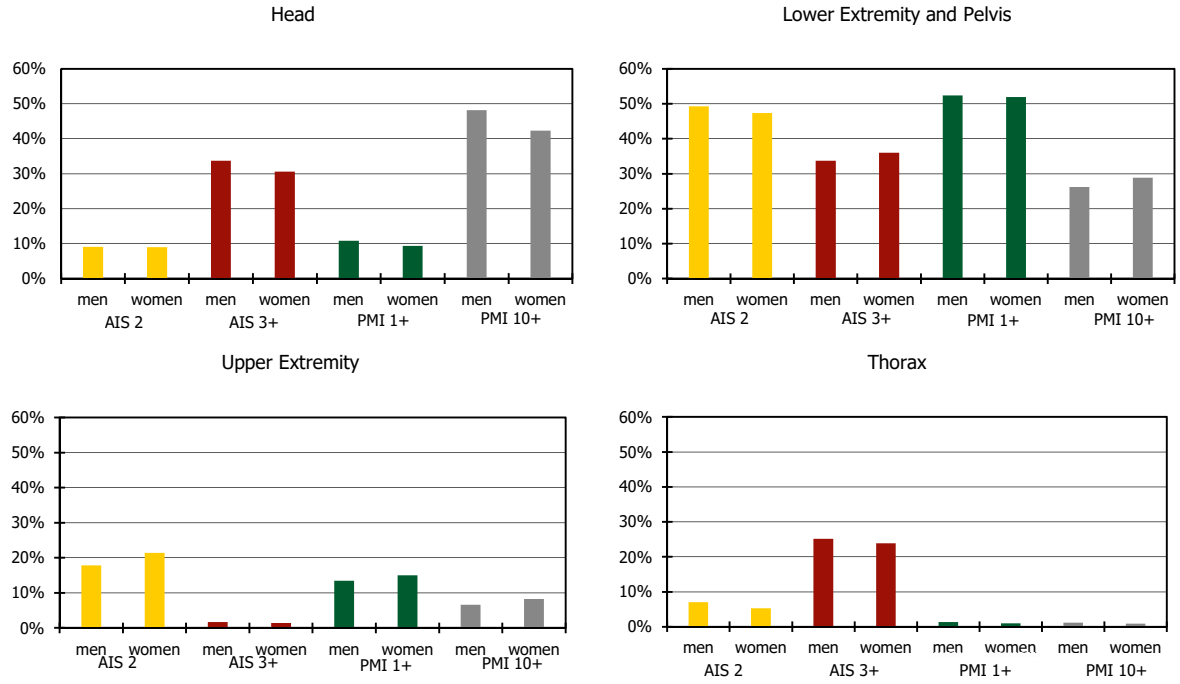

Figure 2-13 Percentage of pedestrian injuries to Upper Extremity, Head, Lower Extremity and Pelvis, and Thorax, of different injury classification (AIS 2, AIS 3+, RPMI 1+ and RPMI 10+) categorised by gender.

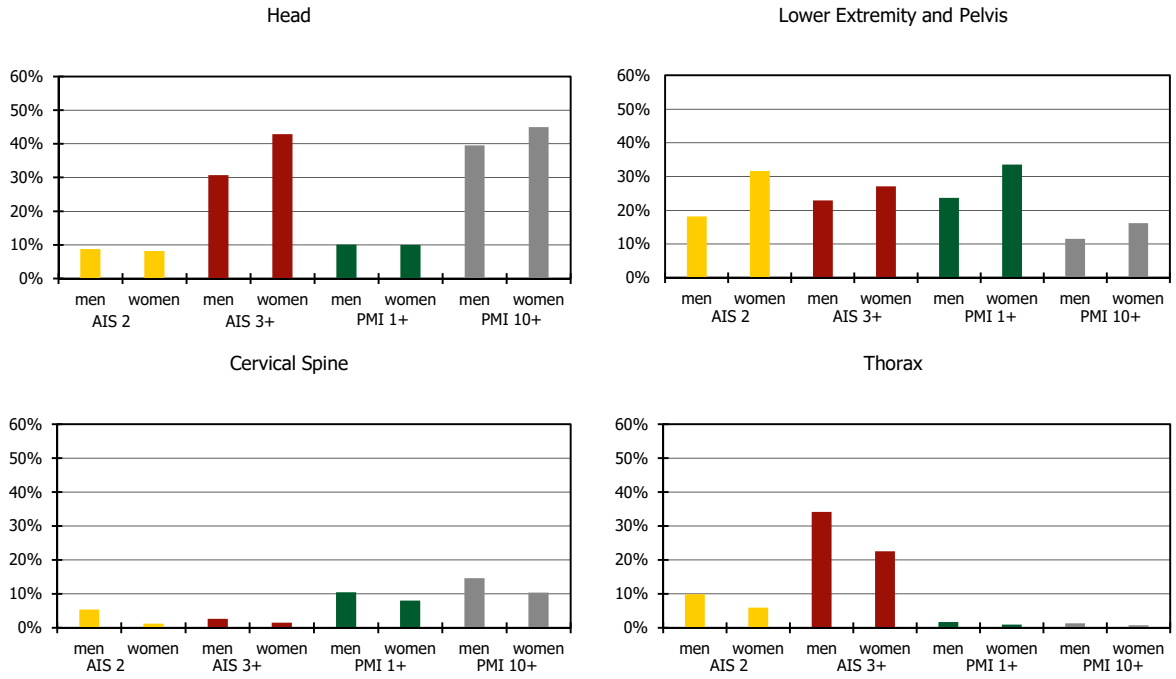

Figure 2-14: Percentage of cyclist injuries to Head, Lower Extremity ad Pelvis, Cervical Spine and Thorax, of different injury classifications (AIS 2, AIS 3+, RPMI 1+ and RPMI 10+) categorised by gender.

In Table 2-6 and Table 2-7 below, the distribution of all injuries among cyclists and pedestrians are shown, categorised by gender. When long-term consequences (predicted PMI 1+ and PMI 10+ injuries) are taken into consideration, there are some conclusions that can be drawn regarding which injuries that should be prioritized for inclusion in virtual testing of cyclists and pedestrians in collision with passenger cars. For cyclists, the body regions that should be considered for virtual testing are Head, Upper extremity, and Lower extremity and Pelvis. For pedestrians, the corresponding body regions are Head and Lower Extremity and Pelvis.

Table 2-6: Injury distribution of cyclists AIS 2 & AIS 3+ and PMI 1+ & PMI 10+ injuries in Sweden 2006-2017 (bicycle-passenger car crashes) categorised by gender.

	AIS 2		AIS 3+		PMI 1+		PMI 10+	
Body region	men	women	men	women	men	women	men	women
Head	11%	11%	32%	49%	12%	12%	46%	52%
Cervical spine	5%	2%	1%	1%	11%	9%	12%	10%
Face	6%	5%	1%	0%	4%	3%	6%	4%
Upper extremity	37%	34%	2%	5%	28%	25%	13%	13%
Lower extremity	19%	32%	23%	20%	24%	32%	12%	14%
Thorax	10%	6%	33%	19%	2%	1%	2%	0%
Thoracic spine	4%	4%	2%	1%	4%	3%	5%	3%
Abdomen	1%	1%	3%	3%	0%	0%	0%	0%
Lumbar spine	4%	4%	3%	1%	5%	4%	3%	3%
External (skin)	3%	1%	0%	0%	10%	11%	1%	1%

Table 2-7: Injury distribution of pedestrians AIS 2 & AIS 3+ and PMI 1+ & PMI 10+ injuries in Sweden 2006-2017 (pedestrian-passenger car crashes) categorised by gender.

	AIS 2		AIS 3+		PMI 1+		PMI 10+	
Body region	men	women	men	women	men	women	men	women
Head	9%	9%	34%	31%	11%	9%	48%	42%
Face	4%	4%	2%	1%	3%	3%	5%	4%
Cervical spine	2%	2%	1%	2%	5%	5%	7%	7%
Upper extremity	18%	21%	2%	1%	13%	15%	7%	8%
Lower extremity	49%	47%	34%	36%	52%	52%	26%	29%
Thoracic spine	3%	2%	0%	2%	2%	3%	2%	4%
Thorax	7%	5%	25%	24%	1%	1%	1%	1%
Abdomen	4%	5%	1%	0%	4%	5%	3%	4%
Lumbar spine	2%	1%	2%	3%	0%	0%	0%	0%
External (skin)	2%	2%	0%	0%	7%	7%	1%	1%

2.2.2.2 Injury Types

The relevance of detailed AIS injury codes was analysed and discussed within the two publications below:

- Leo, C., Klug, C., Ohlin, M. and Linder, A. (2019), "Analysis of pedestrian injuries in pedestrian-car collisions with focus on age and gender", *2019 IRCOBI Conference Proceedings, Florence, Italy, 11.-13.9.2018*, IRCOBI, pp. 256–257. http://www.ircobi.org/wordpress/downloads/irc19/pdf-files/40.pdf

A detailed analysis of injuries was made based on Swedish accident data with the focus on age and gender. The three most commonly injured AIS2+ body regions were identified as lower extremities, head and upper extremities, while bone fractures were the most frequent injuries sustained by pedestrians regardless of their age or gender. Moreover, significant differences between the injuries sustained by males and females were observed and these differences were even more pronounced when younger and elderly pedestrians were compared. The findings highlight the need for an assessment of safety measures that take gender as well as age of pedestrians into consideration. While it is not possible to examine this aspect with the current impactors, this can be addressed by means of Virtual Testing (VT).

- Leo, C., Klug, C., Ohlin, M., Bos, N., Davidse, R. and Linder, A. (2019), "Analysis of Swedish and Dutch accident data on cyclist injuries in cyclist-car collisions", *Traffic Injury Prevention*. Doi: 10.1080/15389588.2019.1679551. https://www.tandfonline.com/doi/full/10.1080/15389588.2019.1679551?af=R

To reduce the number of severe injuries sustained by cyclists in crashes with vehicles, it is important to understand which kind of injuries are occurring to identify what should be assessed by means of VT. A detailed analysis of injuries was made based on Swedish and Dutch accident data. The most frequently injured body regions and the most frequent single injuries of these body regions were analysed. Cyclists

most frequently injured their heads, upper and lower extremities, and bone fractures as well as brain injuries were identified as some of the most important injuries. For the virtual assessment of cyclist protection, injury predictors for long bone, skull and pelvic fractures as well as brain injuries are required in HBMs

2.2.2.3 Injury Severity Probabilities for Each Cluster of Conflict Situation for Car Accidents

The IPF method described in Section 2.1.3 was used to estimate the injury severity probabilities. The initial contingency tables for cyclists and pedestrians consist of accident data from the base level databases STRADA and CARE. The databases consist of a large amount of accidents categorised into slight, severe and fatal injuries for each cluster of conflict situation, which is sufficient to estimate the probability of injury severity for each cluster. Observe that the more detailed databases cannot be used since they, in certain cases, almost exclusively consist of one of the injury severity categories. The final clustering of conflict situations is based on the CARE database since the conflict situations within a cluster are more aggregated for CARE compared to STRADA. The grey parts of Table 2-8 and Table 2-9 show the observed contingency table for cyclists and pedestrians in the CARE clusters, respectively.

From the observed contingency tables, it is possible to derive an estimated contingency table under the assumption of independence between the databases and the corresponding probabilities of slight, severe and fatal for each cluster of conflict situation.

Table 2-8: Results of IPF – Contingency Tables of Injury Severities for Cyclists.

	STRADA			STRADA			CARE			
Conflict situation cluster	**Slight**	**Severe**	**Fatal**	**Slight**	**Severe**	**Fatal**	**Slight**	**Severe**	**Fatal**	**Total**
Car straight on, Cyclist turns	25	7	0							
Car turns, Cyclists oncoming	85	17	0							
Car turns, Cyclist SD	69	9	0	293	55	0	340053	78175	8118	**426346**
Car turns, Cyclist turns	9	0	0							
Car turns, Cyclist crosses	105	22	0							
Car straight on, Cyclist crosses	468	73	1	468	73	1	729372	145395	12321	**887088**
Car and Cyclist in longitudinal traffic	53	10	0	53	10	0	61889	12430	1731	**76113**
Door	7	3	0	7	3	0	2019	382	5	**2416**
Other	67	9	2	67	9	2	200358	37348	1701	**239485**
Total				**888**	**150**	**3**	**1333691**	**273729**	**23877**	

Table 2-9: Results of IPF – Contingency Tables of Injury Severities for Pedestrians.

	STRADA			STRADA			CARE			
Conflict situation cluster	**Slight**	**Severe**	**Fatal**	**Slight**	**Severe**	**Fatal**	**Slight**	**Severe**	**Fatal**	**Total**
Car straight on, Pedestrian crosses	299	84	9	299	84	9	147059	55446	4553	**207450**
Car turns, Pedestrian SD	23	12	0	49	20	1	18085	4564	1861	**22905**
Car turns, Pedestrian oncoming	26	8	1							
Car and Pedestrian in longitudinal traffic	23	11	2	23	11	2	6173	2389	780	**9378**
Reversing	49	10	1	49	10	1	0	0	0	**60**
Unspecified	52	15	2	52	15	2	1242577	428544	82709	**1753899**
Total				**472**	**140**	**15**	**1413894**	**490943**	**88228**	

In Appendix A.2 the observed and estimated number of accidents for each injury severity, slight, severe and fatal, within each cluster of conflict situations are given. It can be concluded that the estimated number of accidents for slight, severe and fatal injuries deviates more from the observations for STRADA compared to CARE. One reason for this is that CARE contains more observations and therefore more weight is given to the CARE dataset. However, the deviation does indicate that the categorisation of accidents into slight severe and fatal, and hence the probabilities, might differ between CARE and STRADA. On the other hand, in most cases with large deviations, the STRADA clusters only consists of few observations and therefore an uncertain distribution of accidents into slight, severe and fatal injuries. One exception is Cluster 2 for cyclists which contains many observations also for STRADA. Furthermore, for Cluster 4 the CARE database does not contain any observations and the final distribution of accidents is only based on the STRADA database. The resulting probabilities are given in Table 2-10 and Table 2-11 for cyclists and pedestrians, respectively.

Table 2-10: Probability of a certain injury severity for each cluster of cyclist conflict situation.

Cluster of conflict situations	**Slight**	**Severe**	**Fatal**	**Total**
1. Car straight on, Cyclist turns + Car turns, Cyclist oncoming + Car turns, Cyclist SD + Car turns, Cyclist turns + Car turns, Cyclist crosses	79.8 %	18.3 %	1.9 %	100%
2. Car straight on, Cyclist crosses	82.2 %	16.4 %	1.4 %	100%
3. Car and Cyclist in longitudinal traffic	81.4 %	16.3 %	2.3 %	100%
4. Door	83.9 %	15.9 %	0.2 %	100%
5. Others	83.7 %	15.6 %	0.7 %	100%

Table 2-11: Probability of a certain injury severity for each cluster of pedestrian conflict situation.

Cluster of conflict situations	Slight	Severe	Fatal	Total
1. Car straight on, Pedestrian crosses	71.0 %	27.8 %	2.2 %	100%
2. Car turns, Pedestrian SD + Car turns, Pedestrian oncoming	79.2 %	20.0 %	0.8 %	100%
3. Car and Pedestrian in longitudinal traffic	66.1 %	25.6 %	8.3 %	100%
4. Reversing	81.6 %	16.7 %	1.7 %	100%
5. Unspecified	70.9 %	24.4 %	4.7 %	100%

For all clusters of conflict situations, the patterns are similar (i.e., the probability of slight injury is (as expected) the largest, followed by severe). The probability of fatal injury is the lowest probability, but the risk of fatal accidents is higher for pedestrians than for cyclists in some of the clusters. For example, the probabilities of a fatality for pedestrians in Clusters 3 and 5 are much higher than all other clusters (i.e., there is a higher risk of fatal accidents if the conflict situation is *Car and Pedestrian in longitudinal traffic* or *Unspecified)*.

In conclusion, the probabilities calculated using the IPF method can be seen as representative for both STRADA and CARE in most cases. If large deviations exist between the observed and estimated number of accidents in STRADA, the few observations result in uncertain representation of the distribution of accidents between slight, severe and fatal injuries. One exception is Cluster 4 for cyclists, although even in this case CARE consists of many more observations than STRADA and the probabilities can probably be based on the CARE dataset.
It was not possible to perform a comparable analysis for tram accidents based on the available data.

2.2.3 Probability of Specific Accident Scenarios

2.2.3.1 Probability of Specific Types of Conflict Situations

The IPF method described in Section 2.1.3 was used to estimate the conflict situation probabilities within each cluster of conflict situations. The conflict situation probabilities are calculated per cluster since it is assumed that the conflict situations within a cluster is distributed similarly within the different databases. Further, the probabilities are calculated per injury severity due to the fact that some of the databases include mainly one category of the injury severity. The in-depth databases V_PAD/V_CAD, GIDAS and CEDATU allow for distribution of accidents into a specific conflict situation, which is necessary when estimating the probabilities of each conflict situation. The intermediate database IGLAD could also be used, but was excluded for two reasons. First, accidents from GIDAS and CEDATU can also occur in IGLAD and hence, there is a risk for double counting of accidents. Second, V_PAD/V_CAD, GIDAS and CEADATU contain European data, unlike IGLAD that consists of data from other parts of the world. Therefore, V_PAD/V_CAD, GIDAS and CEDATU represent our baseline samples, having assumed that they provide probabilities representing Europe within one cluster and severity.

The observed and estimated number of accidents for each conflict situation is given for slight, severe and fatal injuries for cyclists in Appendix A.4 and for pedestrians in A.3. The clusters have been colour coded in the figures since each cluster is assessed individually. Results in the figures are displayed based on the same cluster categories as in STRADA and CARE.

Databases with few observations do not contribute to the result as much as other well populated databases. GIDAS holds the highest number of reported accidents, while CEDATU holds the highest number of reported accidents. For severe accidents, the number of reported cases was comparable among the databases, except for cyclists for which V_CAD only consists of a few accidents. Furthermore,

it can be concluded that in general there are only few observations of severe and fatal accidents resulting in uncertain estimations and results that are sensitive to the cluster division.

The estimated and observed number of accidents correlate for pedestrians, which indicates that independent of database, the distribution of accidents is similar for conflict situations within a cluster. For cyclists, the differences in certain clusters are more significant. This indicates that the distribution of accidents between conflict situations within a cluster is not always similar for the different databases. However, the differences are within an acceptable range. The resulting probabilities per cluster (colour coded) for cyclists and pedestrians are summarised in Appendix A.5.

To obtain the overall probability of each cluster situation, the probabilities within each cluster are multiplied with the probability for an accident belonging to a specific cluster, based on the division of accidents clusters within STRADA and CARE. The clusters *Unspecified* and *Others* are excluded due to the large number of observations in these categories and their resulting impact on the probabilities, especially for cyclists in the CARE database. The accidents categorised as *Unspecified* should belong to one of the other clusters and the hypothesis is that they will have the same distribution as the ones already divided into the other clusters, although it cannot be confirmed.

Tables 2-8 and 2-9 show the derived probabilities for each type of conflict situation for the different injury severities. The final probabilities, in most cases, are comparable for the two databases. Some exceptions exist such as the large probability of fatality for the conflict situation RT/SD in the cluster Car turns, Cyclist SD when using the CARE database compared to 0 in the STRADA database. However, this is probably due to the few observations belonging to the injury severity type fatal in the STRADA database, which results in large uncertainties on the distribution of fatal accidents.

The Iterative Proportional Fitting (IPF) is only useful when the accidents are distributed similar among the different conflict situations for the included databases. In our case, this means that the IPF method is used to calculate the conflict situation probabilities for each cluster separately, since the distribution of accidents between clusters differs for the included databases. Therefore, the final probabilities are calculated based on the cluster distribution of accidents given by CARE or STRADA and the cluster specific conflict probabilities calculated with the IPF

This particular type of analysis was only performed for car accidents, as detailed data on conflict situation distribution was not available for tram accidents.

Table 2-12: Probability for specific types of cyclist conflict situations as a result of IPF.

Conflict situation cluster	Conflict situation	STRADA			CARE		
		Slight	Severe	Fatal	Slight	Severe	Fatal
Car straight on, Cyclist turns	SCPCROD	0.0	0.0	0.0	0.0	0.0	0.0
	SCPCRSD	0.5	1.7	0.0	0.2	6.6	0.0
	SCPCLOD	0.1	0.0	0.0	0.0	0.0	0.0
	SCPCLSD	0.8	1.7	0.0	0.2	6.6	0.0
	Details unknown	1.6	1.7	0.0	0.5	6.6	0.0
Car turns, Cyclist oncoming	LT/OD	5.8	4.0	0.0	6.0	0.0	0.0
	RT/OD	4.5	4.0	0.0	4.7	0.0	0.0
	Details unknown	0.0	4.0	0.0	0.0	0.0	0.0
Car turns, Cyclist SD	LT/SD	1.5	0.0	0.0	1.9	0.0	0.0
	RT/SD	6.9	6.3	0.0	8.3	6.6	36.6
	Details unknown	0.0	0.0	0.0	0.0	0.0	0.0
Car turns, Cyclist turns	LT/ODLD	0.0	0.0	0.0	0.0	0.0	0.0
	LT/ODRD	0.0	0.0	0.0	0.0	0.0	0.0
	LT/SDLD	0.0	0.0	0.0	0.0	0.0	0.0
	LT/SDRD	0.0	0.0	0.0	0.0	0.0	0.0
	RT/ODLD	0.0	0.0	0.0	0.0	0.0	0.0
	RT/ODRD	0.0	0.0	0.0	0.0	0.0	0.0
	RT/SDLD	1.1	0.0	0.0	0.0	0.0	0.0
	RT/SDRD	0.0	0.0	0.0	0.0	0.0	0.0
	Details unknown	0.0	0.0	0.0	0.0	0.0	0.0
Car turns, Cyclist crosses	LT/RD	1.3	0.0	0.0	0.8	0.0	0.0
	LT/LD	0.8	0.0	0.0	0.5	0.0	0.0
	RT/RD	5.7	0.0	0.0	3.6	0.0	0.0
	RT/LD	5.1	15.4	0.0	3.2	6.6	0.0
	Details unknown	0.0	0.0	0.0	0.0	0.0	0.0
Car straight on, Cyclist crosses	SCPCR	37.4	33.4	50.0	42.2	39.7	27.8
	SCPCL	19.2	18.4	50.0	21.7	21.8	27.8
	Details unknown	0.4	0.0	0.0	0.5	0.0	0.0
Car and Cyclist in longitudinal traffic	Oncoming	1.0	3.5	0.0	0.9	2.6	4.1
	SD	5.4	3.5	0.0	4.6	2.6	3.7
	Details unknown	0.0	0.0	0.0	0.0	0.0	0.0
Door	Door	0.9	2.1	0.0	0.2	0.2	0.0
TOTAL		100	100	100	100	100	100

Table 2-13: Probability for specific types of pedestrian conflict situations as a result of IPF..

Conflict situation cluster	Conflict situation	STRADA			CARE		
		Slight	Severe	Fatal	Slight	Severe	Fatal
Car straight on, Pedestrian crosses	SCPPL	26.8	32.5	45	32.3	42.9	53.7
	SCPPR	44.1	31.7	20.9	53.2	41.9	24.9
	SCPPLSD	0.1	1.5	0.6	0.1	2.0	0.7
	SCPPLOD	0.0	0.0	0.0	0.0	0.0	0.0
	SCPPRSD	0.2	0.0	2.7	0.3	0.0	3.3
	SCPPROD	0.0	1.5	0.0	0.0	2.0	0.0
	Details unknown	0.0	0.0	0.0	0.0	0.0	0.0
Car turns, Pedestrian SD	LT/SD	3.7	7.7	0.0	3.9	4.2	0.0
	RT/SD	1.8	1.9	0.0	1.9	1.0	0.0
	LT/SDLD	0.0	0.0	0.0	0.0	0.0	0.0
	RT/SDRD	0.0	0.0	0.0	0.0	0.0	0.0
	Details unknown	0.0	0.0	0.0	0.0	0.0	0.0
Car turns, Pedestrian oncoming	LT/OD	4.7	0.0	3.8	3.6	0.0	1.7
	RT/OD	1.5	3.2	0.0	1.2	1.0	0.0
	LT/ODLD	0.0	3.2	3.8q	0.0	1.0	1.7
	LT/ODRD	0.0	0.0	0.0	0.0	0.0	0.0
	RT/ODLD	0.0	0.0	0.0	0.0	0.0	0.0
	RT/ODRD	0.0	0.0	0.0	0.0	0.0	0.0
	Details unknown	0.0	0.0	0.0	0.0	0.0	0.0
Car and Pedestrian in longitudinal traffic	SD	3.6	5.0	10.3	2.4	2.2	9.4
	Oncoming	1.9	3.8	5.1	1.2	1.6	4.7
	Details unknown	0.0	0.0	0.0	0.0	0.0	0.0
Reversing	Reversing	11.7	8.0	7.7	0	0	0
TOTAL		100	100	100	100	100	100

To further verify the representativeness of the estimated probabilities, the intermediate database IGLAD has been used. The estimated probabilities in Table 2-12 and Table 2-13 were used together with the number of accidents per conflict situation and injury severity from IGLAD. The number of accidents per conflict situations and injury severity were aggregated to the cluster divisions as in STRADA and CARE. In this way it is possible to compare the observed accidents per conflict situation with the number of accidents per conflict situation using the estimated probabilities. The results can be found in Appendix A.7 and A.6 for cyclists and pedestrians, respectively. The verification with IGLAD data gives reasonable results. Some expected differences have been observed, although they are within an acceptable range, (i.e., the deviations between observation and estimation are not too large). When the estimation with IGLAD was based on limited or no data, the deviations were larger and in some conflict situations with no observed accidents in IGLAD resulting in an allocation of accidents in the estimation as a result of this.

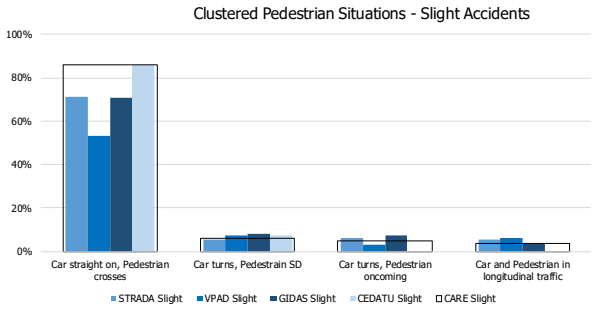

Figure 2-15: Probability for clustered pedestrian conflict situations based on slight accidents.

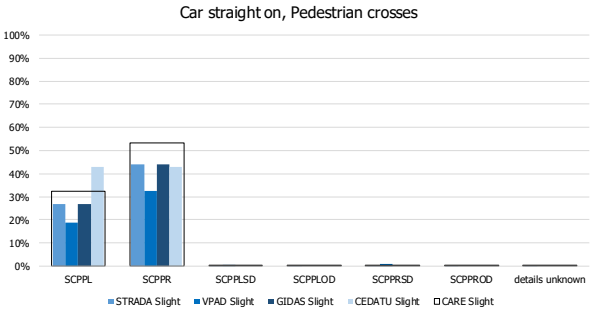

Figure 2-16: Probability of conflict situations within the cluster "Car straight on, Pedestrian crosses" based on slight accidents.

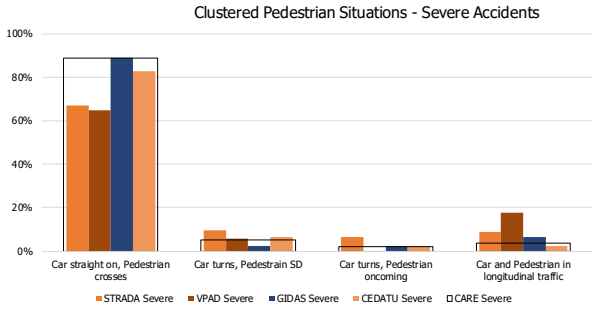

Figure 2-17: Probability for clustered pedestrian conflict situations based on severe accidents.

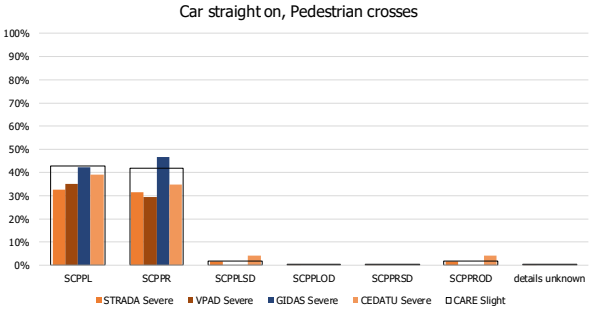

Figure 2-18: Probability of conflict situations within the cluster "Car straight on, Pedestrian crosses" based on severe accidents.

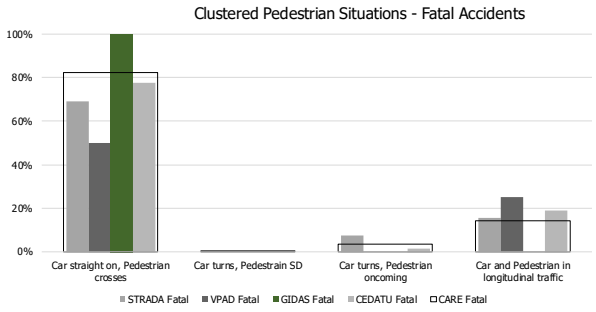

Figure 2-19: Probability for clustered pedestrian conflict situations based on fatal accidents.

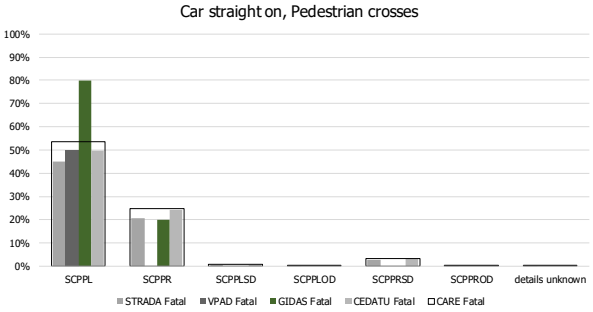

Figure 2-20: Probability for clustered pedestrian conflict situations based on fatal accidents.

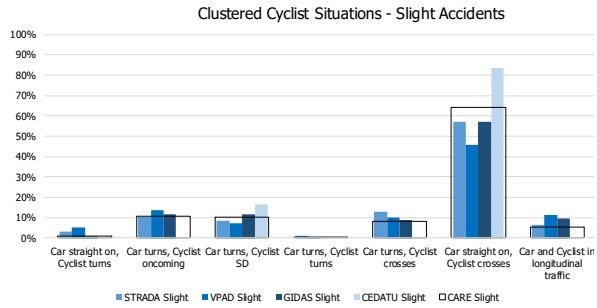

Figure 2-21: Probability for clustered cyclist conflict situations based on slight accidents.

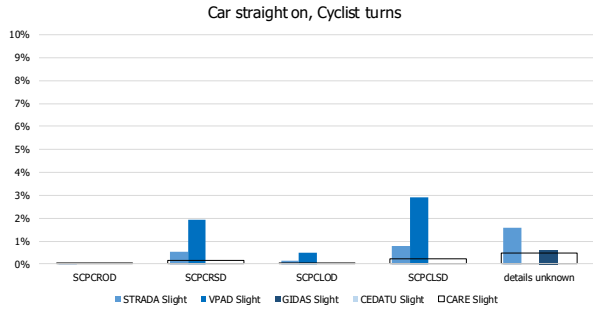

Figure 2-22: Probability of conflict situations within the cluster "Car straight on, Cyclist turns" based on slight accidents.

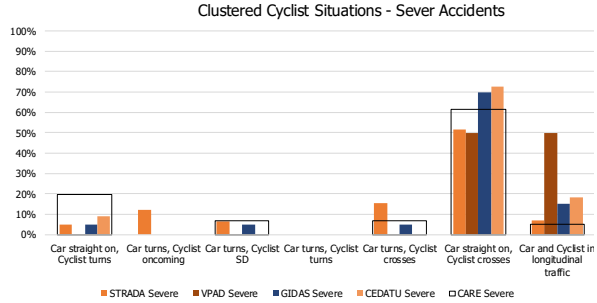

Figure 2-23: Probability for clustered cyclist conflict situations based on severe accidents.

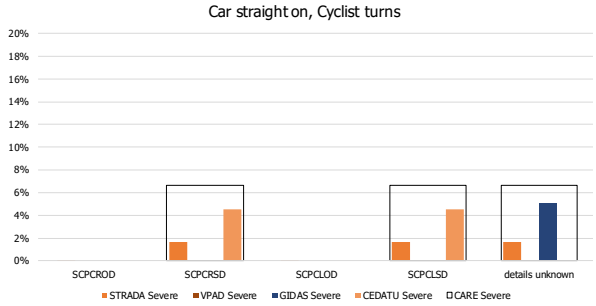

Figure 2-24: Probability of conflict situations within the cluster "Car straight on, Cyclist turns" based on severe accidents.

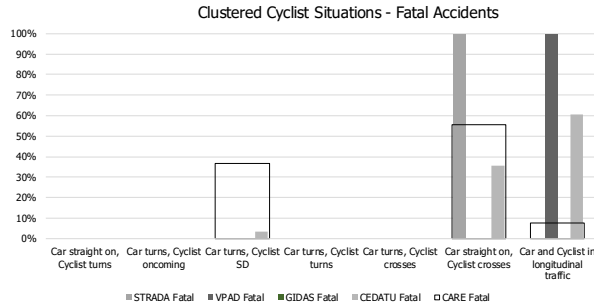

Figure 2-25: Probability for clustered cyclist conflict situations based on fatal accidents.

No data available

Figure 2-26: Probability of conflict situations within the cluster "Car straight on, Cyclist turns" based on fatal accidents.

2.2.3.2 Probability of Accident Parameters

Detailed analysis was performed for each conflict situation and injury severity with the results presented as shown in Figure 2-27. The density of the accident sample data is given in form of bins in the histogram (yellow) as well as a smoothed estimated density line (black) which represents a smoothed version of the histogram. In the same plot the fitted Weibull distribution (red) is also shown. For a first visual inspection of how well the fitted Weibull distribution fits the accident sample data, the cumulative distribution function is given in an extra plot. In the boxplot in the left bottom corner of Figure 2-27, the mean value of the accident data is seen. It is possible to obtain a first impression of how the values change in terms of different injury severities through the mean value. Finally, one table also provides the most important information of the analysed data, namely which data represent the conflict situation, injury severity, number of analysed cases, fitted distribution and related parameters, as well as the p-value of the goodness of fit test. Here only one analysis is shown as an example. To also see the other analyses, please refer to the Appendix B.3.

These types of analyses were only performed for car accidents, as no in-depth data for trams was available.

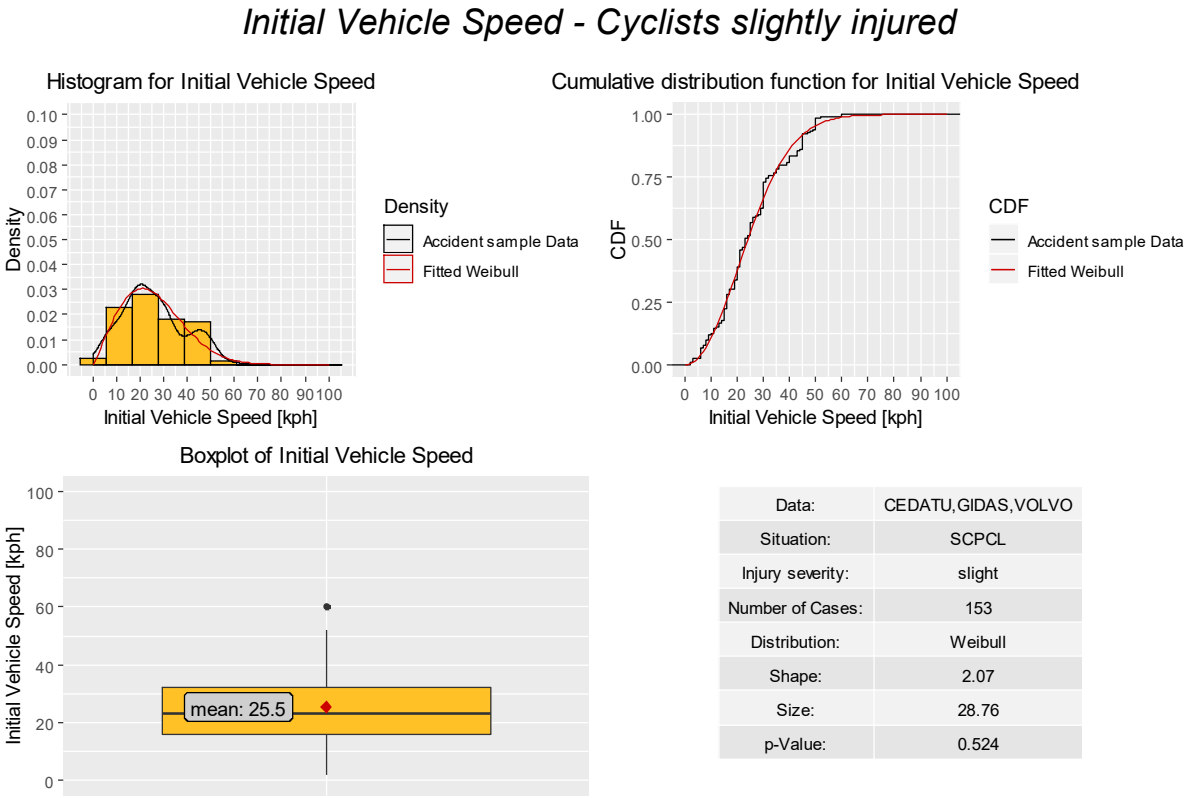

Figure 2-27 Detailed analyses of one specific conflict situation.

Initial Vehicle Speed for Cyclist - Car Accidents

For the initial vehicle speed in cyclist accidents all p-values are above the significant level of α=0.05%. This means that the Weibull distribution can be used to describe the accident data sample and that there are no significant differences between observation and fitted distribution. All results are summarised in Table 2-14. The original data and the fitted distributions are visualised in Figure 2-28 - Figure 2-30 for the different accident severities.

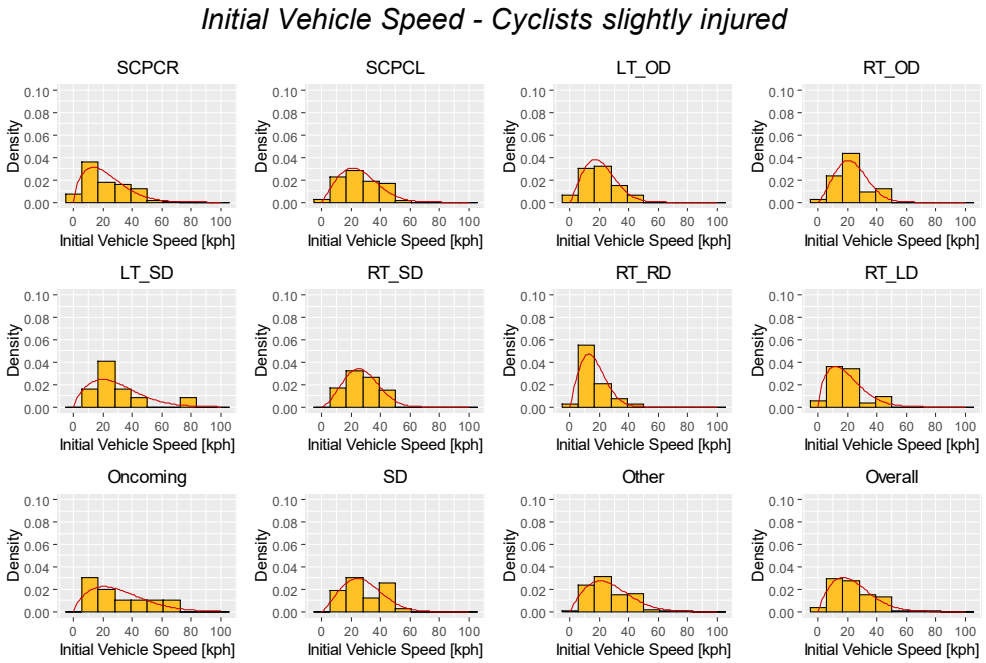

Figure 2-28 Fitted Weibull distribution to accident sample data for different detailed conflict situations for the initial vehicle speed in cyclist accidents with slightly injured cyclists.

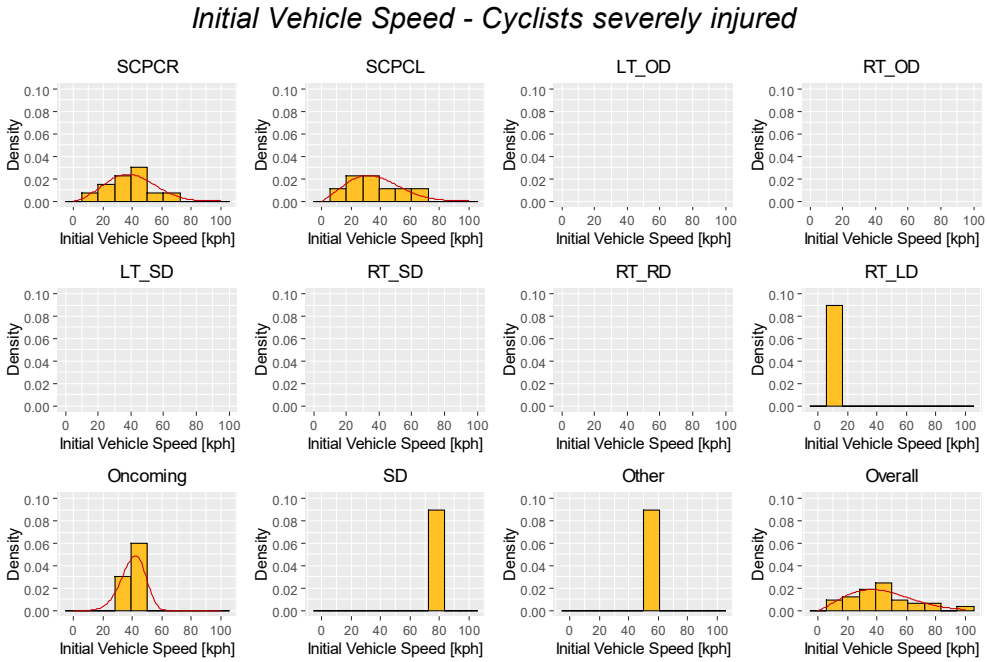

Figure 2-29 Fitted Weibull distribution to accident sample data for different detailed conflict situations for the initial vehicle speed in cyclist accidents with severely injured cyclists.

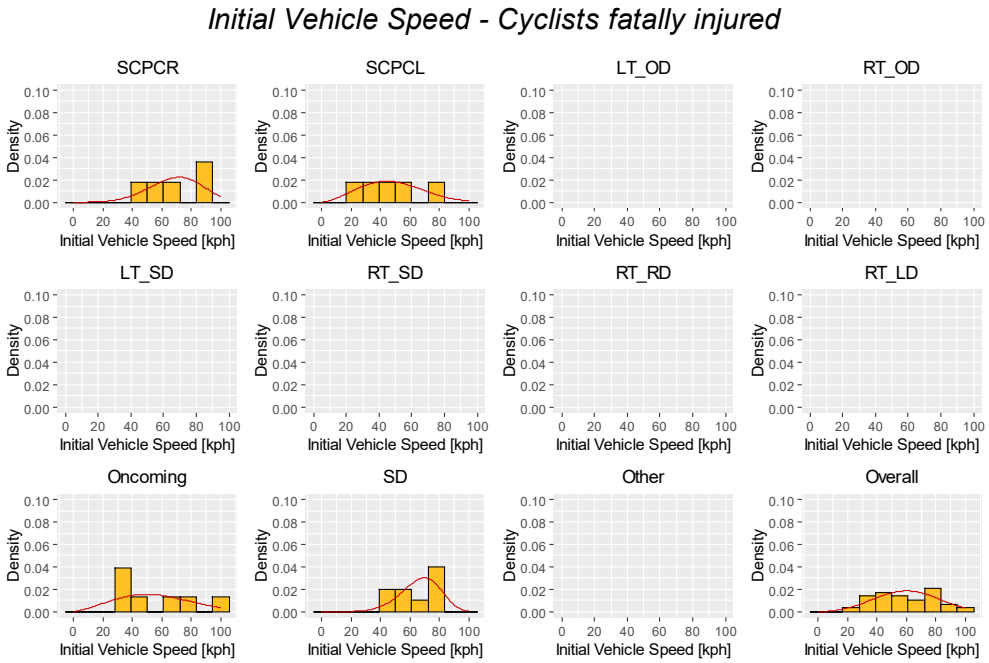

Figure 2-30 Fitted Weibull distribution to accident sample data for different detailed conflict situations for the initial vehicle speed in cyclist accidents with fatally injured cyclists.

Table 2-14 Parameters of fitted Weibull distribution to accident sample data for different detailed conflict situations and different injury severities for the initial vehicle speed in cyclist accidents.

Situation	Severity	Number of Cases:	Shape (λ)	Scale (k)	p-value
SCPCR	slight	238	1.61	24.47	0.494
SCPCL	slight	153	2.07	28.76	0.53
LT/OD	slight	59	2.10	23.31	0.172
RT/OD	slight	31	2.35	25.83	0.774
LT/SD	slight	11	1.74	32.23	0.08
RT/SD	slight	79	2.58	30.47	0.818
RT_RD	slight	60	1.99	18.14	0.036
RT_LD	slight	47	1.62	21.25	0.146
Oncoming	slight	9	1.69	34.89	0.742
SD	slight	128	2.24	31.35	0.324
Other	slight	104	1.91	30.39	0.188
Overall	slight	863	1.81	26.50	0.07
SCPCR	severe	12	2.64	44.17	0.686
SCPCL	severe	8	2.27	40.73	0.362
Oncoming	severe	3	5.67	43.36	0.788
Overall	severe	29	2.17	48.55	0.404
SCPCR	fatal	5	4.46	75.85	0.86
SCPCL	fatal	5	2.51	54.10	0.82
Oncoming	fatal	7	2.37	62.59	0.25
SD	fatal	9	5.84	71.93	0.618
Overall	fatal	26	3.21	67.45	0.926

Initial Vehicle Speed for Pedestrian – Car Accidents

For the initial vehicle speed in pedestrian accidents, not all p-values for the Weibull fit were above the significant level of α=0.05%. The parameters are summarised in Table 2-15. The original data and the fitted distributions are visualised in Figure 2-31 – Figure 2-33 for the different accident severities.

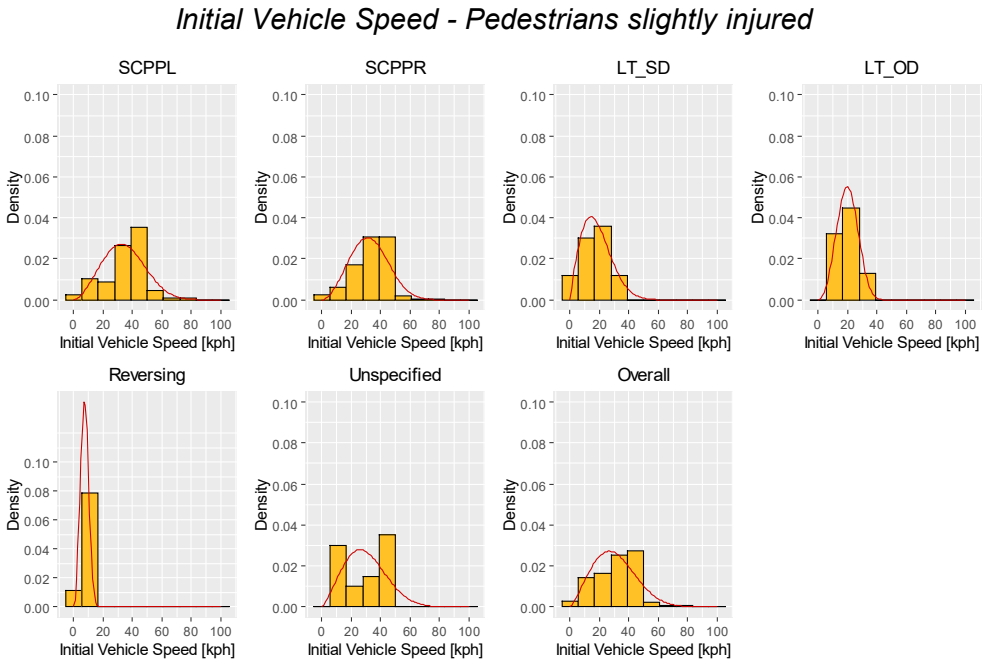

Figure 2-31 Fitted Weibull distribution to accident sample data for different detailed conflict situations for the initial vehicle speed in pedestrian accidents with slightly injured pedestrians.

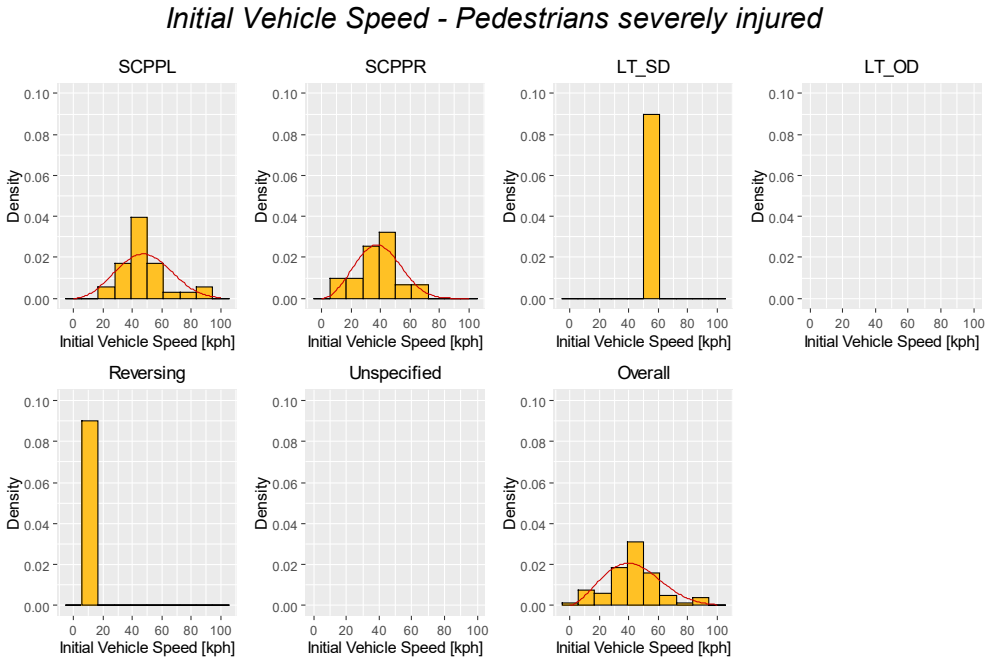

Figure 2-32 Fitted Weibull distribution to accident sample data for different detailed conflict situations for the initial vehicle speed in pedestrian accidents with severely injured pedestrians.

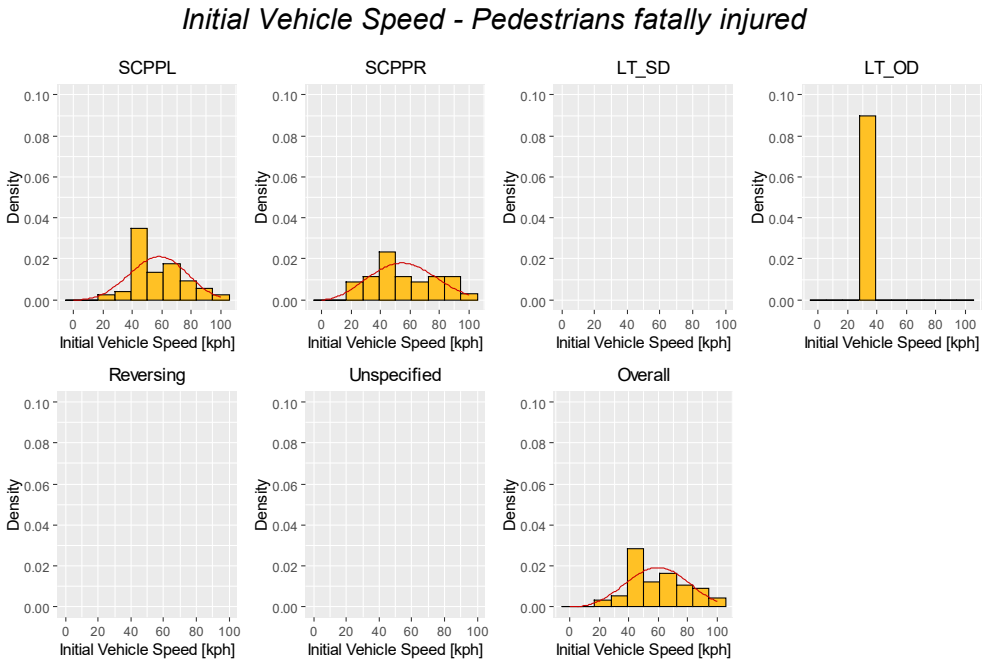

Figure 2-33 Fitted Weibull distribution to accident sample data for different detailed conflict situations for the initial vehicle speed in pedestrian accidents with fatally injured pedestrians.

Table 2-15 Parameters of fitted Weibull distribution to accident sample data for different detailed conflict situations and different injury severities for the initial vehicle speed in pedestrian accidents.

Situation	Severity	Number of Cases:	Shape	Scale	P-value
SCPPL	slight	112	2.64	38.81	0.004
SCPPR	slight	183	2.78	36.49	0.00
LT/SD	slight	15	1.94	20.71	0.148
LT/OD	slight	14	3.16	22.33	0.602
SD	slight	15	1.94	20.71	0.168
Reversing	slight	16	3.07	8.39	0.044
Unspecified	slight	18	2.28	33.66	0.532
Overall	slight	382	2.27	34.43	0.00
SCPPL	severe	32	2.99	54.14	0.098
SCPPR	severe	28	2.89	43.50	0.178
Overall	severe	73	2.48	48.70	0.032
SCPPL	fatal	67	3.51	64.09	0.144
SCPPR	fatal	31	2.87	62.95	0.422
Overall	fatal	127	3.32	66.70	0.160

Initial Cyclist Speed for Cyclist – Car Accidents

The p-value of the Weibull distribution for the majority of initial cyclist speeds for cyclist accidents is above the significant level (Table 2-16). The original data and the fitted distributions are visualised in Figure 2-34 – Figure 2-36 for the different accident severities.

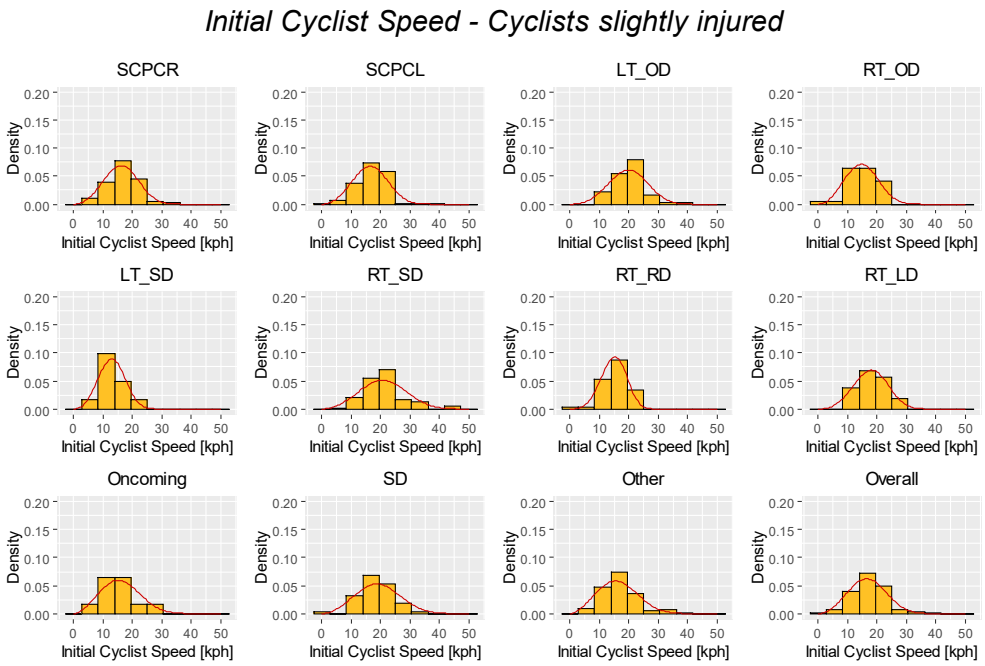

Figure 2-34 Fitted Weibull distribution to accident sample data for different detailed conflict situations for the initial cyclist speed in cyclist accidents with slightly injured cyclists.

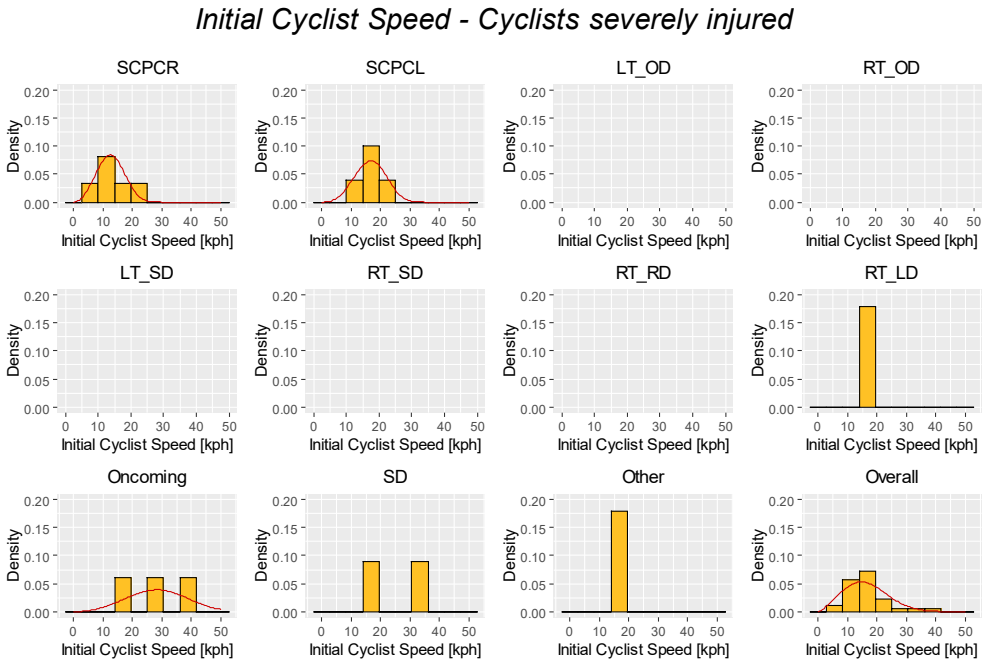

Figure 2-35 Fitted Weibull distribution to accident sample data for different detailed conflict situations for the initial cyclist speed in cyclist accidents with severely injured cyclists.

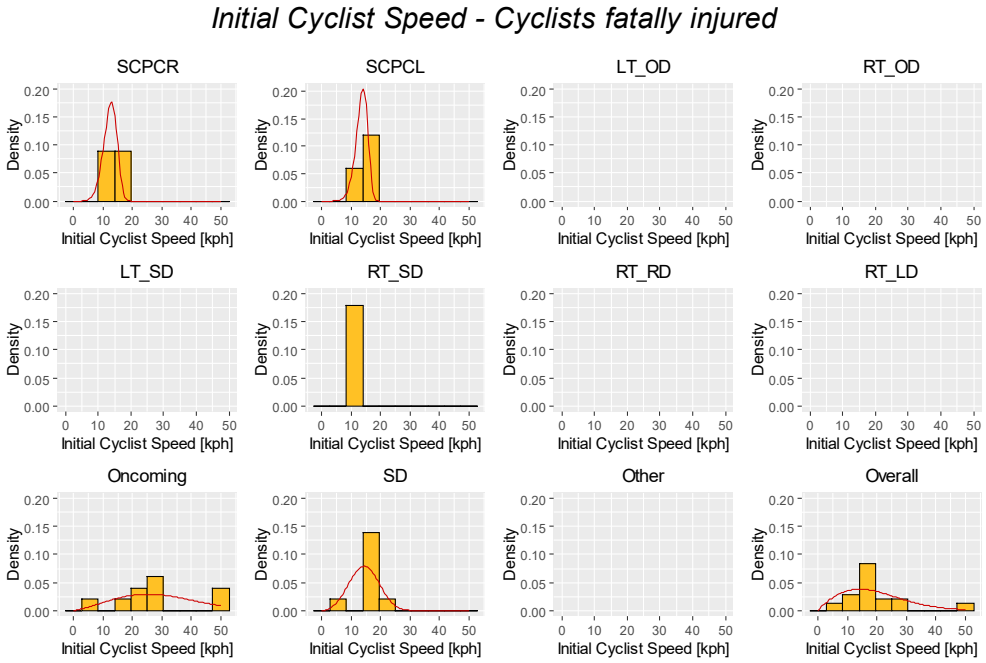

Figure 2-36 Fitted Weibull distribution to accident sample data for different detailed conflict situations for the initial cyclist speed in cyclist accidents with fatally injured cyclists.

Table 2-16 Parameters of fitted Weibull distribution to accident sample data for different detailed conflict situations and different injury severities for the initial cyclist speed in cyclist accidents.

Situation	Severity	Number of Cases:	Shape (λ)	Scale (k)	p-value
SCPCR	slight	297	3.22	18.12	0.142
SCPCL	slight	170	3.21	18.46	0.194
LT/OD	slight	65	3.50	22.01	0.03
RT/OD	slight	31	3.04	16.69	0.138
LT/SD	slight	11	3.33	14.48	0.522
RT/SD	slight	83	3.06	23.45	0.004
RT_RD	slight	68	4.02	16.38	0.002
RT_LD	slight	58	3.58	19.87	0.018
Oncoming	slight	11	2.70	18.03	0.112
SD	slight	144	2.90	21.63	0.198
Other	slight	112	2.69	18.40	0
Overall	slight	1000	2.99	18.87	0.024
SCPCR	severe	11	3.06	14.18	0.55
SCPCL	severe	9	3.54	18.39	0.362
Oncoming	severe	3	3.19	31.80	0.696
Overall	severe	32	2.38	18.33	0.006
SCPCR	fatal	4	6.26	13.21	0.902
SCPCL	fatal	3	7.87	14.28	0
Oncoming	fatal	9	2.30	32.49	0.502
SD	fatal	10	3.28	16.11	0.112
Overall	fatal	26	1.85	21.50	0.096

Initial Pedestrian Speed for Pedestrian-Car Accidents

For the initial pedestrian speeds for pedestrian accidents the same results can be obtained as for the other parameters when fitting a Weibull distribution to the sample data (Table 2-17). The original data and the fitted distributions are visualised in Figure 2-37 – Figure 2-39 for the different accident severities.

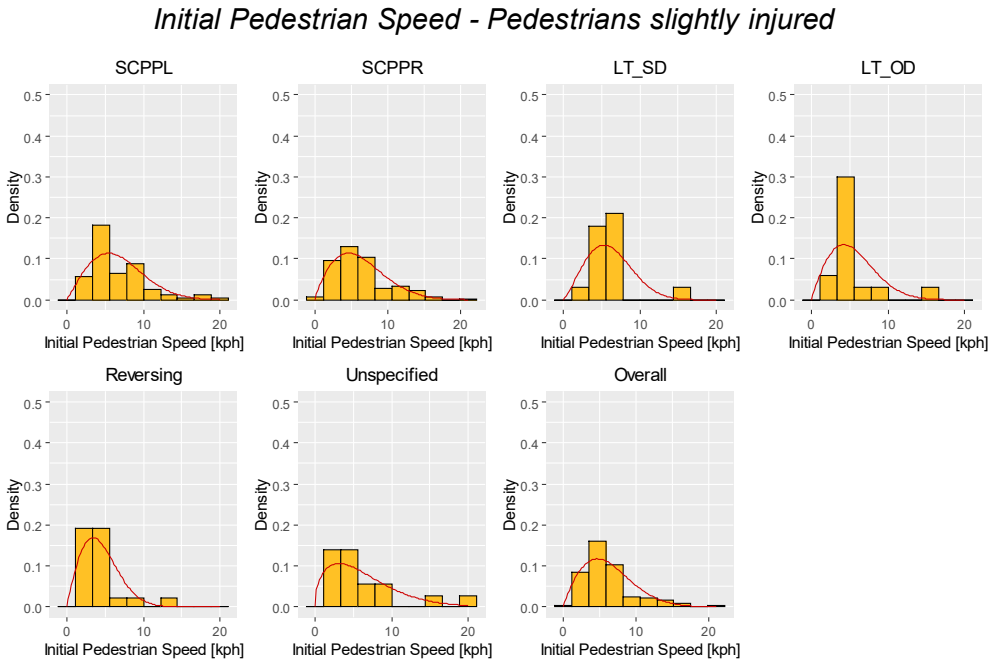

Figure 2-37 Fitted Weibull distribution to accident sample data for different detailed conflict situations for the initial pedestrian speed in pedestrian accidents with slightly injured pedestrians.

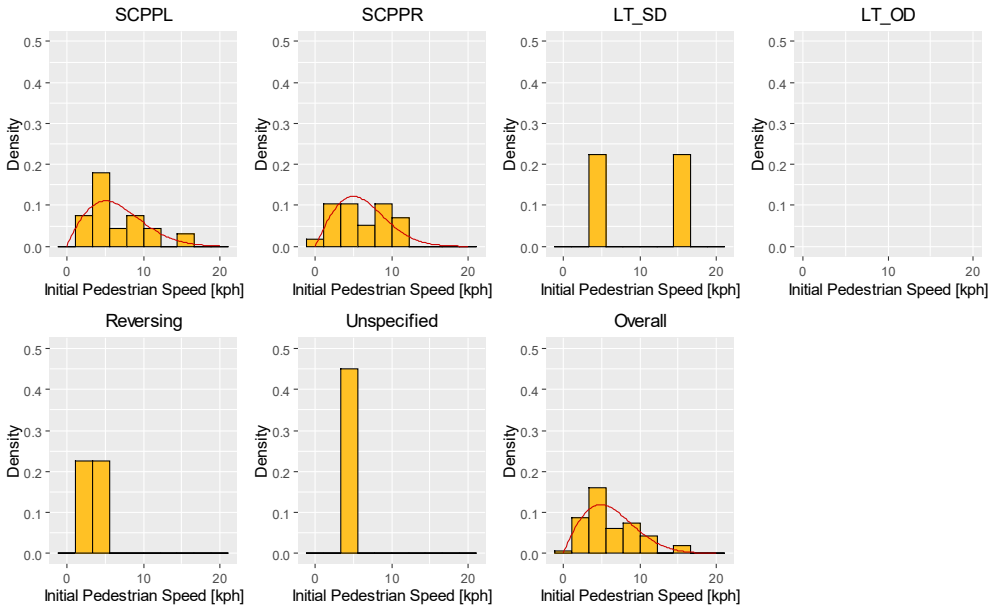

Figure 2-38 Fitted Weibull distribution to accident sample data for different detailed conflict situations for the initial pedestrian speed in pedestrian accidents with severely injured pedestrians.

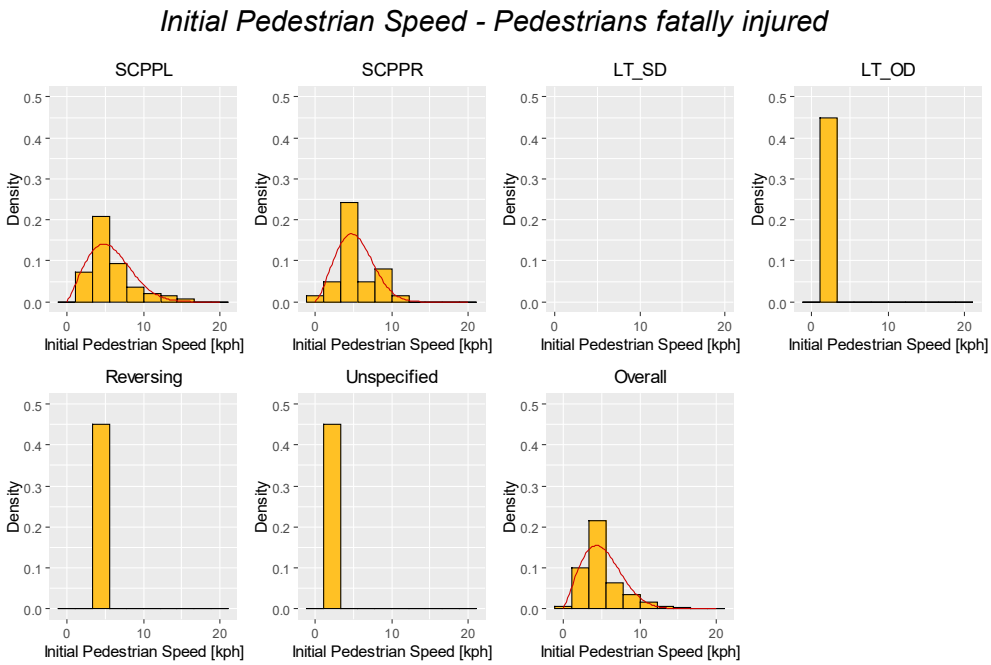

Figure 2-39 Fitted Weibull distribution to accident sample data for different detailed conflict situations for the initial pedestrian speed in pedestrian accidents with fatally injured pedestrians.

Table 2-17 Parameters of fitted Weibull distribution to accident sample data for different detailed conflict situations and different injury severities for the initial pedestrian speed in pedestrian accidents.

Situation	Severity	Number of Cases:	shape	scale	p-value
SCPPL	slight	111	2.02	7.61	0
SCPPR	slight	186	1.82	7.11	0
LT/SD	slight	15	2.23	6.93	0.306
LT/OD	slight	15	1.91	6.20	0.278
SD	slight	15	2.23	6.93	0.294
Reversing	slight	21	1.94	4.97	0.048
Unspecified	slight	16	1.45	6.97	0.016
Overall	slight	385	1.87	7.01	0
SCPPL	severe	30	1.90	7.48	0.136
SCPPR	severe	26	2.00	7.04	0.888
Overall	severe	73	1.95	7.06	0.038
SCPPL	fatal	63	2.16	6.43	0.002
SCPPR	fatal	28	2.41	5.92	0.938
Overall	fatal	126	2.14	5.81	0

With all the probabilities derived from the data and presented in this section it is now possible to determine the initial speeds for the pre-cash simulations for the vehicle and the VRU.

2.2.3.3 Road Conditions

In Figure 2-40 and Figure 2-41 a first analysis of road conditions based on CARE data is shown for car - pedestrian and car - cyclist accidents. Figure 2-42 shows the same for tram accidents based on the consolidated dataset consisting of Austrian, German and Latvian data.

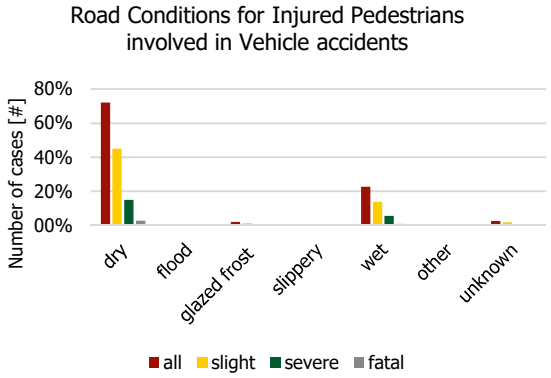

Figure 2-40 Road Conditions for Injured Pedestrians involved in Vehicle accidents based on CARE Data.

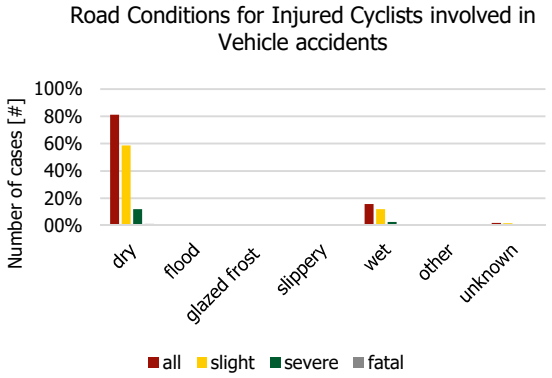

Figure 2-41 Road Conditions for Injured Cyclists involved in Vehicle accidents based on CARE Data.

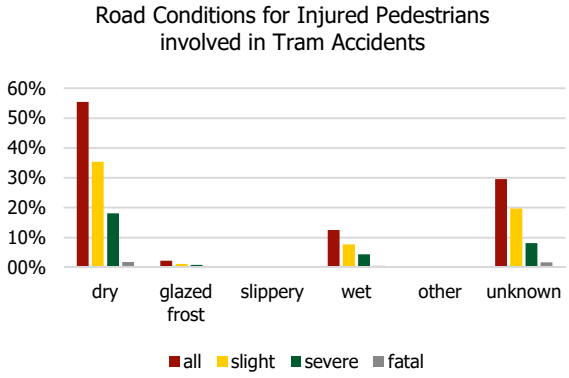

Figure 2-42 Road Conditions for Injured Pedestrians involved in Tram Accidents based on data from Austria, Germany, Switzerland and Latvia for the years 2010 to 2017.

The detailed probabilities for dry and non-dry roads are given in Table 2-18 and Table 2-19 for the different conflict situations and injury severities for car - pedestrian and cyclist accidents. As GIDAS, VOLVO, and CEDATU had applied slightly different classification systems for road conditions, it was decided to combine all categories not belonging to dry road conditions in the category "not-dry".

Table 2-18 Probabilities of dry and non-dry road conditions for different injury severities in pedestrian accidents per conflict situation for GIDAS, VOLVO and CEDATU.

	Slight		Severe		Fatal	
Road Condition	**dry**	**not dry**	**dry**	**not dry**	**dry**	**not dry**
SCPPL	61%	39%	74%	26%	55%	45%
SCPPR	71%	29%	59%	41%	69%	31%
SCPPLSD	100%	0%	100%	0%	100%	0%
SCPPLOD	0%	0%	0%	0%	0%	0%
SCPPRSD	0%	100%	100%	0%	100%	0%
SCPPROD	0%	0%	0%	100%	0%	0%
LT/SD	35%	65%	25%	75%	0%	0%
RT/SD	46%	54%	0%	100%	0%	0%
LT/SDLD	0%	0%	0%	0%	0%	0%
RT/SDRD	0%	0%	0%	0%	0%	0%
LT/OD	66%	34%	0%	0%	0%	100%
RT/OD	50%	50%	100%	0%	0%	0%
LT/ODLD	0%	0%	0%	100%	100%	0%
LT/ODRD	0%	0%	0%	0%	0%	0%
RT/ODLD	0%	0%	0%	0%	0%	0%
RT/ODRD	0%	0%	0%	0%	0%	0%
SD	67%	33%	20%	80%	75%	25%
Oncoming	64%	36%	33%	67%	67%	33%
Reversing	62%	38%	67%	33%	100%	0%
Stationary Pedestrian	72%	28%	67%	33%	100%	0%
Unspecified	70%	30%	50%	50%	50%	50%
Overall	65%	35%	60%	40%	65%	35%

Table 2-19 Probabilities of dry and non-dry road conditions for different injury severities in cyclist accidents per conflict situation for GIDAS, VOLVO and CEDATU.

	Slight		Severe		Fatal	
Road Condition	**dry**	**not dry**	**dry**	**not dry**	**dry**	**not dry**
SCPCROD	0%	0%	0%	0%	0%	0%
SCPCRSD	50%	50%	33%	67%	0%	0%
SCPCLOD	100%	0%	0%	0%	0%	0%
SCPCLSD	83%	17%	0%	100%	0%	0%
SCPCR	85%	15%	52%	48%	100%	0%
SCPCL	75%	25%	33%	67%	80%	20%
LT/OD	73%	27%	0%	100%	0%	0%
RT/OD	83%	17%	0%	100%	0%	0%
LT/SD	65%	35%	0%	100%	0%	0%
RT/SD	87%	13%	25%	75%	100%	0%
LT/ODLD	0%	0%	0%	0%	0%	0%
LT/ODRD	0%	0%	0%	0%	0%	0%
LT/SDLD	0%	0%	0%	0%	0%	0%
LT/SDRD	0%	0%	0%	0%	0%	0%
RT/ODLD	0%	0%	0%	0%	0%	0%
RT/ODRD	0%	0%	0%	0%	0%	0%
RT/SDLD	0%	100%	0%	100%	0%	0%
RT/SDRD	0%	0%	0%	0%	0%	0%
LT/RD	85%	15%	0%	100%	0%	0%
LT/LD	83%	17%	0%	100%	0%	0%
RT/RD	90%	10%	0%	100%	0%	0%
RT/LD	66%	34%	25%	75%	0%	0%
Oncoming	79%	21%	75%	25%	90%	10%
SD	83%	17%	27%	73%	78%	22%
Door	58%	42%	0%	100%	0%	0%
Reversing	83%	17%	50%	50%	0%	0%
Other	85%	15%	19%	81%	0%	0%
Overall	82%	18%	28%	72%	87%	13%

3 Future Accident and Impact Scenarios

Previous studies (Gruber *et al.*, 2019; Detwiller and Gabler, 2017) have shown that the introduction and anticipated market penetration of new active safety systems, such as autonomous emergency braking (AEB) (Cieślik *et al.*, 2019) will positively affect the impact scenarios of VRU - vehicle conflicts in the future. Such prospective analyses can only be performed by means of simulations although these types of systems have already been implemented in certain new cars. The average age of passenger cars on European roads is 11.1 years (ACEA, 2019), hence, it will take several years until the effect of new safety systems will be visible in accident databases.

In order to define future accident and impact scenarios, the analysis described in the previous chapter were used to derive a catalogue of VT scenarios, which are subsequently further simulated with and without an AEB system. The database analyses described in Section 2, and in particular the results of Section 2.2.3, determine the probabilities of VRU - vehicle conflict situations and their initial velocities.

The **VIRTUAL VRU Pre-crash Tool** has been developed as an open-source project for the generation of the VT scenario catalogue, as well as the simulation thereof. The description of the tool, the further creation of the scenario catalogue and scenario weighting according to the obtained accident investigations, are outlined in the first part of this section. In the second part the introduced methodology has been applied with the generated scenario catalogue (based on the database investigation). In order to determine future accidents and impact scenarios, the weighted simulated results of the baseline cases are compared with the AEB cases

3.1 Method

An overview of the method for the analysis of future impact scenarios is shown in Figure 3-1. The generation of VT scenarios, was based on the main accident influencing factors (initial velocity and conflict situation), which were described in Section 2.2.3. Simulations of determined VT scenarios have been carried out with the VIRTUAL VRU Pre-crash Tool. The method to determine future accidents and impact locations involves several components: a) Documents the scenario generation and simulation; b) Describes the main properties of the implemented active system (AEB) and its simulation parameters; c) Addresses the generation of the entire scenario catalogue based on variations of the main accident influencing factors; and d) Introduces methods to assess the effect of the active safety system on the generated scenario catalogue, and the methodology to weight the results according to their probability of occurrence.

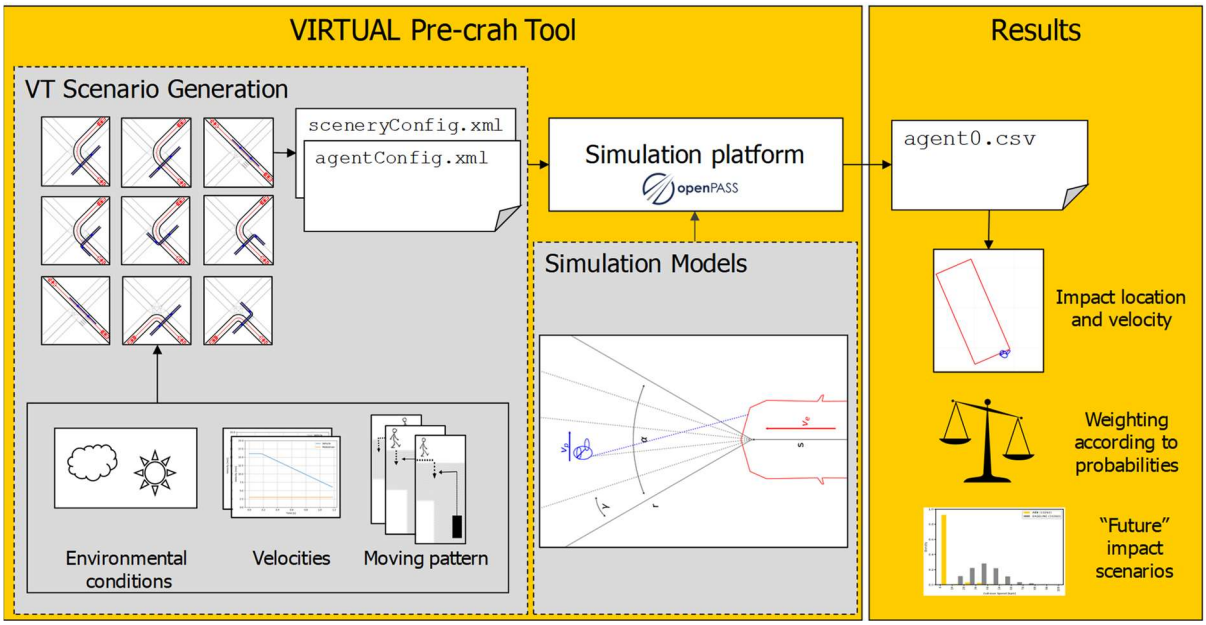

Figure 3-1: Overview of the method to derive future impact scenarios.

3.1.1 VIRTUAL VRU Pre-crash Tool

The developed VIRTUAL VRU Pre-crash Tool utilises the OpenPASS framework, which is an agent- based simulation environment, implementing driving physics and other environmental influencing factors. The OpenPASS framework is open-source and intends to harmonise the effectivity assessment of active safety systems. (Wang *et al.*, 2018; Dobberstein *et al.*, 2017).

Based on the identified requirements for the VIRTUAL project and the existing capabilities of the simulation platform, several functions have been extended and newly developed for the VIRTUAL VRU Pre-crash Tool. New features include scenario generation by using OpenDRIVE road layouts, AEB functions, pedestrian motion, data visualisation, and further assessment methods to compare results. The entire source code, to generate and simulate scenarios, is available on:
https://virtual.openvt.eu/wp-4/vru-precrash-tool

The VIRTUAL VRU Pre-crash Tool comprises four main parts, as shown in Figure 3-2 and defines the outline of this section:

1. **Simulation platform** (OpenPASS)
2. **Scenario generation**
3. **Simulation models**
4. **Scenario evaluation**

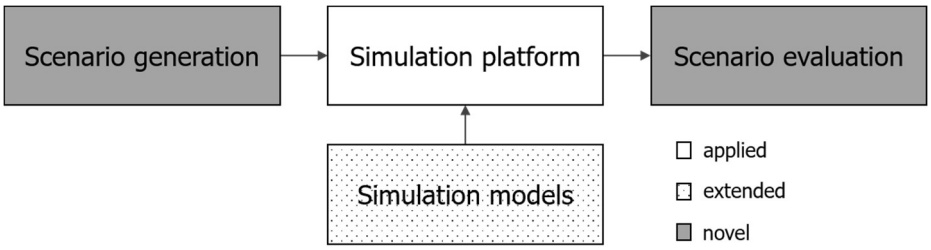

Figure 3-2: The primary components of the VIRTUAL VRU Pre-crash Tool.

A manuscript introducing the developed tool in detail has already been submitted to AAP (Schachner *et al.*, 2020)

Schachner, Martin; Sinz, Wolfgang; Thomson, Robert; Klug, Corina (2020): An open source framework to generate and evaluate potential safety-critical car - pedestrian scenarios based on road layouts. In: *Submitted*.

Abstract: This study describes a method to generate and evaluate a scenario catalogue, based on conflict situations. The scenario catalogue is the combination of OpenDRIVE road layouts (description of plausible paths according to different conflict situations) and potential motion profiles for both participants. This approach enables a relatively easy way to generate a large number of possible conflict scenarios for a specific road layout. In the proposed method, the scenarios are simulated with the open source framework OpenPASS. The simulation is based on a conventional two-track vehicle dynamics model with an implemented trajectory follower, which was equipped with a generic autonomous emergency braking (AEB) system. The AEB system intervenes in the event of an impending collision and affects the outcome of a baseline scenario. The comparison of the simulated results for different system setups thus allows the prediction of system capabilities to decrease the relative collision velocities and collision configurations such as the point of impact. In addition to the indicated change in the collision configuration, the study also identifies conflict situations less affected by the system. A particularly interesting finding is that some scenarios even became worsened by the AEB intervention in comparison to the baseline case. The implemented methods are open source, freely available, and thus allow a transparent evaluation of safety system. Replicable and flexible tools are needed for future use cases, such as studies on the effect of injuries using in-crash simulations and more detailed system models.

3.1.1.1 Simulation Platform

A simulation platform, has to be capable of modelling certain aspects of the physical reality, comprising information about the road network and other environmental influencing factors (Page *et al.*, 2015). Further, the platform has to be capable of modelling the dynamic behaviour of traffic participants, which consists of vehicle dynamics, sensors, safety systems and a driver model in the case of a car.

Within the simulation world, it is necessary for participants to interact dynamically to safeguard their behaviour is mutually influenced such that particular effects of safety systems can be assessed. Another prerequisite for a simulation platform is the simulation logic, which ensures correct scheduling of all traffic participants (internally referred to as agents) within the simulation.

The open source project under the Eclipse Public License, OpenPASS ("open platform for the assessment of safety systems") fulfils these requirements and has been selected as the simulation platform for the VIRTUAL VRU Pre-crash Tool, as it provides the necessary components of a "simulation platform" for the assessment of conflicts between VRUs and pedestrians. The simulation platform is also in line with the requirements for the effectiveness assessment of Advanced Driver Assistance Systems (ADAS) as

described by (Page et al. 2015). The authors (Wang *et al.*, 2018) (Dobberstein *et al.*, 2017) postulate further performance, flexibility and transparency as the three main properties of OpenPASS.

OpenPASS already incorporates the requirements of the Prospective Effectiveness Assessment for Road Safety (P.E.A.R.S.) project, as described by (Wang *et al.*, 2018).

The simulation platform is written in QT C++ programme and involves a rather complex but flexible code framework, which can be split into three main parts: **Core Framework**, **Scenario Modules** and **System Definitions**. The simulated dynamics are written to output files for each agent (*dataLog_0.csv, dataLog_1.csv* etc.) and can be used for further investigation of impact locations and velocities.

From a software developer point of view, the **Core Framework** involves various interfaces, datatypes and further mechanisms which guarantee the internal flexibility and extensibility. One central point of the core framework is the implementation of the scheduler, which executes all agents in a quasi-parallel manner, forwards the signals of the internal subsystems and thus guarantees the correct execution of the simulation.

Agents represent the dynamic traffic elements such as a vehicle or pedestrian, which are required be modelled in algorithmically, usually referred to as the **System Definitions**. Each agent is defined by its potential motion dynamics and may consist of subsystems. Users can define the characteristics for each agent to represent different capabilities and ADAS functions.

The **World Module** includes the logic to build a virtual simulation environment. The world is a central concept in the simulation, it is a container class, which stores all information within the simulation. Agents have access to continuously retrieve information from within this world description, such as current velocities, positions or distances to other agents. The world container also stores the entire history of the simulation and its intended future course, the target trajectory.

3.1.1.2 Scenario Generation

Particular focus was set on the methods to derive scenarios as input for the simulation environment. The generation of such a scenario is strongly connected to the *runConfiguration*, *sceneryConfiguration* and in particular to the trajectories defined in the input file for the simulation platform. Thus, the described methodology focuses mainly on the definition of "meaningful" (i.e., feasible) trajectories.

Accidents vary greatly in their appearance. They are affected by many different parameters throughout the entire event. In order to derive future accident scenarios, the influencing factors must be modelled in the simulation environment. The most relevant parameters for the pre-crash phase and their mapping to the simulation framework in form of their corresponding input files are highlighted Table 3-1

Table 3-1: Input parameters used in the VIRTUAL VRU Pre-crash Tool, highlighting the most important influencing factors based on the database investigation

Parameters	Related input	Name of variable
Deceleration	sceneryConfiguration	TargetTrajectory
Initial Speed Vehicle/VRU (v0)	sceneryConfiguration	TargetTrajectory
Collision Speed Vehicle/VRU t0	sceneryConfiguration	TargetTrajectory
Road condition	runConfiguration	Friction
Weather Condition	runConfiguration	Friction
Light Condition	runConfiguration	TimeOfDay
Conflict situation	sceneryConfiguration	TargetTrajectory

Speed and acceleration information define the agents' trajectories leading to a conflict. However, in order to describe full trajectories, path information must be included. The estimated initial paths (comprising motion history and the respective participant's intention) are stored together with a road layout. Paths cannot be compared easily among different accidents. One approach for coping with this issue, is to classify accidents in motion patterns (Lindman *et al.*, 2011; Lindman *et al.*, 2015), termed conflict situations, facilitating comparison of accidents based on the conflict situations. Section 2.1.2.2 describes the classification of conflict situations applied within the project.

In order to derive realistic paths and driving intentions, it is assumed that drivers and VRUs intend to use designated lanes to reach a certain target destination. The detailed method of finding a path based on the OpenDRIVE road layouts is described in (Schachner *et al.*, 2020). From the analysis of current accident scenarios (Section 2), the corresponding conflict situation (defining the path points) and the initial velocity of both, the vehicle and the VRU define the main influencing factors to generate the trajectories of the vehicle and the VRU as shown in Figure 3-3.

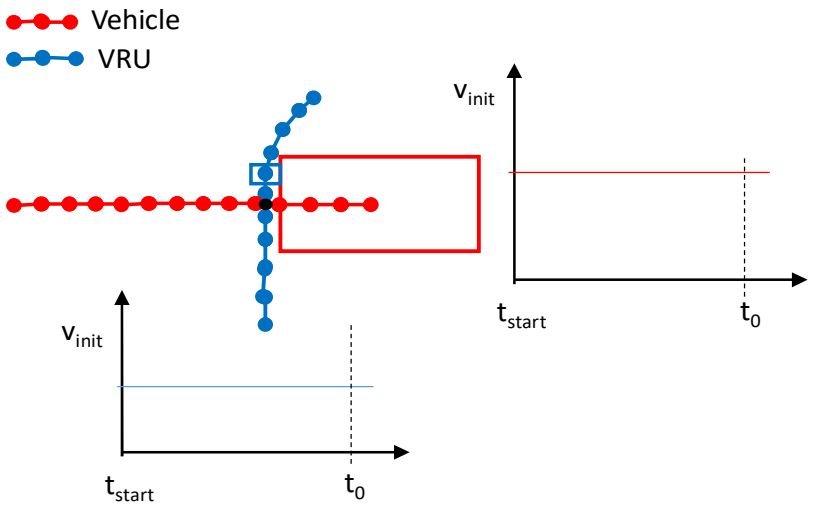

Figure 3-3 The target trajectory of the vehicle and the VRU can be generated based on the initial velocity and the path point and the conflict situation.

In order to generate scenarios compliant with the database investigations, they have to end in a collision in the baseline case, determined at the time t_0. In order to generate such scenarios, they are defined from a collision point between the VRU and the vehicle front. The vehicle front as modelled in the simulation environment is shown in Figure 3-4. The location of the collision point is determined relative to the centre of the front. The right front vehicle corner is thus determined as 50% of the vehicle width, while the left front corner is -50%. As shown in Figure 3-5, the collision point is defined as the mean distance of the intersection points between the vehicle front and the VRU contour.

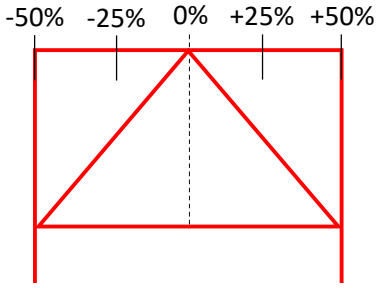

Figure 3-4 The collision point is defined as the distance from the centre of the vehicle front. The right front vehicle corner is thus determined as 50% resp. 0.5, for the left front corner this is -50% resp. -0.5.

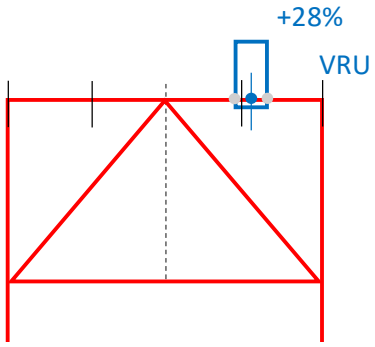

Figure 3-5 The collision point is defined as the mean distance of the intersection points between vehicle front and the VRU contour.

To generate an impact scenario, it is necessary to select the corresponding motion states such that the VRU and the vehicle meet at the predefined collision point at time t_0. In order to do so, the respective path points of the collisions must be found. Therefore, an algorithm, comprising four steps as shown in Figure 3-6, has been developed.

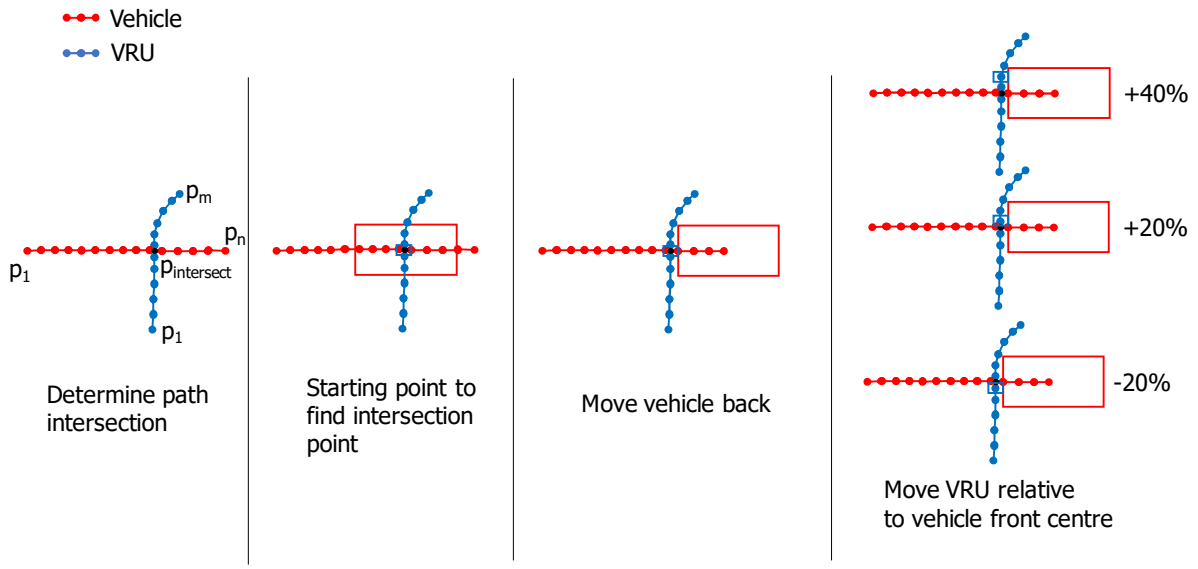

Figure 3-6: The methodology to determine the collision point between the vehicle and the VRU. In the initial step, both paths are intersected to derive the point $p_{interscet}$. The vehicle is moved backwards along the path until the two contours stop intersecting each other. The VRU is further moved in the direction of the target collision point.

Path Intersection

Due to the design of the OpenDRIVE road layout descriptions, it is possible to derive path points for the conflict situation in arbitrary granularity. For the scenario generation, a point magnitude of 0.1 [m] was used. Since the path p is described by means of connected points p_i, p_j, it is necessary to find the segment of the overlapping points. The exact intersection point is usually not directly part of the derived path and hence additionally inserted as $p_{intersect}$ into both paths.

Finding the Contour Intersection

The vehicle is first moved backwards to the index, where the object contours still overlap each other. From this point the VRU is moved towards the intended collision point. The trajectory is determined by the angle δ between the intended VRU path vector, and the vector from the current collision point to the target point, as shown in Figure 3-7.

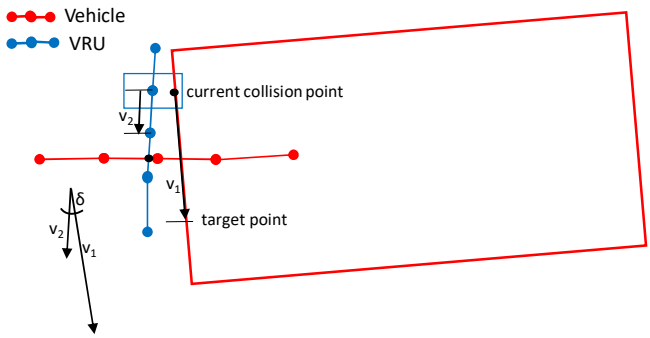

Figure 3-7: The trajectory definition for the collision point between the vehicle and VRU.

Move Vehicle and VRU to Meet Collision Point Configuration

For each path point, the distance to the target point is checked. The VRU is moved in the intended direction. If the relative distance is under a certain threshold, the algorithm terminates and the collision configuration (collision indices on the path) is found. The velocities are subsequently generated from these indices using motion states. The concept of motion states is described further in the following section. The algorithm to determine the indices of the VRU and the vehicle at time t_0 can be found in Appendix C.2.

Motion States

To generate trajectories from the obtained collision point, the initial–collision speeds of the VRU and vehicle are utilised. The deceleration/acceleration from the initial to the collision speed describes the entire dynamics of the VRU and vehicle prior to the collision. The time t_{start} results from the minimum length of the extracted paths of the VRU and the vehicle, and the applied dynamics (initial/collision speed and acceleration), which has been limited to -10[s] to avoid unnecessarily long simulation times. The determined trajectory is inverted, meaning that t_{start} is zero and the collision time t_0 is the time required for all pre-collision kinematics until the time of collision. An example motion sequence and the corresponding times t_0 and t_{start} are shown in Figure 3-8.

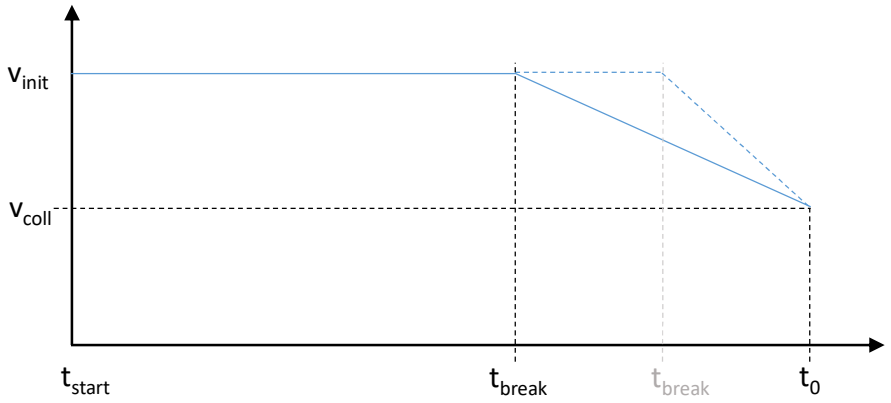

Figure 3-8: Exemplary visualisation of the velocity profile, which is determined theoretically by the initial and collision velocity, as well as the deceleration/acceleration prior to the collision.

3.1.1.3 Simulation Models

Table 3-2 lists the relevant modules for the implementation of the VIRTUAL VRU Pre-crash Tool. The table also shows which components of the code remained unchanged from the original OpenPASS framework, components modified and implemented specifically for the VIRTUAL VRU Pre-crash Tool. The detailed description of these newly developed components in OpenPASS has been submitted in a manuscript to AAP (Schachner *et al.*, 2020).

Table 3-2: Overview of the components of the simulation models in the VIRTUAL pre-crash simulation platform

Original OpenPASS Components	Modified OpenPASS Components	New Components
Ego_Sensor	Algorithm_Selector	Ideal_Object_Detector
Init_Agent		Algortihm_Brake_Assistant
AlgorithmicTrajectory_Follower		Pedestrian_Trajectroy_Follower
Dynamic_TwoTrack		
SensorCollision		
DynamicsCollision		

3.1.1.4 Visualisation and Evaluation of Scenarios

The simulation output is written to a .csv file, containing information about the observed state, information containing the agent position (x, y) in the global coordinate system, velocity v as well as the yaw angle ψ for each simulated time step. The control signals (throttle, brake, steering), as calculated by the *algorithmic_selector*, are also written to the output files, as well as the time to collision (TTC) calculated by the *algorithm_brake_assistant* and the occurrence of a collision.

The output information is used to visualise the simulated results, to observe possible system malfunctioning or to investigate the reasons why a collision occurred in the scenario. The visualisation uses the *plot.ly* framework, which utilises JavaScript for the front end visualisation. Using this type of framework provides three particular advantages:

- The JavaScript engine, in combination with the respective frameworks allows a high degree of interaction between the user and the respective application.
- Web applications can be easily developed and deployed, since the JavaScript frameworks are continuously being enhanced.
- HTML content allows interpretation of the data visualisation by any web browser. Thus, sharing information does not require any additional software components and is relatively user friendly.

A sample layout including the driving trajectories is shown from top view on the left side of Figure 3-9, showing the contour of both the vehicle and the pedestrian. Additionally, the sensor view of the *ideal_object_detector* has also been sketched, to further provide insight into the simulated scenario and draw conclusions about the functionality of each respective ADAS system.

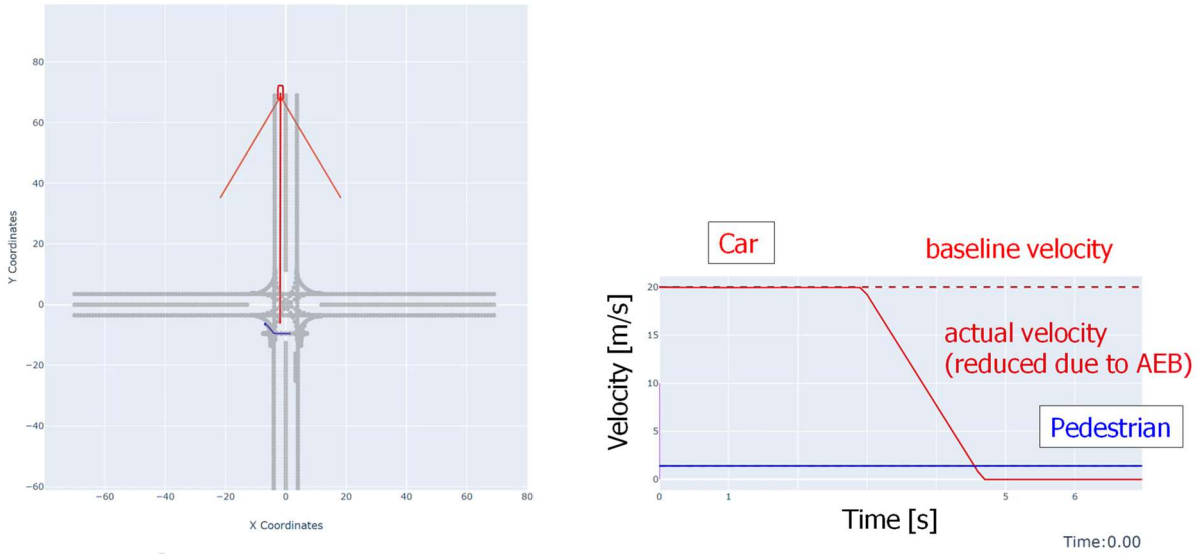

Figure 3-9: Visualisation of pre-crash simulation results with the VIRTUAL Pre-crash Tool.

The reason for developing the visualisation is due predominantly to developed debugging. In case of an unavoidable accident (i.e., a collision between vehicle and VRU) the .csv file also contains information about the collision time $t_{collision}$.

3.1.2 Conceptual AEB System

A conceptual AEB system, modelled on previous studies (Gruber *et al.*, 2019; TRL *et al.*, 2018; Barrow *et al.*, 2018), was applied.–A geometric sensor with a range of 80 m and a field of view of 60° was positioned 0.25 m behind the most frontal point of the vehicle (2.2 m ahead of vehicle CoG). The VRU was detected when fully in view for 150 ms while braking was induced when the TTC was ≤ 1s. The geometric sensor was modelled with an azimuthal resolution of 0.5° and a time resolution of 10 ms. After the brake delay, the acceleration was increased in line with the braking gradient until the maximum acceleration (depending on road friction) was reached.

Table 3-3: Parameters of the conceptual AEB System.

Sensor range [m]	Field of view (sensor angle) [°]	Acquisition time [s]	TTC threshold [s]	Azimuthal resolution [°]	Brake delay [s]	Braking gradient [m/s³]
60	60	0.15	1.0	0.5	0.2	36.0

3.1.3 Simulation Matrix

The VT catalogue was created from the analysis of current accident scenarios. Therefore, only a subset of all possible conflict situations has been considered for different injury severities. In order to define meaningful trajectories, the initial velocity of the VRU and the vehicle have been considered together with each defined type of conflict situation and varying baseline collision points. The simulated trajectories were simulated with different friction coefficients of **dry** and **wet** road conditions (μ: 0.5 and 0.8) (Warner *et al.*, 1983), and with and without the AEB system.

Table 3-4: Parameters for the generated scenarios

Trajectory definition	Environment
Vehicle Initial Velocity	Friction Coefficient μ
VRU Initial Speed	
Conflict Situation	
Collision Points	

The initial velocities for both the VRU and the vehicle have been selected in constant percentile steps of the cumulative Weibull distribution, which are described within the database analysis in Section 2.2.3.2. For each conflict situation, 19 initial velocities (5th to the 95th percentile of the initial speeds in 5 percentile steps) of the vehicle and nine initial velocities (10th to the 90th percentile in 10 percentile steps) of the VRU were combined. Additionally, the conflict point between the VRU and the vehicle front has been varied as described in Section 3.1.1.2. Steps between -0.4 and 0.4 have been used with a step size of 0.2. for the vehicle and 10 percentile steps for the VRU. Hence, a total of 1,710 impact scenarios resulting in a conflict with the vehicle front per conflict situation, has been included in the simulation matrix.

3.1.3.1 Catalogue of Virtual Pedestrian - Car Scenarios

In order to define the trajectories for the different conflict situations, a meaningful road layout facilitating the identification of paths for both the pedestrian and the car was established. Figure 3-10 shows the utilised OpenDRIVE road layout, a generic standard junction based on Euro NCAP test protocol (Euro NCAP, 2019), expanded by additional pavements and pedestrian crossings.

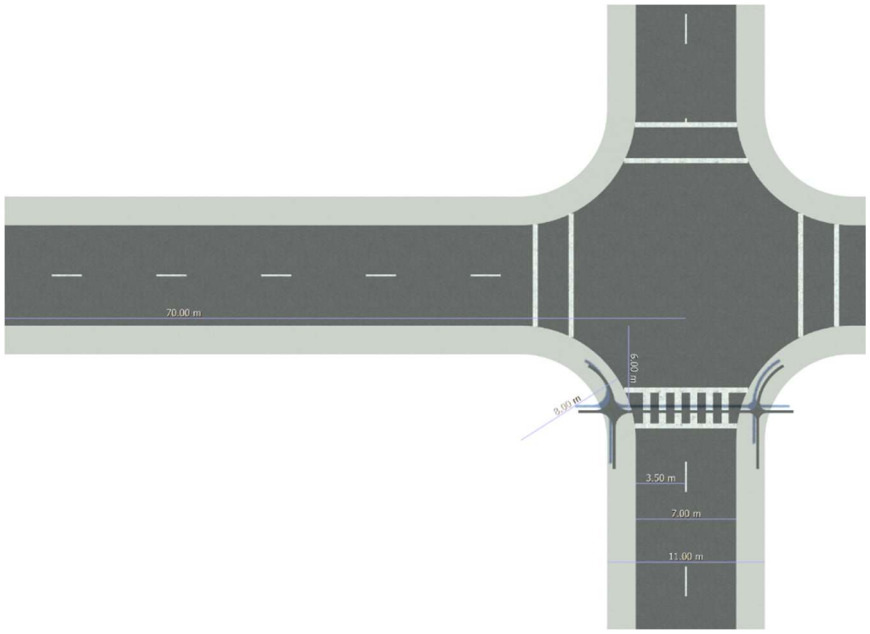

Figure 3-10: The OpenDRIVE road layout, able to define car - pedestrian conflict situations, in line with the generic crossing of the Euro NCAP test protocol (Euro NCAP, 2019).

Table 3-5 shows the derived paths for the considered car - pedestrian conflict situations. A complete table for all derived paths, with respect to the car – pedestrian conflict situations (Lindman *et al.*, 2011), can be found in Appendix D.1.

Table 3-5: Overview of considered car - pedestrian conflict situations. Paths are retrieved with the start and end ID of the road identifiers of each respective OpenDRIVE file.

Conflict Situation	Pictogram (Lindman *et al.*, 2011)	ID Start-End Road	Derived paths
Straight Crossing Path, pedestrian from left (SCPPL)	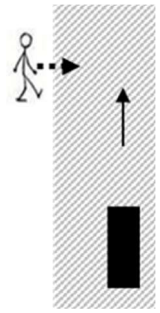	Vehicle: 2 – 3 Pedestrian: 6 – 4	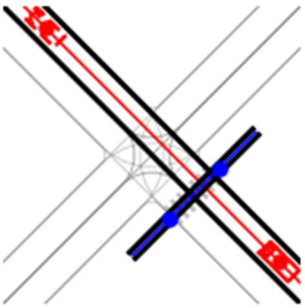
Straight Crossing Path, pedestrian from right (SCPPR)	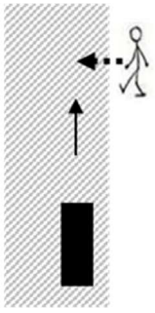	Vehicle: 2 – 3 Pedestrian: 4 - 6	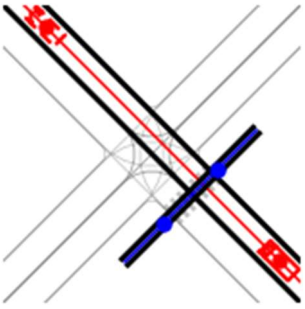

3.1.3.2 Catalogue of Virtual Cyclist - Car Scenarios

In order to define the trajectories for the different cyclist - car conflict situations, a meaningful road layout facilitating the identification of paths for both the cyclist and the car was established. Figure 3-11 shows the developed OpenDRIVE road layout, a generic standard junction, which has been expanded by additional bicycle lanes and crossings.

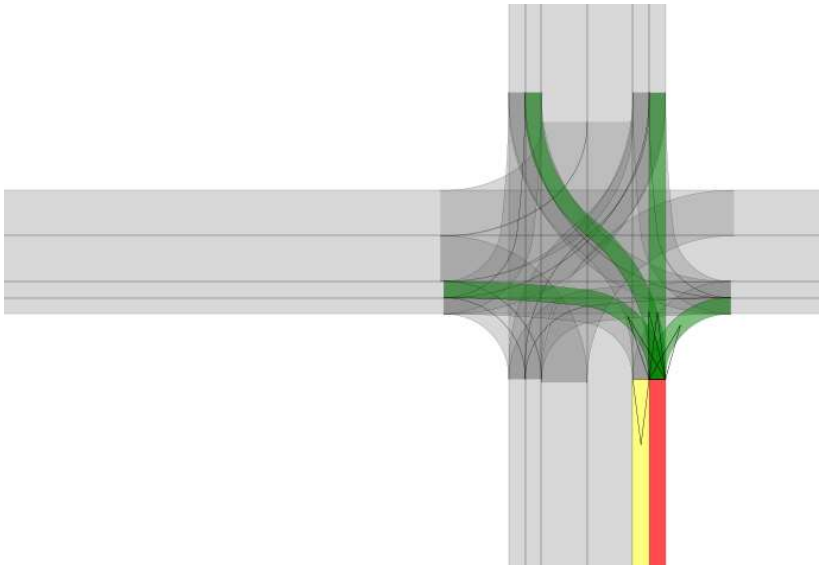

Figure 3-11: OpenDRIVE layout of the cyclist junction.

Table 3-6 shows the derived paths for the considered cyclist - car conflict situations. A complete table for all derived paths, with respect to the cyclist - car conflict situations (Lindman *et al.*, 2015), can be found in Appendix D.2.

Table 3-6 Overview of considered car - cyclist conflict situations. Paths are retrieved with the start and end ID of the road identifiers of each respective OpenDRIVE file.

Conflict Situation	Pictogram (Lindman *et al.*, 2011)	ID Start-End Road	Derived paths
Straight Crossing Path, cyclist from right (SCPCR)	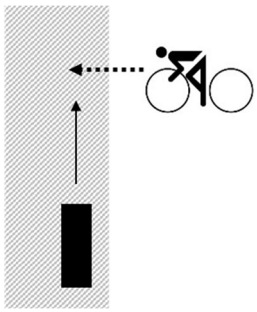	Vehicle: 0 – 1 Cyclist: 6 – 2	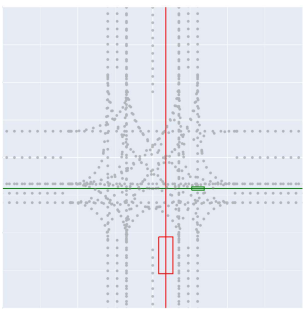
Straight Crossing Path, cyclist from left (SCPCL)	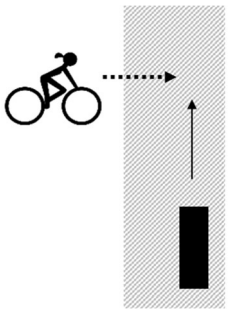	Vehicle: 0 – 1 Cyclist: 2 – 6	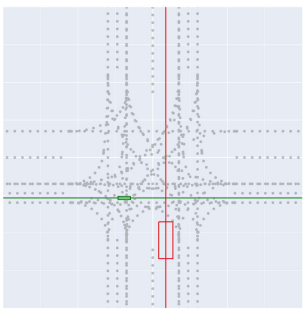

3.1.3.3 Catalogue of Virtual Pedestrian - Tram Scenarios

The generic junction used for the definition of pedestrian - tram scenarios is shown in Figure 3-12.

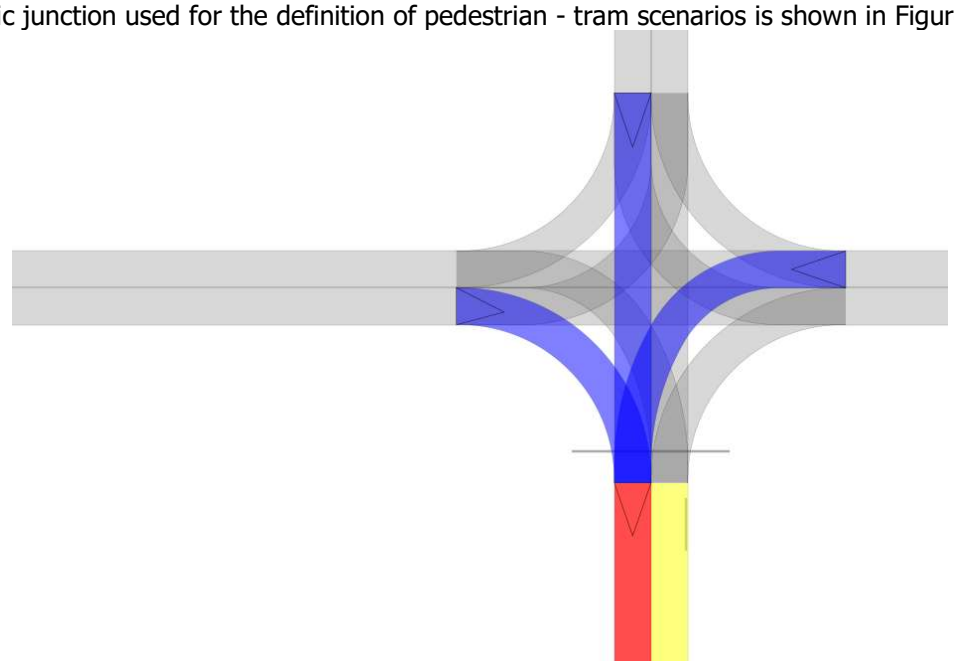

Figure 3-12 OpenDRIVE layout of the pedestrian - tram junction.

An example of the derived conflict situation is shown in Table 3-7.

Table 3-7: Example of simulated tram - pedestrian conflict situations. Paths are retrieved with the start and end ID of the road identifiers of the respective OpenDRIVE file.

Conflict Situation	**Pictogram** (Lindman *et al.*, 2011)	**ID Start-End Road**	**Derived paths**
Straight Crossing Path, pedestrian from right (SCPPR)	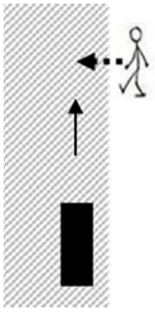	Vehicle: 2 – 3 Pedestrian: 4 - 6	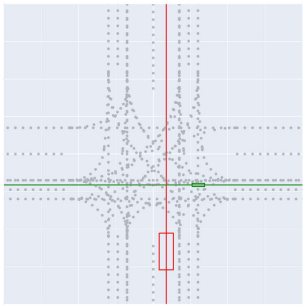
Straight Crossing Path, pedestrian from right (SCPPL)	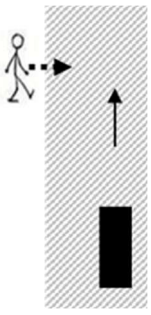	Vehicle: 2 – 3 Pedestrian: 6 - 4	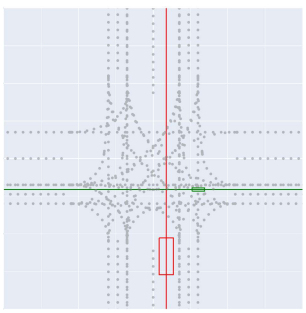

In comparison to the pedestrian/cyclist - car conflicts the database investigations did not reveal a distribution of initial velocities with respect to a certain injury severity. Hence, the initial velocities have been assumed to be equally distributed in a range from 10 km/h to 50 km/h (using 19 equally distributed velocity values). The same has also been applied for initial pedestrian speeds, ranging from 2 km/h to 11 km/h (using nine equally distributed velocity values).
For the friction coefficients, a value of μ: 0.5 has been selected which corresponds to an emergency brake with magnetic pads, sanding, etc. The derived trajectories have further been simulated with and without the AEB system.

3.1.4 Data Analysis

Collision speeds and impact positions of the baseline simulations (vehicle without the generic AEB system) were analysed. Therefore the results follow the initial distributions of the database analysis and hence the corresponding simulation matrix, as described in Section 3.1.3. These baseline results have been further compared with the results of the AEB cases (vehicle equipped with the conceptual AEB system as described in Section 3.1.2). The collision speed $v_{collision}$ is defined as the vehicle speed at the time when the vehicle first intersects the VRU shape. For the analysis of $v_{collision}$ a step size of 10 km/h has been chosen.

In order to determine future accident scenarios and their impact configurations holistically, the database investigations must be included into the data analysis, as done in Section 2.2.3. Therefore a weighting methodology has been developed to derive the probability of the generated scenarios.
As shown in Figure 2-5, the probabilities of the influencing parameters (conflict situation (CS), the initial velocity of the vehicle and the VRU (v_{veh}, v_{VRU}) and the road condition (RC)) are conditionally dependent (i.e., derived with a certain precondition, on the injury severity (IS), for instance). In order to determine the probability of a testing scenario Equation 3-1. has been used.

$$p(testing_scenario) = p(conflict_situation) * p(v_{veh}) * p(v_{vru}) * p(road_{condition}) \quad 3\text{-}1$$

$$p(testing_scenario) = p(IS) * p(CS|IS) * p(v_{veh}|CS, IS) * p(v_{vru}|CS, IS) * p(RC|CS, IS) \quad 3\text{-}2$$

The probability of the initial velocities for the VRU and the vehicle are considered by the simulation matrix (Weibull cumulative density function in 5% and 10% steps), meaning that the simulated velocities represent the observed distributions from the accident analysis. This is however not the case for the observed road conditions of the database analysis, as shown in Table 2-17. The road conditions have been initialised equally distributed within the simulation matrix (each scenario was run once with baseline and once with reduced friction).

$$p(v_{coll} = x) = \sum_{i=1}^{m} p\left(v_{coll_i} = x\right) p(\mu_i) \quad 3\text{-}3$$

In order to consider this environmental effect, the observed results have been discretised (10km/h steps for the collision velocity $v_{collision}$). These discretised distributions have further been weighted according to the overserved road condition probability.

Figure 3-13 and Figure 3-14 show exemplary the weighting procedure for the conflict situation SCPPL for slight injury severities. The simulated results (collision velocity) can be seen in the Figure 3-13. The distribution between **not dry** (wet, icy, snowy,..) and **dry** road conditions is 0.39 and 0.61, respectively. Figure 3-14 shows the weighted probability distribution for the collision velocity of the conflict situation

SCPPL, slight injuries. For the not dry scenarios, collision velocities up to 30 km/h and for the dry scenarios, collision velocities up to 10 km/h were observed. In the combined results, velocities up to 30 km/h are probable, but less likely than **not dry** scenarios.

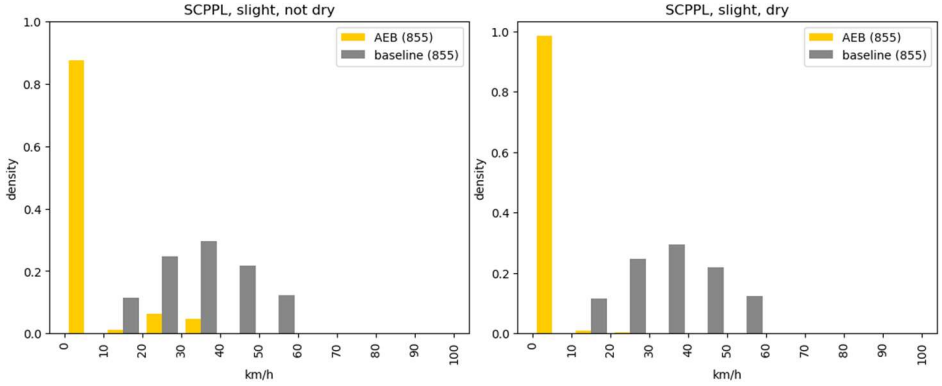

Figure 3-13: The simulated discretised collision velocity distribution for the baseline and the AEB cases, for dry (μ=0.8) and not dry (μ=0.5) road conditions.

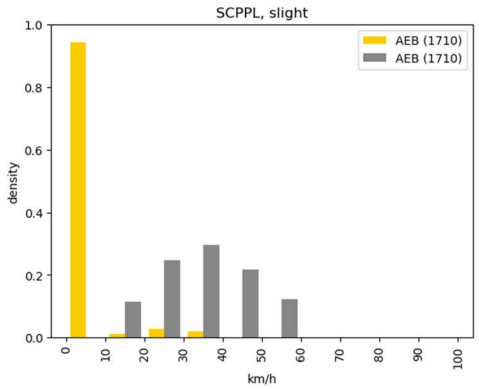

Figure 3-14: The weighted result collision velocity according to the probability of the road conditions.

This method has further been applied to cluster each conflict situation with respect to the observed probability and further to weight the collision velocity for the different injury severities.

The baseline testing scenarios are based on current accident data. Due to the simulations with a virtual AEB system, these same scenarios can either be avoided or lead to an accident. The probability of avoiding a testing scenario can be summarised by using the probabilities of each testing scenario, that did not lead to a collision between vehicle and VRU.

$$p(avoided_scenario) = \sum_{i=1}^{m} p(testing_scenario_i) \quad 3\text{-}4$$

For each unavoidable testing scenario that led to an accident, a collision velocity of the vehicle and an impact location of the VRU, relative to the vehicle is obtained. The probabilities of scenarios which led to $v_{collision_k}$ at $location_impact_j$ are summarised to reach the probability of a specific impact scenario, described with Equation 3-5.

$$p(collision_scenario_1) = \sum_{i=1}^{m} p\left(testing_scenario_i \ , v_{collision_k}, location_impact_j\right) \quad 3\text{-}5$$

3.2 Results

A large number of scenarios for different conflict situations and different injury severities can be generated by applying the introduced simulation approach This section has been categorised into results for pedestrian - car conflicts and cyclist - car conflicts.

For both types, examples of future accident configurations for the conflict situations **SCPPL/SCPCL** and **SCPPR/SCPCR** were evaluated. These conflict situations have been selected due to their frequency and the availability of data in the different injury severity classes: **slight**, **severe** and **fatal.** For the assessment, each scenario was simulated with and without the AEB system, which have been further denoted as AEB and baseline cases. The scenario assessment was performed with respect to **impact location** and emerging **collision velocities**. All other results have been summarised in two manuscripts, awaiting submission once the manuscript outlining the VIRTUAL pre-crash simulation tool has been published (submitted at time of deliverable submission).

3.2.1 Future Pedestrian - Car Accident Scenarios

The treatment simulation results of the VT scenarios representing SCPPL and SCPPR conflict situations are summarised in Table 3-9. The results are graphically presented in Figure 3-15 - Figure 3-20. Due to the applied generic AEB system, the majority of SCPPL and SCPPR baseline test scenarios were avoided in the simulations. No AEB intervention and therefore no change of the baseline scenario was observed in a maximum of 1% of the scenarios. A drastic reduction in the collision velocity was observed in cases with AEB intervention without no crash avoidance.

Table 3-8: Overview of the effect of a generic AEB system on SCPPL and SCPPR pedestrian - car conflict situations

		Slight		Severe		Fatal	
		SCPPL	SCPPR	SCPPL	SCPPR	SCPPL	SCPPR
Conflicts	Baseline	1710	1710	1710	1710	1710	1710
	AEB	120	67	410	174	642	654
	Shift [%]	-93.0	-96.1	-76.0	-89.8	-62.5	-61.8
V_coll[m/s]	Baseline	9.7	9.2	13.5	10.9	16.1	15.6
	AEB	7.5	6.8	10.3	8.6	11.7	12.0
	Shift [%]	-23.4	-26.3	-23.6	-21.1	-26.9	-22.7
AEB avoidance							
	Conflicts	1590	1643	1300	1536	1068	1056
Reduced collision velocity by AEB							
	Conflicts	100	53	408	168	642	654
V_col [m/s]	Baseline	14.6	13.8	17.7	15.7	19.2	19.8
	AEB	7.9	7.3	10.3	8.7	11.7	12.0
	Shift [%]	-45.5	-47.3	-41.7	-44.8	-38.8	-39.2
No AEB intervention							
	Conflicts	20 (1.2%)	14 (0.8%)	2 (0.11%)	6 (0.35%)	0 (0.0%)	0 (0.0%)

3.2.1.1 Impact Locations

The distribution of the impact locations is shown in Figure 3-15 - Figure 3-17. The impact location (baseline collision point) between VRU and vehicle in the baseline case was assumed to be equally distributed among all the generated scenarios. For the simulations with AEB treatment, the impact location shifted towards the right side of the vehicle front (-40%) for all SCPPL scenarios and to the left for (+40%) for SCPPR scenarios.

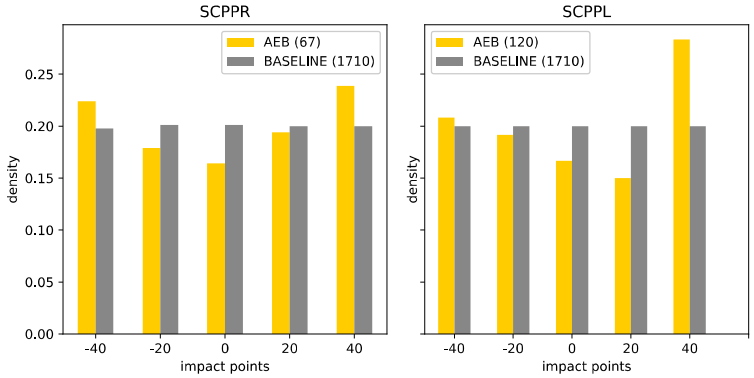

Figure 3-15: Distribution of the impact locations for slight conflict scenarios, between cars and pedestrians. The baseline is shown in grey and the AEB cases in yellow.

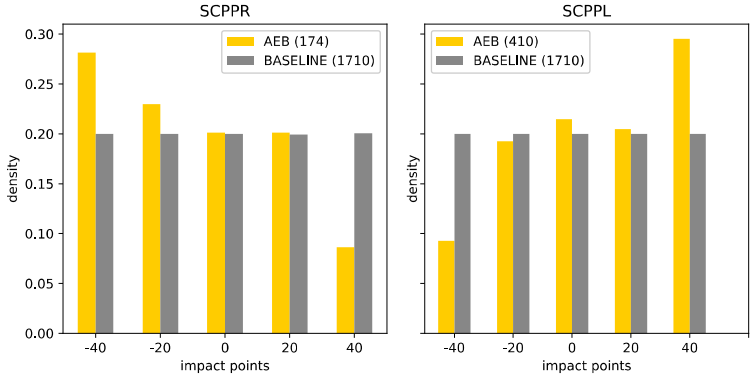

Figure 3-16: Distribution of the impact locations for severe conflict scenarios, between cars and pedestrians. The baseline is shown in grey and the AEB cases in yellow.

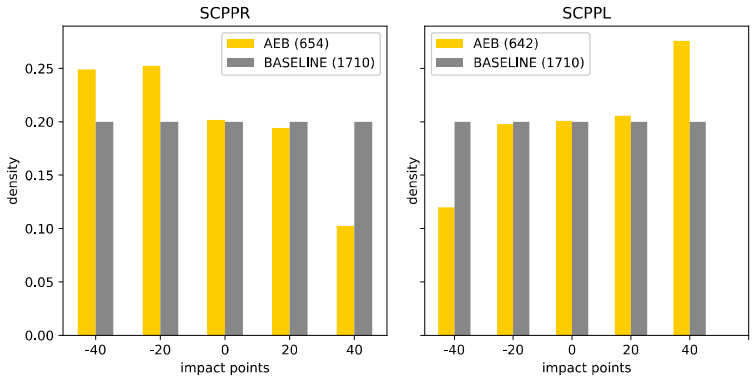

Figure 3-17: Distribution of the impact locations for fatal conflict scenarios, between cars and pedestrians. The baseline is shown in grey and the AEB cases in yellow.

It has been observed that the shift in impact location for severe and fatal accidents has been moved towards the side of the vehicle opposite to the approaching side of the VRU (the left half of the vehicle for scenarios in which the VRU is approaching from the right). This seems reasonable, due to the emergency brake allowing the pedestrian to move further across the vehicle before impact.

(i.e. to the left side for scenarios in which the VRU is approaching from the right). This seems reasonable, due to the emergency braking giving the pedestrian time to move further across the front of vehicle before impact.
However, for slight injuries the opposite trend has been detected (i.e., a higher number of impacts on the same side of the vehicle, from which the pedestrian is originally approaching), which can be explained mainly by the different ratio between vehicle and VRU speed compared to the more severe scenarios. This issue can lead to scenarios leaving pedestrians undetected by the sensor, as shown exemplary in Figure 3-25, and for slight scenarios exposing pedestrians to later detection. It is more likely that accidents will be avoided when the pedestrian has already almost passed the vehicle (i.e., the pedestrian is on the right edge when originally approaching from the left). A higher number of slight injury scenarios was observed for injuries without AEB intervention compared to the more severe baseline scenarios, shown in Table 3-8.

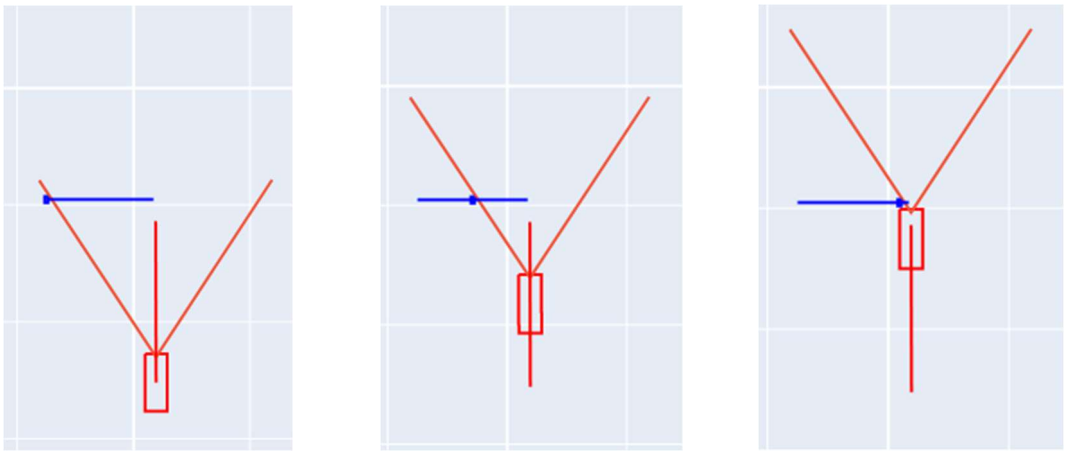

Figure 3-18: VRU to vehicle scenario, in which the VRU is not detected by the sensor because the speed of the VRU is equal to the vehicle speed.

3.2.1.2 Collision Velocities

The distributions of the collision velocity for the pedestrian - car conflict situation, SCPPL and SCPPR, was weighted with respect to the road condition distribution for each injury severity. The results are shown in Figure 3-20 - Figure 3-21. The mean collision velocity was reduced in the analysed conflict situations and for all (baseline) accident severities. The baseline distributions are based on the Weibull functions for each respective accident severity. The yellow bars on the left side showing 0 km/h represent the avoided AEB cases.

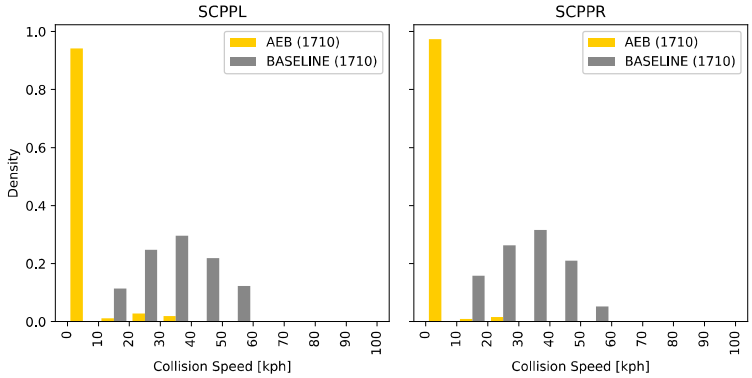

Figure 3-19: Distribution of collision velocities for slight conflict scenarios, between cars and pedestrians. The baseline is shown in grey and the AEB cases in yellow.

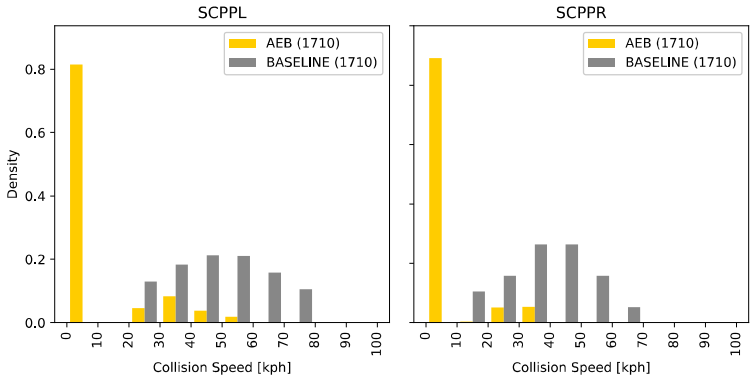

Figure 3-20: Distribution of collision velocities for severe conflict scenarios, between cars and pedestrians. The baseline is shown in grey and the AEB cases in yellow.

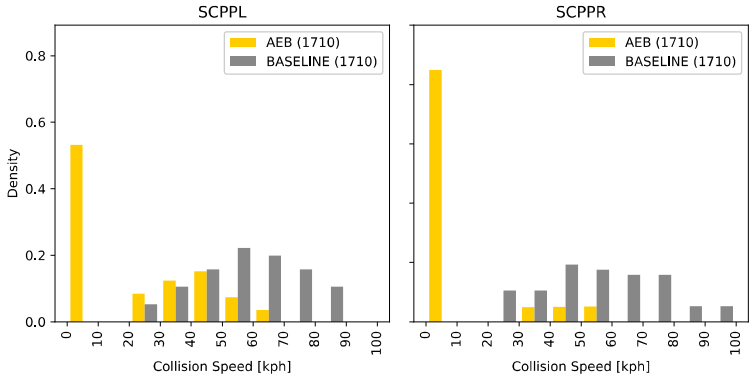

Figure 3-21: Distribution of collision velocities for fatal conflict scenarios, between cars and pedestrians. The baseline is shown in grey and the AEB cases in yellow.

The collision distributions for the conflict situation SCPPL and SCPPR have been further combined according to the weighting schema (described in Section 3.1.4). The probability of a certain conflict situation as shown in Table 2-13, was utilised for the weighting. Figure 3-22 shows the weighted distribution of the collision velocity for different injury severities.

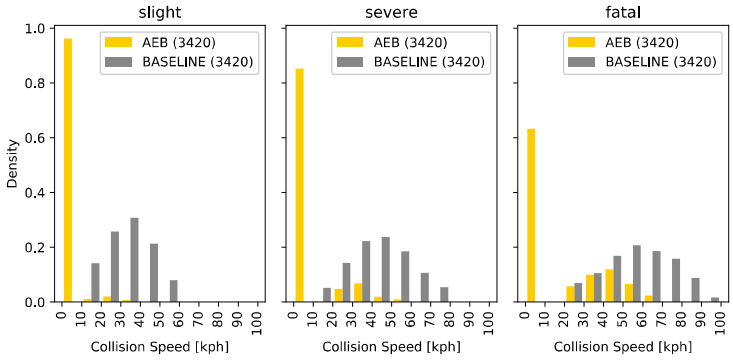

Figure 3-22 Weighted collision velocity for the slight, severe and fatal injuries for car - pedestrian conflicts.

The weighted distribution, with respect to the injury severity (shown in Table 2-13), for the overall collision velocities for car - pedestrian conflicts is shown in Figure 3-23.

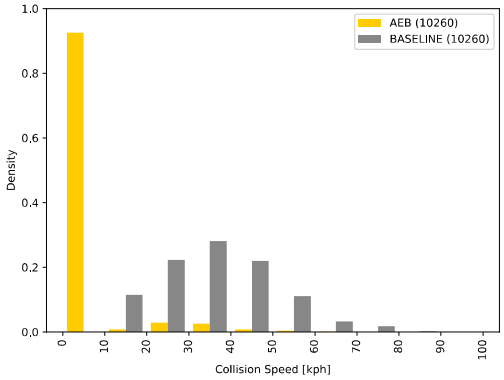

Figure 3-23 Overall weighted collision velocity distribution for car - pedestrian conflicts.

3.2.2 Future Cyclist - Car Accident Scenarios

The treatment simulation results of the VT scenarios representing SCPCL and SCPCR conflict situations are summarised in Table 3-9. The results are graphically presented in Figure 3-26.
Between 31.3% (fatal SCPCR scenarios) and 75% (severe SCPCR scenarios) of the baseline test scenarios were avoided in the simulations, due to the AEB system. No AEB intervention and therefore no change of the baseline scenario was observed in up to 13% of the scenarios. Cases with intervention, without avoidance, showed a drastic reduction in collision velocity.

Table 3-9: Overview of the effect of generic an AEB system on SCPCL and SCPCR cyclist - car conflict situations.

		Slight		Severe		Fatal	
		SCPCL	SCPCR	SCPCL	SCPCR	SCPCL	SCPCR
Conflicts	Baseline	1706	1529	1710	1710	1710	1710
	AEB	721	635	615	428	625	1174
	Shift [%]	-57.7	-58.5	-64.0	-75.0	-63.5	-31.3
V_coll [m/s]	Baseline	8.6	8.1	11.1	11.5	13.8	19.5
	AEB	7.0	6.7	7.8	7.5	9.7	12.5
	Shift [%]	-18.5	-17.8	-29.5	-34.8	-29.6	-36.2
AEB avoidance							
	Conflicts	985	894	1095	1282	1085	536
Reduced collision velocity by AEB							
	Conflicts	493	427	152	366	577	1174
V_col [m/s]	Baseline	8.1	7.9	11.9	14.6	17.8	21.0
	AEB	6.7	6.5	7.7	7.5	9.9	12.5
	Shift [%]	-17.4	-17.8	-35.7	-48.4	-44.2	-40.7
No AEB intervention							
	conflicts	228 (13.4%)	208 (13.6%)	152 (8.9%)	62 (3.6%)	48 (2.8%)	0 (0%)

3.2.2.1 Impact Locations

The effect of the AEB system on impact location is shown in Figure 3-24 - Figure 3-26. A similar trend, as for the pedestrian conflicts, is visibly showing a slight shift towards the left for SCPCL and to the right for SCPCR conflict situations.

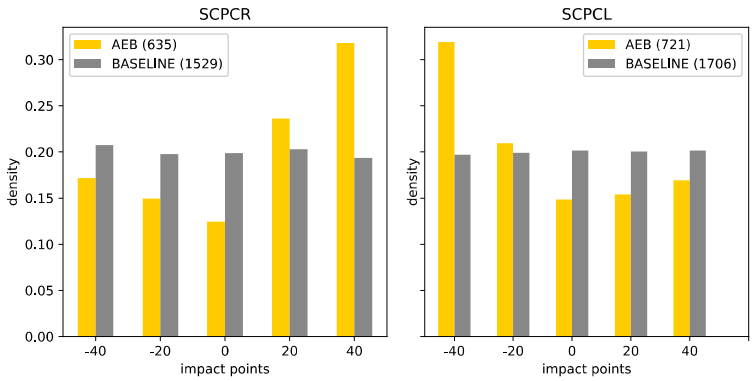

Figure 3-24: Distribution of the impact locations for slight conflict scenarios, between car and cyclist. The baseline is shown in grey and the AEB cases in yellow.

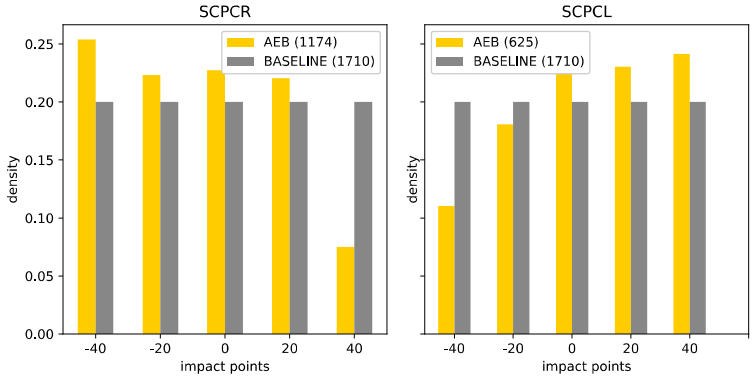

Figure 3-25: Distribution of the impact locations for severe conflict scenarios, between car and cyclist. The baseline is shown in grey and the AEB cases in yellow.

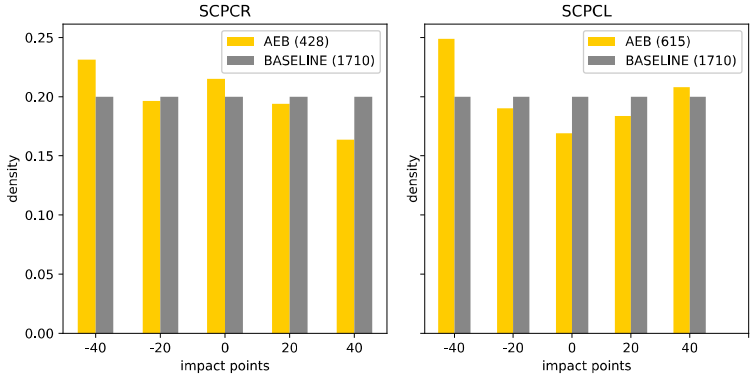

Figure 3-26: Distribution of the impact locations for fatal conflict scenarios, between car and cyclist. The baseline is shown in grey and the AEB cases in yellow.

3.2.2.2 Collision Velocities

The distributions of the collision velocity for the pedestrian - car conflict situation SCPCL and SCPCR have been weighted with respect to the road condition distribution for each injury severity. The results are shown in Figure 3-27 - Figure 3-29. The mean collision velocity has been reduced in the analysed conflict situations and for all (baseline) accident severities. The baseline distributions are based on the Weibull functions for each respective accident severity. The yellow bars on the left side showing 0 km/h represent the avoided AEB cases.

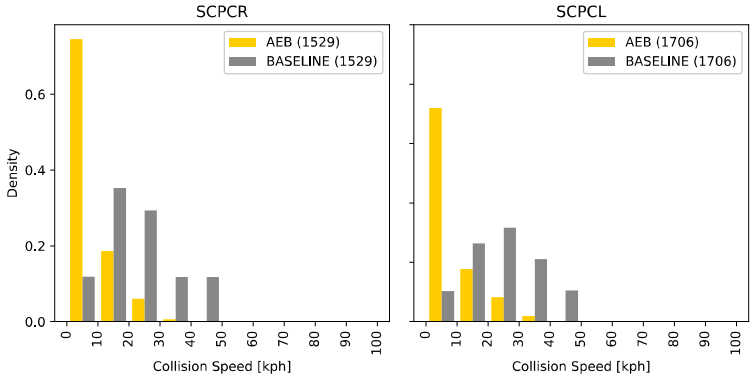

Figure 3-27: Distribution of collision velocities for slight conflict scenarios, between car and cyclist. The baseline is shown in grey and the AEB cases in yellow.

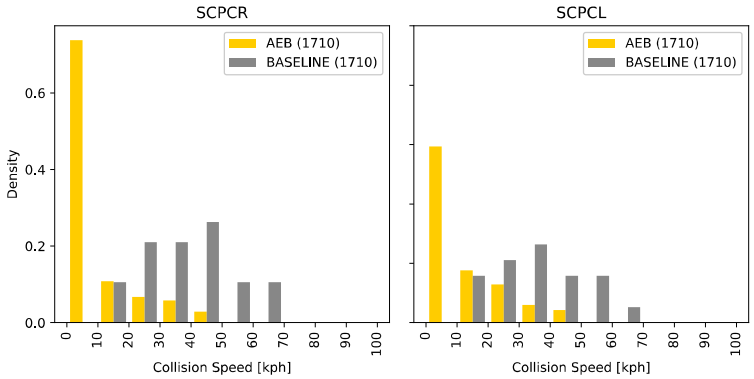

Figure 3-28: Distribution of collision velocities for severe conflict scenarios, between car and cyclist. The baseline is shown in grey and the AEB cases in yellow.

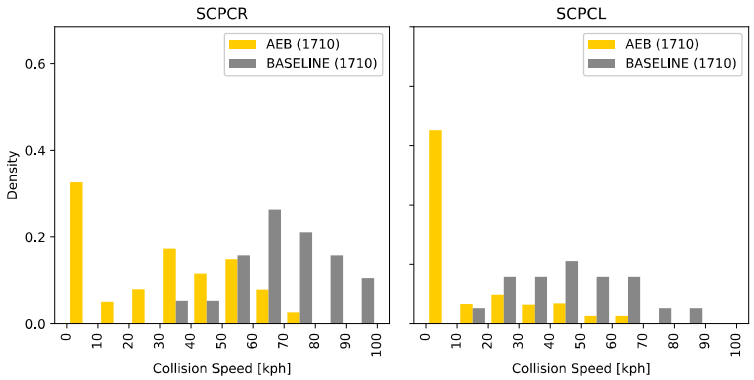

Figure 3-29: Distribution of collision velocities for fatal conflict scenarios, between car and cyclist. The baseline is shown in grey and the AEB cases in yellow.

The collision distributions for the conflict situation SCPCL and SCPCR have been further combined according to the weighting schema as described in Section 3.1.4. The probability for the occurrence of a certain cyclist - car conflict situation (given in Table 2-12) has been utilised. Figure 3-30 shows the weighted distribution of the collision velocity for different injury severities.

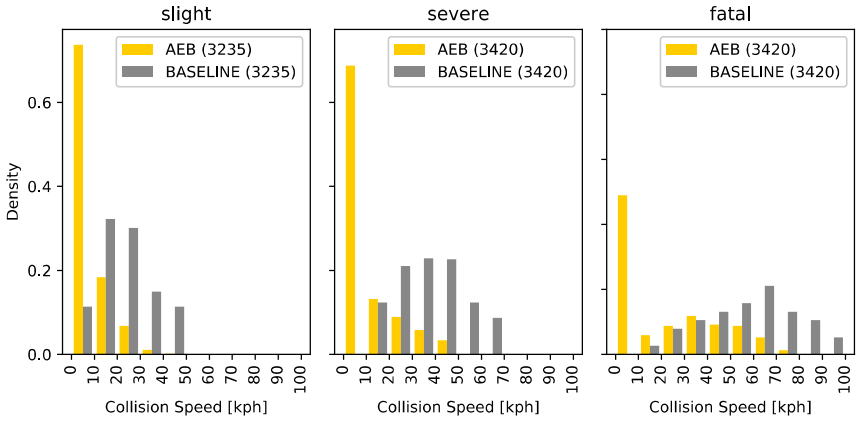

Figure 3-30: Weighted collision velocity for the slight, severe and fatal injuries for car - cyclist conflicts.

The weighted distribution of the overall collision velocity for car - cyclist conflicts is shown in Figure 3-31. The weighting has been done with respect to the injury severity as given in Table 2-10.

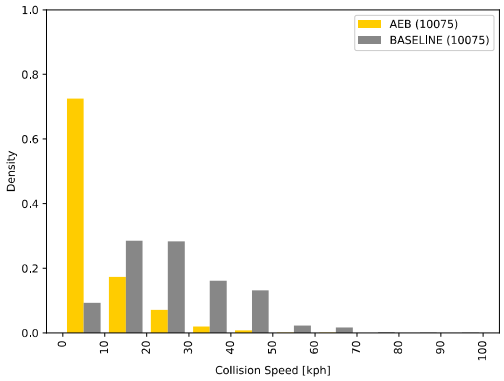

Figure 3-31: Overall weighted collision velocity distribution between car and cyclist.

3.2.3 Future Pedestrian - Tram Accident Scenarios

In comparison to pedestrian/cyclist - car conflict situations, the quality of pedestrian - tram accidents data is rather poor. Therefore, the simulation matrix has been set up differently, displaying exemplary results for this type of conflict scenarios.
The treatment simulation results of the VT scenarios representing SCPPL and SCPPR conflict situations are summarised in Table 3-10. The results are graphically presented in Figure 3-32 and Figure 3-33.
The observed results for SCPPL and SCPPR are quite similar. Approximately 76% of the baseline test scenarios were avoided due to the AEB system. No AEB intervention and therefore no change in the baseline scenario was observed in 2.5% of the scenarios. In cases with intervention, without avoidance, a drastic reduction in the collision velocity was observed.

Table 3-10: Overview of the effect of a generic AEB system on SCPPL and SCPPR tram - pedestrian conflict situations.

		SCPPL	SCPPR
Conflicts	Baseline	855	855
	AEB	200	199
	Shift [%]	-76.6	-76.7
V_coll [m/s]	Baseline	8.3	8.3
	AEB	4.3	4.3
	Shift [%]	-48.2	-48.3
AEB avoidance			
	Conflicts	655	656
Reduced collision velocity by AEB			
	Conflicts	179	180
V_col [m/s]	Baseline	12.1	12.3
	AEB	4.4	4.4
	Shift [%]	-64.1	-64.4
No AEB intervention			
	Conflicts	21 (2.46%)	19 (2.22%)

3.2.3.1 Impact Locations

The effect the AEB system has on the impact locations from the treatment simulations is shown in Figure 3-32. A similar trend as for the pedestrian/cyclist - car conflict can be seen, showing a slight shift towards the right for SCPPL and to the left for SCPPR conflict situations with AEB treatment, compared to the baseline.

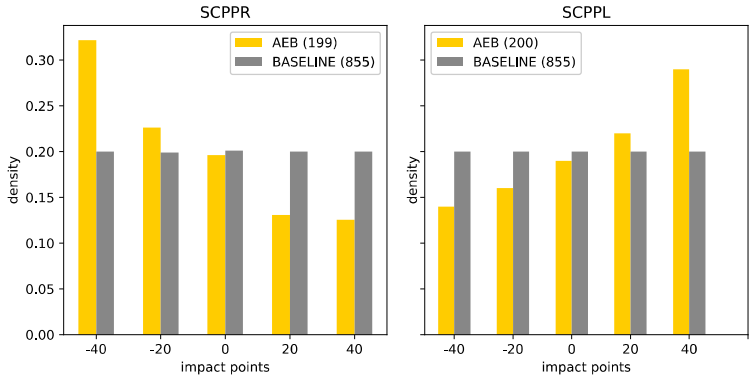

Figure 3-32: Distribution of the impact locations for conflict scenarios, between tram and pedestrian. The baseline is shown in grey and the AEB cases in yellow.

3.2.3.2 Collision Velocities

The results of the collision velocity for tram - pedestrian conflict situations are shown in Figure 3-33. The collision velocities have been reduced in the AEB treatment simulations compared to the baseline and 80% of the VT scenarios were avoided for SCPPR and SCPPL.

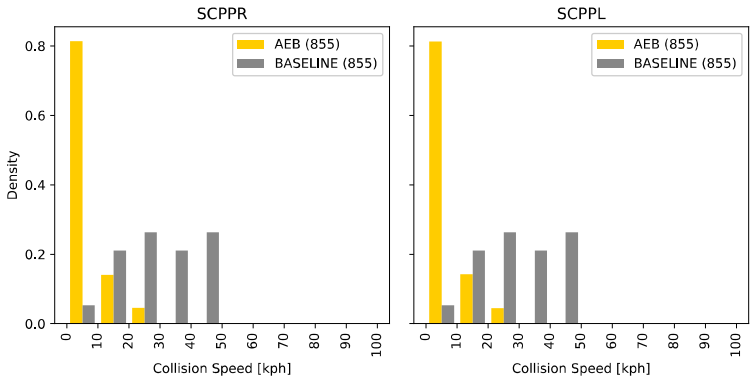

Figure 3-33: Distribution of collision velocities for the conflict scenarios, between tram and pedestrian. The baseline is shown in grey and the AEB cases in yellow.

To the best of the authors knowledge, trams equipped with AEBs are not available. Hence, this analysis is very conceptual and should be viewed as the initial step in researching this issue. Further specifications of possible concepts will be performed within the next few tasks of the project.

4 Discussion

The next few stages of the project will investigate certain significant differences identified for male and female accident statistics (i.e.., higher share of lower extremity injuries for female cyclists compared to male) by means of simulations.

The analysis of injuries of pedestrians and cyclists showed using HBMs for virtual assessment would be suitable to assess the risk of the following:

- long bone fractures of lower extremities
- pelvic bone fractures
- rib fractures
- knee ligament ruptures
- brain injuries
- skull fractures

The classification of accident scenarios is not harmonised among European countries. Hence, data available in CARE were therefore limited by the data sources, Neither is the evaluation of injury severities. Especially in reference to cyclists, the majority of cases have been categorised as "other". It was only possible to achieve very rough clustering because CARE does not explicitly define which vehicle is the car and which one is the bicycle.
To estimate the distributions inside a cluster, more detailed information held on in-depth databases was investigated. However, this method has three significant limitations; 1) driving behaviour and general traffic behaviour is not homogenous throughout Europe, 2) only Austrian, German and Swedish in-depth data was available, and 3) the infrastructure for cyclists can vary significantly among different European countries.

The overall probabilities have been calculated using the distribution of accidents to specific clusters for STRADA and CARE, applying the IPF method. The Iterative Proportional Fitting (IPF) method is useful when estimating probabilities based on databases that have been assumed to hold similar distributions of accidents. Please note that cluster probabilities might sometimes differ in the STRADA and CARE database. The CARE database consists of many more observations and might therefore provide more representative estimates of the cluster probabilities on European roads. Furthermore, for severe and fatal injuries in certain clusters, IPF results in uncertain estimates for conflict situations with few observations. Therefore, these values should be considered with caution, as they are associated with a relatively large degree of uncertainty.
Exclusion of data belonging to certain clusters might change the results. This is particularly important for the cluster "*Unspecified*" and "*Others*" containing a large number of observations. As the probability of an "*unspecified*" type of conflict situation is not useful for our purposes (i.e., does not describe the design of the simulations and cannot be used for the specification of the VT catalogue), these categories were excluded in the current analysis, although they can significantly affect the resulting probabilities. The plausibility checks with the in-depth databases showed that the derived probabilities are reasonable, at least for the countries where access to in-depth data is available.

It is highly recommended that a sustainable, representative, European-wide, long-term and in-depth database is established to eliminate the limitation mentioned above.

Certain categories of conflict situations (for pedestrian e.g., LT/SDLD, RT/SDRD,…) did not expose any cases in the investigated data sources. Whether this is because they never occur, or that, these

particular conflict situations have never been classified (which seems more likely), remains unknown. Improved accident classification, especially for VRUs, is a prerequisite for addressing the lack of cyclist accidents in the sourced databases and identifying whether these theoretical conflict situations never occur in real traffic. These types of conflict situations will be monitored for the integrated assessment in VIRTUAL WP4. However, as the probability based on the current available data is 0, the results will not affect the overall assessment results.

The Weibull distributions showed a better fit than Normal distributions for describing the initial velocities of vehicles and VRUs. For cases involving low sample sizes, some deviations leading to poor p-values were observed in the Weibull distribution. Once the quality of data improves in the future, it would be possible to identify an even more appropriate distribution.

Although the quality of the data available for the pedestrian – tram accidents not being comparable to pedestrian – car accidents, the collection of data compiled within the VIRTUAL project represent an important initial stage in the process of establishing more comprehensive databases. Therefore, the results will be published in order to highlight the need to extend current data sources. Unfortunately, based on currently available data, it has not been viable to incorporate a weighted integrated assessment, in the same manner as will be performed for the car use-cases.

The simulations performed for the prospective analysis of future accident scenarios clearly show that the AEB systems have the potential to avoid a high percentage of collisions. Despite excluding visual obstructions, not all scenarios were avoided through the idealised generic AEB system. However, as a result of AEB system intervention, the collision velocity for the exemplary conflict situations in the remaining cases was also significantly reduced. In order to estimate the overall benefit, the effect of the reduced collision speed should be analysed further by means of HBM simulations. No clear conclusions can be drawn yet as to the effect the AEB systems has on the impact location relative to the vehicle. The impact location would also be highly affected by the pre-crash reaction of the VRU, which is not considered. However, a trend towards a higher number of impacts to the outer edges of the vehicles was observed, which seems plausible and should therefore be further investigated in the in-crash simulations.

For the first time, simulations for a tram model equipped with a conceptual AEB system has been performed. Based on promising results of the initial analyses,, further investigations will be undertaken in the next phase of the project.

Future accident scenarios presented in this report are based on one conceptual generic AEB system. However, the AEB system parameters significantly influence the simulated results. In particular the braking strategy can impact the outcome (Gruber *et al.*, 2019) significantly.

In the next few steps of WP4 of the VIRTUAL project, the selected parameters will be validated and specific systems will be assessed. For the integrated assessment procedure developed in VIRTUAL, the VT testing catalogue, as described in this deliverable will be used to assess the overall benefit of integrated VRU safety systems.
The specific AEB system parameters should be input to the VIRTUAL Pre-crash Tool to derive future impact scenarios relevant for a specific vehicle. For the remaining impact scenarios, in-crash simulations with the VIVA+ HBMs will be performed-

5 Outlook and the Next Steps

For the unavoidable scenarios, in-crash simulation conditions will be selected and simulated with Human Body Models to finally establish an overall assessment for the integrated VRU assessment.

The following manuscripts have been prepared, awaiting submission on publication of the Pre-crash Tool paper, as it is required as a reference:

- Corina Klug, Christoph Leo, Martin Schachner, Ellen Grumert, Maria Rizzi, Ragnhild Davidse, Astrid Linder: Future pedestrian and cyclist accident scenarios – how will autonomous emergency braking systems of passenger cars affect the impact conditions in accidents with pedestrians and cyclists?

- Philipp Heinzl, Peter Klager, Martin Schachner, Christoph Leo, Maria Rizzi, Corina Klug: Relevance and scenarios of tram - pedestrian accidents – What data is available and how can accidents be avoided?

Titles and authors might be subject to change before the final submission.

6 References

AAAM (2005), *Abbreviated Injury Scale 2005*, Des Plaines IL.

ACEA (2019), "Average Vehicle Age", available at: https://www.acea.be/statistics/tag/category/average-vehicle-age (accessed 30 March 2020).

Aparicio, A., Sanz, L., Burnett, G., Stoll, H., Arbitmann, M., Kunert, M., Flohr, F., Seiniger, P. and Gavrila, D. (2017), "Advancing active safety towards the protection of vulnerable road users: the PROSPECT project", *The 25th ESV Conference Proceedings, Michigan, USA, 5.-8.6.2017*, NHTSA, available at: https://www-esv.nhtsa.dot.gov/Proceedings/25/25ESV-000193.pdf.

Baker, S.P., O'Neill, B., Haddon, W. and Long, W.B. (1974), "The injury severity score: a method for describing patients with multiple injuries and evaluating emergency care", *The Journal of Trauma*, Vol. 14 No. 3, pp. 187–196.

Bakker, J., Jeppson, H., Hannawald, L., Spitzhüttl, F., Longton, A. and Tomasch, E. (2017), "IGLAD - International Harmonized In-Depth Accident Data", *The 25th ESV Conference Proceedings, Michigan, USA, 5.-8.6.2017*, NHTSA, available at: http://indexsmart.mirasmart.com/25esv/PDFfiles/25ESV-000248.pdf.

Bakker, J., Ockel, D. and Schöneburg, R. (2014), "Multinational in-depth accident data: From concept to reality", paper presented at 6th International Conference ESAR, 20.-21.06.2014, Hannover.

Barrow, A., Edwards, A., Smith, L., Khatry, R., Kalaiyarasan, A. and Hynd, D. (2018), *Effectiveness estimates for proposed amendments to the EU's General and Pedestrian Safety Regulations, Published project report / Transport Research Laboratory, TRL PPR*, Vol. 844, v3.0, TRL, Wokingham, Berkshire, United Kingdom. ISBN: 978-1-912433-06-3.

Brunner, Horst, Krettek, Christian, Otte, Dietmar, Zwipp and Hans (2003), "Scientific Approach and Methodology of a New In-depth Investigation Study in Germany so called GIDAS", paper presented at International Technical Conference on the Enhanced Safety of Vehicles, 19.-22.5.2003, Nagoya, Japan.

Chen, Q., Lin, M., Dai, B. and Chen, J. (2015), "Typical Pedestrian Accident Scenarios in China and Crash Severity Mitigation by Autonomous Emergency Braking Systems", *SAE 2015 World Congress Proceedings, 24.4.2015*, SAE International.

Cieślik, I., Kovaceva, J., Bruyas, M.-P., Large, D., Kunert, M., Krebs, S. and Arbitmann, M. (2019), "Improving the effectiveness of active safety systems to significantly reduce accidents with vulnerable road users - the project PROSPECT (Proactive Safety for Pedestrians and Cyclists)", *The 26th ESV Conference Proceedings, Eindhoven, Netherlands, 10-13 June*, NHTSA, available at: https://www-esv.nhtsa.dot.gov/Proceedings/26/26ESV-000277.pdf.

del Pozo de Dios, E., Ferrer, A., Hill, J., Fagerlind, H., Giustiniani, G. and Persia, L. (2013), "Towards a Global and Harmonized Database for In–Depth Accident Investigation in Europe: The Dacota Project", *The 23rd ESV Conference Proceedings, Seoul, Republic of Korea, 27.-30.5.2013*, NHTSA, pp. 1–9, available at: https://www-esv.nhtsa.dot.gov/Proceedings/23/isv7/main.htm.

Department of Transport (2013), "Road accident in-depth studies (RAIDS)", available at: https://www.gov.uk/government/publications/road-accident-investigation-road-accident-in-depth-studies/road-accident-in-depth-studies-raids#further-information (accessed 13 August 2018).

Detwiller, M. and Gabler, H.C. (2017), "Potential Reduction in Pedestrian Collisions with an Autonomous Vehicle", *The 25th ESV Conference Proceedings, Michigan, USA, 5.-8.6.2017*, NHTSA, pp. 1–8, available at: https://www-esv.nhtsa.dot.gov/Proceedings/25/25ESV-000404.pdf.

Dobberstein, J., Bakker, J., Wang, L., Vogt, T., Düring, M., Stark, L., Gainey, J., Prahl, A., Mueller, R. and Blondelle, G. (2017), "The Eclipse Working Group openPASS – an Open Source Approach to Safety Impact Assessment Via Simulation", *The 25th ESV Conference Proceedings, Michigan, USA, 5.-8.6.2017*, NHTSA, available at: http://indexsmart.mirasmart.com/25esv/PDFfiles/25ESV-000094.pdf.

Ds 2016:20 (2016), *In Swedish: Strada Transportstyrelsens olycksdatabas*.

Erik, Källhammer, J.-E., Eriksson, D., Nentwich, M., Fredriksson, R. and Smith, K. (2010), "Pedestrian injury mitigation by autonomous braking", *Accident Analysis & Prevention*, Vol. 42 No. 6, pp. 1949–1957. doi: 10.1016/j.aap.2010.05.018.

Euro NCAP (2019), *Test Protocol - AEB VRU systems*.

European Commission (2018), *Annual Accident Report 2018*.

European Parliament and European Council (2019), *Type-approval requirements for motor vehicles and their trailers, and systems, components and separate technical units intended for such vehicles, as regards their general safety and the protection of vehicle occupants and vulnerable road users* No. 2019/2144.

Försäkringsförbundet (Insurance Sweden) (2004), *Medicinsk Invaliditet – Gradering av Medicinsk Invaliditet (Medical Impairment - Grading of Medical Impairment, in Swedish)*, Stockholm, Sweden.

González-Estrada, E. and Villaseñor, J.A. (2018), "An R package for testing goodness of fit: goft", *Journal of Statistical Computation and Simulation*, Vol. 88 No. 4, pp. 726–751. doi: 10.1080/00949655.2017.1404604.

Gruber, M., Kolk, H., Klug, C., Tomasch, E., Feist, F., Schneider, A. and Roth, F. (2019), "The effect of P-AEB system parameters on the effectiveness for real world pedestrian accidents", *The 26th ESV Conference Proceedings, Eindhoven, Netherlands, 10-13 June*, NHTSA, available at: http://indexsmart.mirasmart.com/26esv/PDFfiles/26ESV-000130.pdf.

Hummel, T., Kühn, M., Bende, J. and Lang, A. (2011), *Advanced Driver Assistance Systems: An investigation of their potential safety benefits based on an analysis of insurance claims in Germany, Forschungsbericht / Gesamtverband der Deutschen Versicherungswirtschaft e.V FS, Fahrzeugsicherheit / Unfallforschung der Versicherer*, Vol. 03, GDV, Berlin. ISBN: 978-3-939163-37-4.

Isaksson-Hellman, I. and Lindman, M. (2019), "Real-world evaluation of driver assistance systems for vulnerable road users based on insurance crash data in Sweden", *The 26th ESV Conference Proceedings, Eindhoven, Netherlands, 10-13 June*, NHTSA, available at: https://www-esv.nhtsa.dot.gov/Proceedings/26/26ESV-000300.pdf.

Isaksson-Hellman, I. and Werneke, J. (2017), "Detailed description of bicycle and passenger car collisions based on insurance claims", *Safety Science*, Vol. 92, pp. 330–337. doi: 10.1016/j.ssci.2016.02.008.

Jeppsson, H., Östling, M. and Lubbe, N. (2018), "Real life safety benefits of increasing brake deceleration in car-to-pedestrian accidents: Simulation of Vacuum Emergency Braking", *Accident Analysis & Prevention*, Vol. 111, pp. 311–320. doi: 10.1016/j.aap.2017.12.001.

Klager, P. (2019), "Collection of Data Regarding Light Rail Vehicle Accidents Resulting in Personal Injuries", Masterthesis, Technische Universität Wien, Vienna, 2019.

Klug, C., Weinberger, M., Tomasch, E., Feist, F., Sinz, W., Steffan, H., Kinsky, T., Roth, F., Praxl, N. and Buenger, B. (2015), "Pelvic and femoral injuries in car-to-pedestrian accidents", *2015 IRCOBI Conference Proceedings, Lyon, France, 9.-11.9.2015*, IRCOBI, pp. 49–63, available at: http://www.ircobi.org/wordpress/downloads/irc15/pdf_files/15.pdf.

Lenard, J., Morris, A., Tomasch, E., Nehmzow, D., Otte, D., Cant, L., Haddak, M., Vallet, G., Ebbinger, H., Barnes, J., Vries, Y. de, van Kampen, B. and Paez, J. (2006), "PENDANT: A European Crash Injury Database", *2nd International Conference on ESAR "Expert Symposium on Accident Research", Hanover, Germany, 1.-2.9.2006*, ESAR, available at: https://dspace.lboro.ac.uk/dspace-jspui/bitstream/2134/2635/1/PUB460.pdf.

Leo, C., Klug, C., Ohlin, M., Bos, N., Davidse, R. and Linder, A. (2019a), "Analysis of Swedish and Dutch accident data on cyclist injuries in cyclist-car collisions", *Traffic injury prevention*. doi: 10.1080/15389588.2019.1679551.

Leo, C., Klug, C., Ohlin, M. and Linder, A. (2019b), "Analysis of pedestrian injuries in pedestrian-car collisions with focus on age and gender", *2019 IRCOBI Conference Proceedings, Florence, Italy, 11.-13.9.*, IRCOBI, pp. 256–257, available at: http://www.ircobi.org/wordpress/downloads/irc19/pdf-files/40.pdf.

Li, G., Lyons, M., Wang, B., Yang, J., Otte, D. and Simms, C. (2017), "The influence of passenger car front shape on pedestrian injury risk observed from German in-depth accident data", *Accident Analysis & Prevention*, Vol. 101, pp. 11–21. doi: 10.1016/j.aap.2017.01.012.

Li, G., Wang, F., Otte, D., Cai, Z. and Simms, C. (2018), "Have pedestrian subsystem tests improved passenger car front shape?", *Accident Analysis & Prevention*, Vol. 115, pp. 143–150. doi: 10.1016/j.aap.2018.03.014.

Linder, A., Davidse, R, J, Iraeus, J., John, J.D., Keller, A., Klug, C., Krašna, S., Leo, C., Ohlin, M., Silvano, A.P., Svensson, M., Wågström, L. and Schmitt, K.-U. (2020), "VIRTUAL - a European approach to foster the uptake of virtual testing in vehicle safety assessment", paper presented at Transport Research Arena, 26.4.-30.4., Helsinki, Finland.

Lindman, M., Jakobsson, L. and Jonsson, S. (2011), "Pedestrians interacting with a passenger car; a study of real world accidents", *2011 IRCOBI Conference Proceedings, Krakow (Poland), 14.-16.9.2011*, IRCOBI, pp. 255–264, available at: http://www.ircobi.org/wordpress/downloads/irc0111/2011/Session6/61.pdf.

Lindman, M., Jonsson, S., Jakobsson, L., Karlsson, T., Gustafson, D. and Fredriksson, A. (2015), "Cyclists interacting with passenger cars; a study of real world crashes", *2015 IRCOBI Conference Proceedings, Lyon, France, 9.-11.9.2015*, IRCOBI, pp. 1–12, available at: http://www.ircobi.org/wordpress/downloads/irc15/pdf_files/10.pdf.

Lindman, M., Ödblom, A., Bergvall, E., Eidehall, A., Svanberg, B. and Lukaszewicz, T. (2010), "Benefit Estimation Model for Pedestrian Auto Brake Functionality", paper presented at 4th International Conference on ESAR, September 16-18, Hanover, Germany, available at: https://www.saferresearch.com/library/benefit-estimation-model-pedestrian-auto-brake-functionality.

Luttenberger, P., Tomasch, E., Willinger, R., Bourdet, N., Mayer, C. and Ewald, C. (2013), *Methodical analysis on future accident scenarios involving SEV's, Deliverable*.

Luttenberger, P., Tomasch, E., Willinger, R., Mayer, C., Bakker, J., Bourdet, N., Ewald, C. and Sinz, W. (2014), "Method for future pedestrian accident scenario prediction", in *Transport Research Arena*, .

Malm, S., Krafft, M., Kullgren, A., Ydenius, A. and Tingvall, C. (2008), "Risk of permanent medical impairment (RPMI) in road traffic accidents", *Annals of advances in automotive medicine.*

Association for the Advancement of Automotive Medicine. Annual Scientific Conference, Vol. 52, pp. 93–100.

Mattsson, K. and Ungerbäck, A. (2013), *In Swedish: "Vägtrafikolyckor - handledning vid rapportering," in Transportstyrelsen*, Borlänge.

Morris, A., Brace, C., Reed, S., Fagerlind, H., Bjorkman, K., Jaensch, M., Otte, D., Vallet, G., Cant, L., Giustiniani, G., Parkkari, K., Verschragen, E. and Hoogvelt, B. (2010), "The development of a European fatal accident database", *International Journal of Crashworthiness*, Vol. 15 No. 2, pp. 201–209. doi: 10.1080/13588260903102476.

Morris, A. and Thomas, P. (2003), "PENDANT - Pan-European Coordinated Accident and Injury Databases", paper presented at International Technical Conference on the Enhanced Safety of Vehicles, 19.-22.5.2003, Nagoya, Japan.

Morris, A.P., Brown, L.A., Thomas, P., Davidse, R.J., Phan, V., Margaritis, D., Robibaro, M., Krupińsk, A., Sicińska, K., Ziakopoulos, A., Theofilatos, G., Usami, M. and Yannis, G. (2018), *SAFERWHEELS - Study on powered two-wheeler and bicycle accidents in the EU*.

National Board of Health and Welfare (Socialstyrelsen) (2010), *International Statistical Classification of Diseases and Related Health Problems - Systematic listing: Swedish version 2011 (ICD-10-SE)*.

NHTSA (2017), "Crash Investigation Sampling System (CISS)", available at: https://www.nhtsa.gov/crash-data-systems/crash-investigation-sampling-system (accessed 27 March 2020).

NHTSA (2018), "National Automotive Sampling System (NASS)", available at: https://www.nhtsa.gov/research-data/national-automotive-sampling-system-nass (accessed 13 August 2018).

Ockel, D., Bakker, J. and Schöneburg, R. (2012), "An initiative towards a simplified international in-depth accident database", paper presented at 5th International Conference on ESAR, September 7-8, Hanover, Germany.

OECD (2019), "IRTAD Road Safety Database", available at: https://www.itf-oecd.org/irtad-road-safety-database.

Otte, D., Jänsch, M. and Haasper, C. (2012), "Injury protection and accident causation parameters for vulnerable road users based on German In-Depth Accident Study GIDAS", *Accident Analysis & Prevention*, Vol. 44 No. 1, pp. 149–153. doi: 10.1016/j.aap.2010.12.006.

Page, Y., Fahrenkrog, F., Fiorentino, A., Gwehenberger, J., Helmer, T., Lindman, M., Op den Camp, O., van Rooij, L., Puch, S., Fränzle, M., Sander, U. and Wimmer, P. (2015), "A Comprehensive and Harmonized Method for Assessing the Effectiveness of Advanced Driver Assistance Systems by Virtual Simulation: The P.E.A.R.S. Initiative", *The 24th ESV Conference Proceedings, Gothenburg, Sweden, 8.-11.6.2015*, NHTSA, available at: https://www-esv.nhtsa.dot.gov/Proceedings/24/files/24ESV-000370.PDF.

Pastor, C. (2013), "Correlation between pedestrian injury severity in real-life crashes and Euro NCAP pedestrian test results", *The 23rd ESV Conference Proceedings, Seoul, Republic of Korea, 27.-30.5.2013*, NHTSA, pp. 1–9, available at: https://www-esv.nhtsa.dot.gov/Proceedings/23/files/23ESV-000308.PDF.

Piantini, S., Mangini, M., Baldanzini, N., Pierini, M., Franci, A. and Peris, A. (2017), "Prediction of motorcyclist serious injury in powered two-wheeler to other vehicle urban crash", *2017 IRCOBI Conference Proceedings, Antwerp, Brussels, 13.-15.9.2017*, IRCOBI, pp. 54–62, available at: http://www.ircobi.org/wordpress/downloads/irc17/pdf-files/16.pdf.

R Core Team (2019), *R: A Language and Environment for Statistical Computing*, Vienna, Austria, available at: https://www.R-project.org/.

Rosén, E. and Sander, U. (2009), "Pedestrian fatality risk as a function of car impact speed", *Accident Analysis & Prevention*, Vol. 41 No. 3, pp. 536–542. doi: 10.1016/j.aap.2009.02.002.

Ross, R., Thomas, P., Sexton, B., Otte, D., Koßmann, I., Vallet, G., Martin, J., Laumon, B. and Lejeune, P. (1998), "An Approach to the Standardisation of Accident and Injury Registration Systems (STAIRS) in Europe", *The 16th ESV Conference Proceedings, Ontario, Canada, 31.5.-4.6.1998*, NHTSA, p. 1298-305, available at: https://www-nrd.nhtsa.dot.gov/pdf/esv/esv16/98s6p16.pdf.

Roth, F., Labenski, V., Gruber, M. and Kolk, H. (2018), "Future Traffic Scenario under Consideration of AEB Systems", paper presented at Praxiskonferenz Fußgängerschutz, June, 2018, Bergisch-Gladbach.

Samin, O.A. and Civil, I.D. (1999), "The New Injury Severity Score Versus the Injury Severity Score in Predicting Patient Outcome: A Comparative Evaluation on Trauma Service Patients of the Auckland Hospital", *Annual Proceedings / Association for the Advancement of Automotive Medicine*, Vol. 43, p. 1.

Schachner, M., Sinz, W., Thomson, R. and Klug, C. (2020), "An open source framework to generate and evaluate potential safety-critical car to pedestrian scenarios based on road layouts", *submitted*.

Shapiro, S.S. and Wilk, M.B. (1965), "An Analysis of Variance Test for Normality (Complete Samples)", *Biometrika*, Vol. 52 No. 3/4, p. 591. doi: 10.2307/2333709.

Strandroth, J., Nilsson, P., Sternlund, S., Rizzi, M. and Krafft, M. (2016), "Characteristics of future crashes in Sweden – identifying road safety challenges in 2020 and 2030", *2016 IRCOBI Conference Proceedings, Malaga, Spain, 14.-16.9.2016*, IRCOBI, pp. 47–60, available at: http://www.ircobi.org/wordpress/downloads/irc16/pdf-files/15.pdf.

Strandroth, J., Rizzi, M., Sternlund, S., Lie, A. and Tingvall, C. (2011), "The correlation between pedestrian injury severity in real-life crashes and Euro NCAP pedestrian test results", *Traffic injury prevention*, Vol. 12 No. 6, pp. 604–613. doi: 10.1080/15389588.2011.607198.

Swedish Government Offices (1965), *SFS 1965:561: last update in SFS 2014:1244, 2014*.

SWOV (2016), *Data Sources*, The Hague.

Thomas, P., Morris, A., Otte, D. and Breen, J. (2003), "Real-world Accident Data Coordinated Methodologies for Data Collection to Improve Vehicle and Road Safety", paper presented at International Technical Conference on the Enhanced Safety of Vehicles, 19.-22.5.2003, Nagoya, Japan, available at: http://www-nrd.nhtsa.dot.gov/pdf/esv/esv18/CD/proceed/00181.pdf.

Thomas, P., Muhlrad, N., Hill, J., Yannis, G., Dupont, E., Martensen, H., Hermitte, T. and Bos, N. (2013), *Final Project Report: DaCoTA - Road Safety Data, Collection, Transfer and Analysis*.

Tomasch, E. and Steffan, H. (2006a), "ZEDATU - Zentrale Datenbank tödlicher Unfälle in Österreich - A Central Database of Fatalities in Austria", *2nd International Conference on ESAR "Expert Symposium on Accident Research", Hanover, Germany, 1.-2.9.2006*, ESAR.

Tomasch, E. and Steffan, H. (2006b), "ZEDATU (Zentrale Datenbank tödlicher Unfälle in Österreich). A central database of fatalities in Austria", *2nd International Conference on ESAR "Expert Symposium on Accident Research", Hanover, Germany, 1.-2.9.2006*, ESAR.

Tomasch, E., Steffan, H. and Darok, M. (2008), "Retrospective accident investigation using information from court", April 21-24, Ljubljana.

TRL, CEESAR and ACEA (2018), *Accident Analysis*.

Verma, S., Heymans, L. and Sanz Villegas, M.T. (2017), *CARE Database - Common Accident Data Set*.

Vertal, P. and Steffan, H. (2016), "Evaluation of the Effectiveness of Volvo's Pedestrian Detection System Based on Selected Real-Life Fatal Pedestrian Accidents", *SAE 2016 World Congress Proceedings, 12.4.2016*, SAE International.

Wang, L., Vogt, T., Dobberstein, J., Bakker, J., Jung, O., Helmer, T. and Kates, R. (2018), "Multi-functional open-source simulation platform for development and functional validation of ADAS and automated driving", in Isermann, R. (Ed.), *Fahrerassistenzsysteme 2016: Von der Assistenz zum automatisierten Fahren 2. Internationale ATZ-Fachtagung*, *Proceedings*, 1. Auflage 2018, Springer Fachmedien Wiesbaden GmbH; Springer Vieweg, Wiesbaden, pp. 135–148.

Warner, C.Y., Smith, G.C., James, M.B. and Germane, G.J. (1983), "Friction Applications in Accident Reconstruction", *SAE Technical Paper Series, FEB. 28, 1983*, SAE International.

WHO (2010), *International Statistical Classification of Diseases and Related Health Problems,* 10th Revision.

Wisch, M., Lerner, M., Vukovic, E., Hynd, D., Fiorentino, A. and Fornells, A. (2017), "Injury Patterns of Older Car Occupants, Older Pedestrians or Cyclists in Road Traffic Crashes with Passenger Cars in Europe – Results from SENIORS", *2017 IRCOBI Conference Proceedings, Antwerp, Brussels, 13.-15.9.2017*, IRCOBI, pp. 63–78, available at: http://www.ircobi.org/wordpress/downloads/irc17/pdf-files/17.pdf.

Wisch, M., Seiniger, P., Edwards, M., Schaller, T., Pla, M., Aparicio, A., Geronimi, S. and Lubbe, N. (2013), "European project AsPeCSS - interim result: Development of Test Scenarios based on identified Accident Scenarios", *The 23rd ESV Conference Proceedings, Seoul, Republic of Korea, 27.-30.5.2013*, NHTSA.

Yamazaki, R. (2018), *Strada bortfallshandbok 2018 – Information om täckning och bortfall i rapportering till Transportstyrelsens vägolycksdatabas*.

Zander, O., Gehring, D.-U. and van Ratingen, M. (2015), "Beyond Safety Legislation: Contribution of Consumer Information Programmes to Enhanced Injury Mitigation of Pedestrians during Accidents with Motor Vehicles", *The 24th ESV Conference Proceedings, Gothenburg, Sweden, 8.-11.6.2015*, NHTSA, pp. 1–14, available at: https://www-esv.nhtsa.dot.gov/Proceedings/24/files/24ESV-000258.PDF.

Appendix

A. Methods and Results from the IPF

A.1 Outline of the Iterative Proportional Fitting (IPF) Algorithm

The IPT algorithm can be described as follows:

1. Start with an initial contingency matrix T consisting of ones
2. Check constraint 1: Each row should total exactly the row sums, if not scale all elements in each row r as $\frac{\sum_{c=1}^{m} w_{rc}}{\sum_{c=1}^{m} t_{rc}}$
3. Check constraint 2: Each column should total exactly the column sums, if not scale all elements in each row c as $\frac{\sum_{r=1}^{n} w_{rc}}{\sum_{r=1}^{n} w_{rc}}$

```
INPUT

T: nxm non-negative input matrix (if cell is 0 use 0.0001 to avoid 0 for column and row
sums)
R: nx1 observed vector of row sums
C: 1xm observed vector column sums
Epsilon: precision for convergence
max_it=maximum number of iterations

OUTPUT
EST: IPF'd version of T

function EST = ipf(T, R, C, Epsilon,max_it)

#Check the correctness of the inputs
st = size(T);
sr = size(R);
sc = size(C);
if (st(1) ~= sr(1))
 #Test if T or R has wrong size.
end
if (st(2) ~= sc(2))
 #Test if T or C has wrong size.
end
if (sum(sum(T < 0)) > 0)
 #Check so T does not contain negative values.
end
if (sum(R<=0)>0 | sum(C<=0)>0)
 #Test that R and C are positive.
end
if (abs(sum(R)-sum(C)) > 1e-6*sum(R))
 #Test that the total number of accidents in column and row sums are the same.
end
if (sum(sum(T,1)==0)>0 | sum(sum(T,2)==0)>0)
 #Check that row and column sum of T is non-zero.
end

#Calculate the initial error as the difference between the estimated contingency tables row
and column sums and the observed row and column sums:

tot_error = sum(abs(sum(T,2)-R)) + sum(abs(sum(T,1)-C));
```

```
EST = T;
count = 1;
n = st(1);
m = st(2);
while (tot_error > epsilon & count < max_it)
 # Iterate while the error is larger than epsilon and the maximum number of iterations
  below the maximum number of allowed iterations.

 #scale the rows
 for i=1:n
  EST(i,:) = EST(i,:) * R(i) / sum(EST(i,:));
 end

 #scale the columns
 for j=1:m
  EST(:,j) = EST(:,j) * C(j) / sum(EST(:,j));
 end

 #Calculate the total error after the scaling process
 total_error = sum(abs(sum(EST,2)-R)) + sum(abs(sum(EST,1)-C));
 count = count + 1;

end
```

A.2 Observed and Estimated Accidents for each Injury Severity

The observed and estimated accidents per injury severity within each cluster of conflict situation, are shown below. Pedestrian results are shown in the left column and cyclist results are shown in the right column. The clusters are categorised according to CARE, due to the clustering in STRADA being more aggregated.

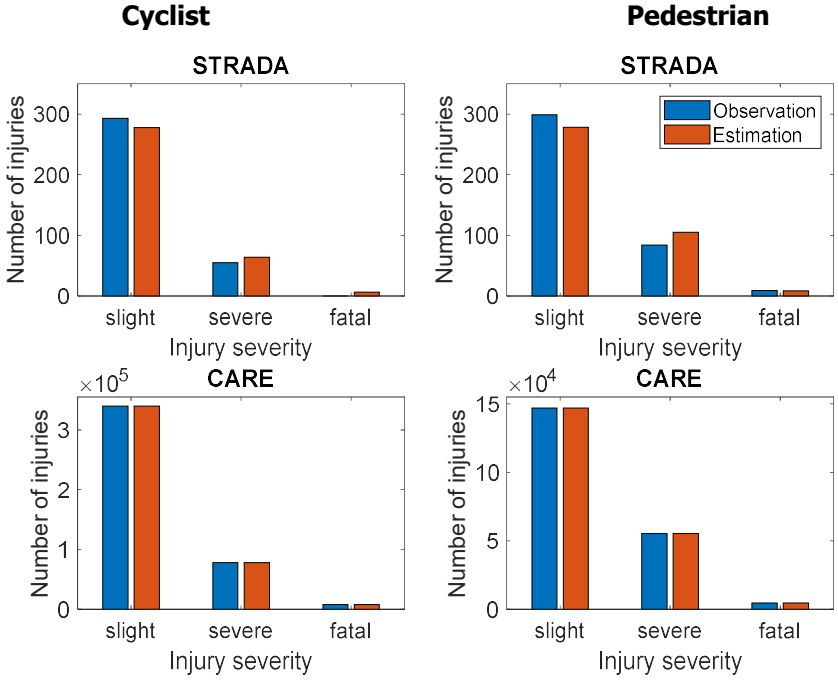

Figure -1: Cluster 1 – Car straight on, Pedestrian crossing

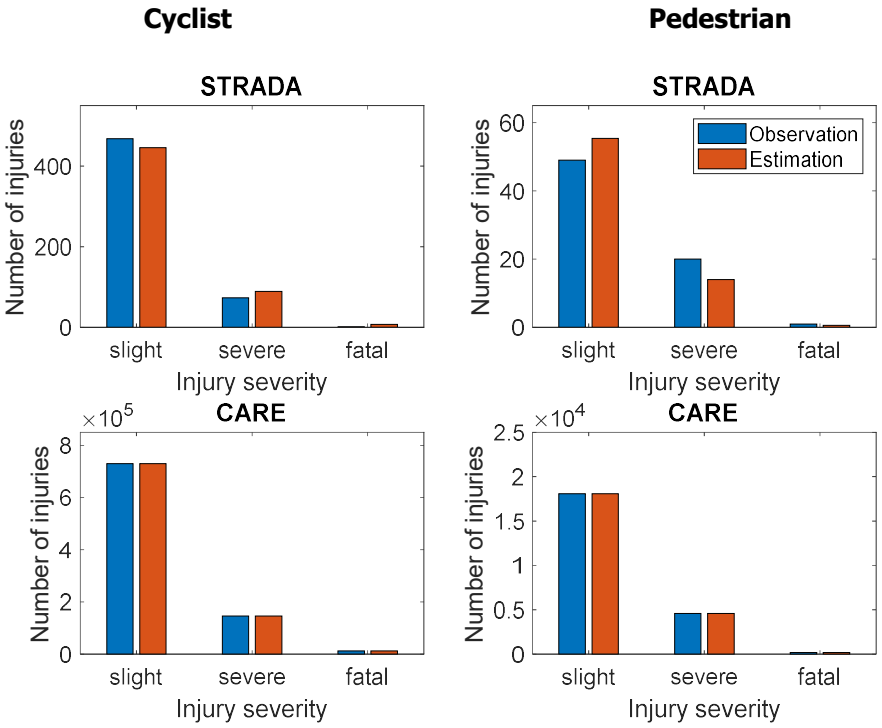

Figure A-2: Cluster 2 – Car turns, Pedestrian SD + Car turning, Pedestrian oncoming

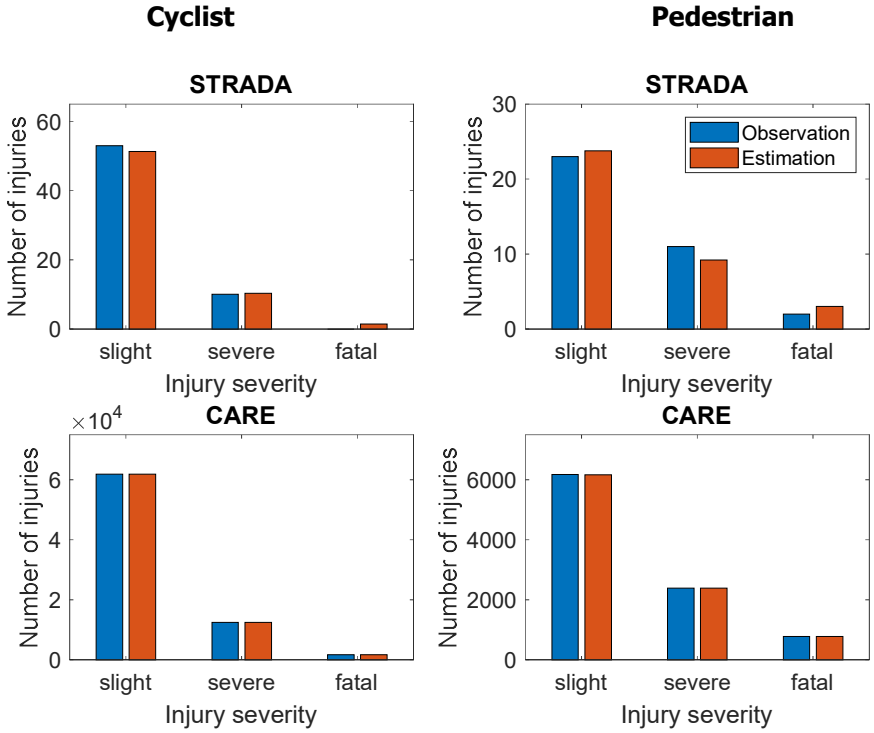

Figure A-3: Cluster 3 – Car and Pedestrian in longitudinal traffic

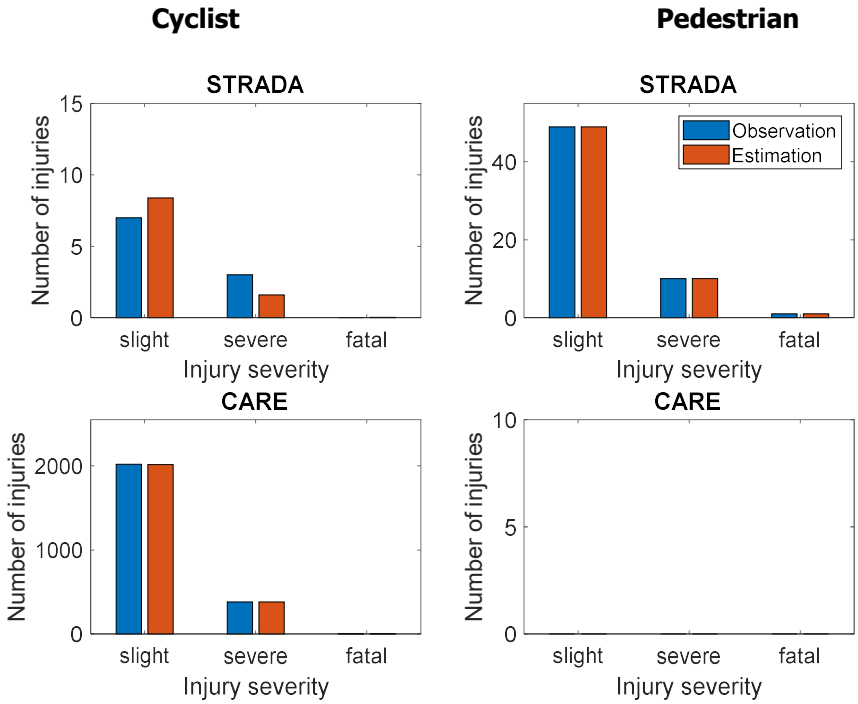

Figure A-4: Cluster 4 – Reversing

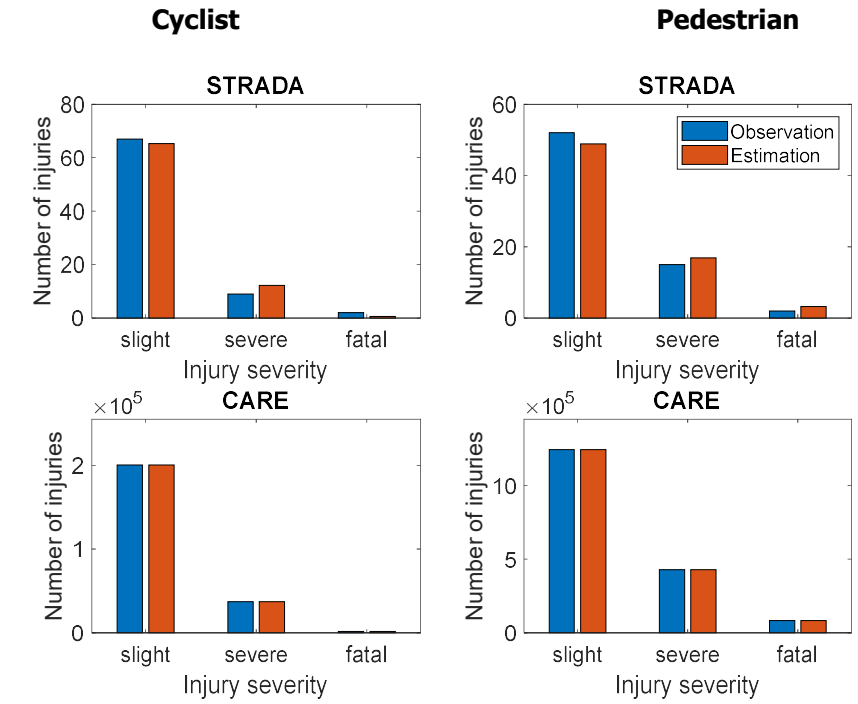

Figure A-5: Cluster 5 – Unspecified

A.3 Pedestrian - Observed and Estimated Accidents per Conflict Situation

The observed and estimated accidents per conflict situation and different databases are shown below. Slight, severe and fatal injuries have been estimated and presented separately. The different clusters are colour coded according to STRADA in Figure A-6 – Figure A-8 and according to CARE in Figure A-9 – Figure A-11.

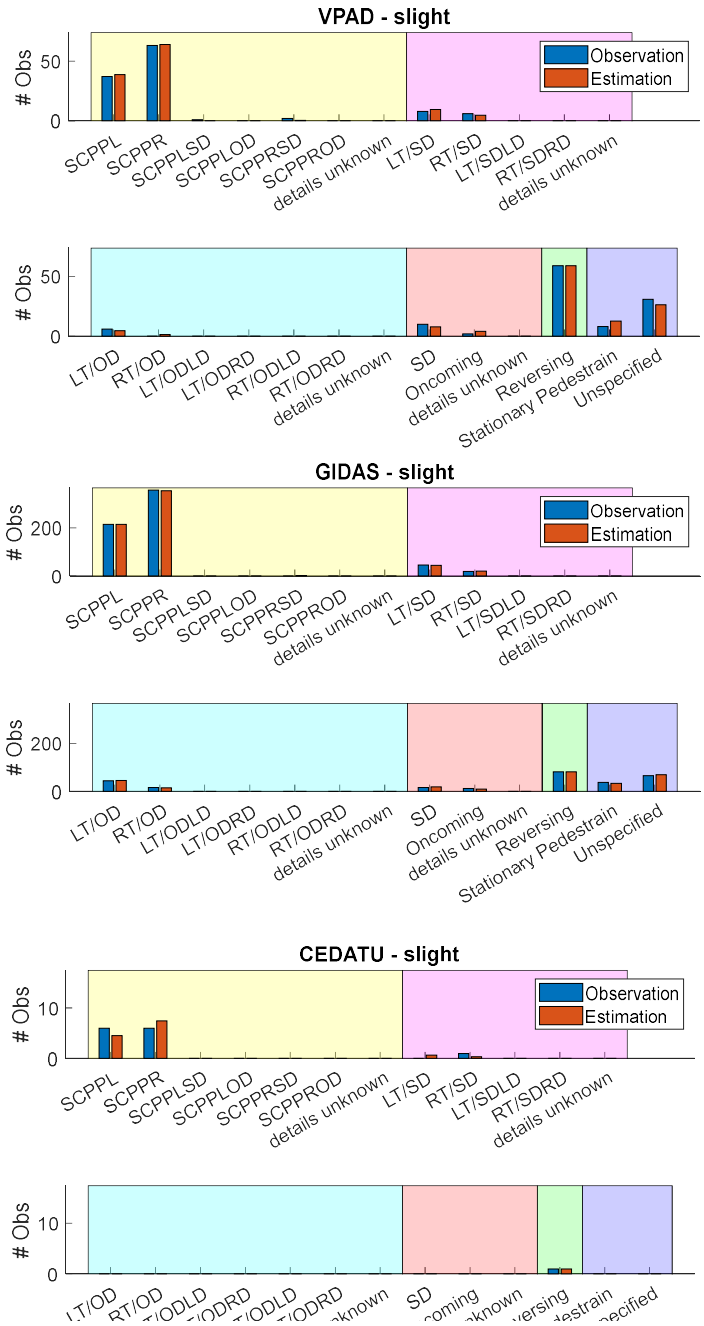

Figure A-6: Slight – observed and estimated accidents for conflict situations. Cluster are colour coded as in STRADA.

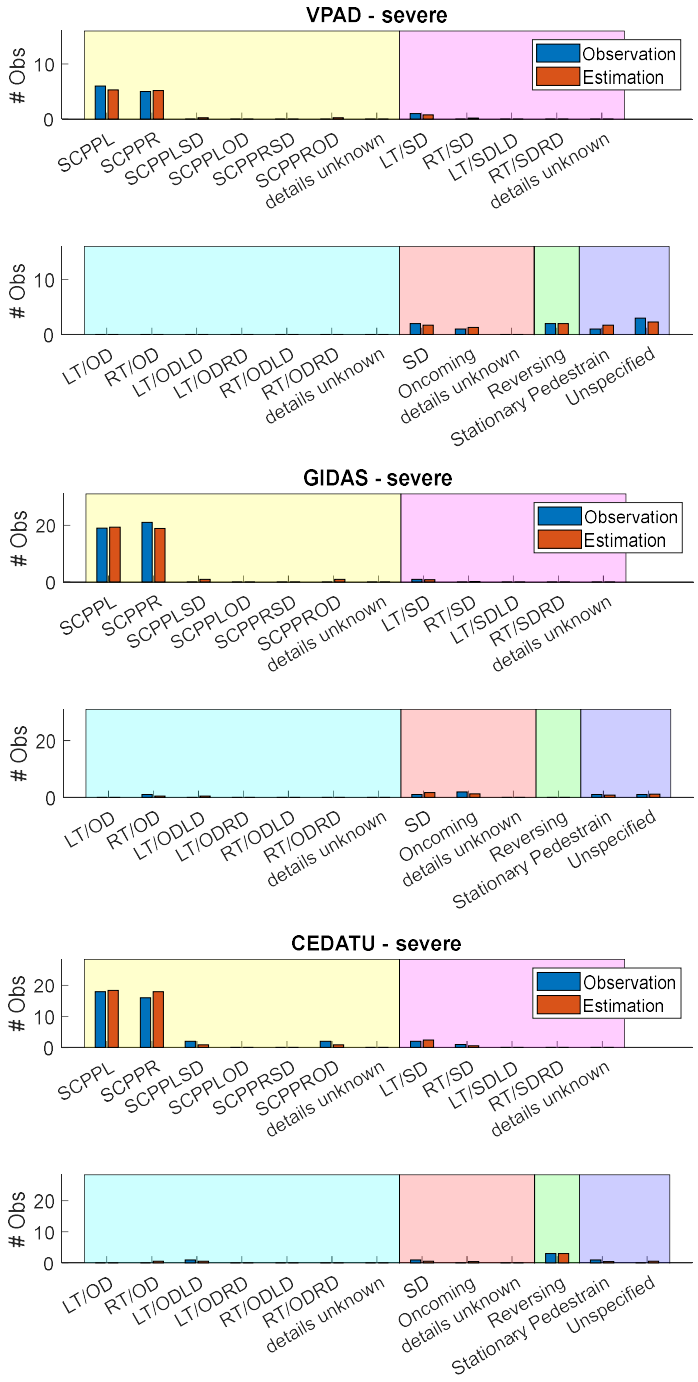

Figure A-7: Severe – observed and estimated accidents for investigated conflict situations. Clusters are colour coded as in STRADA.

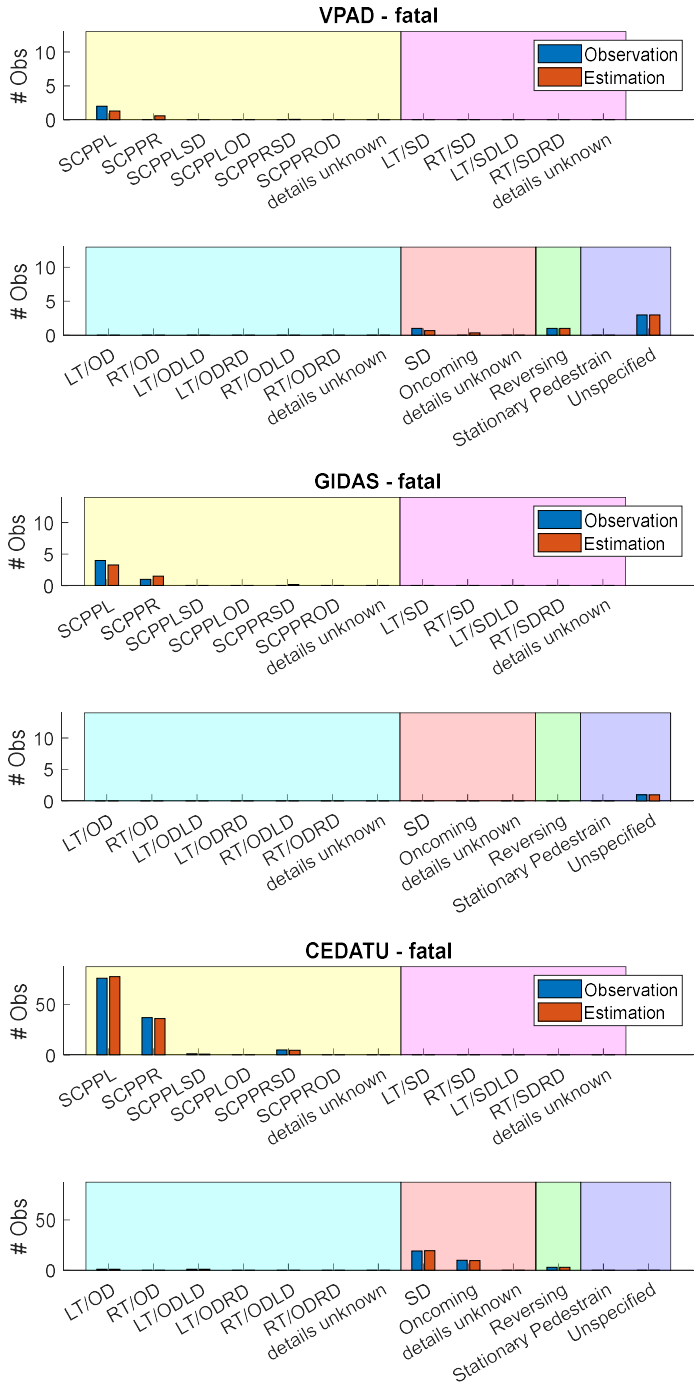

Figure A-8: Fatal – observed and estimated accidents for investigated conflict situations. Clusters are colour coded as in STRADA.

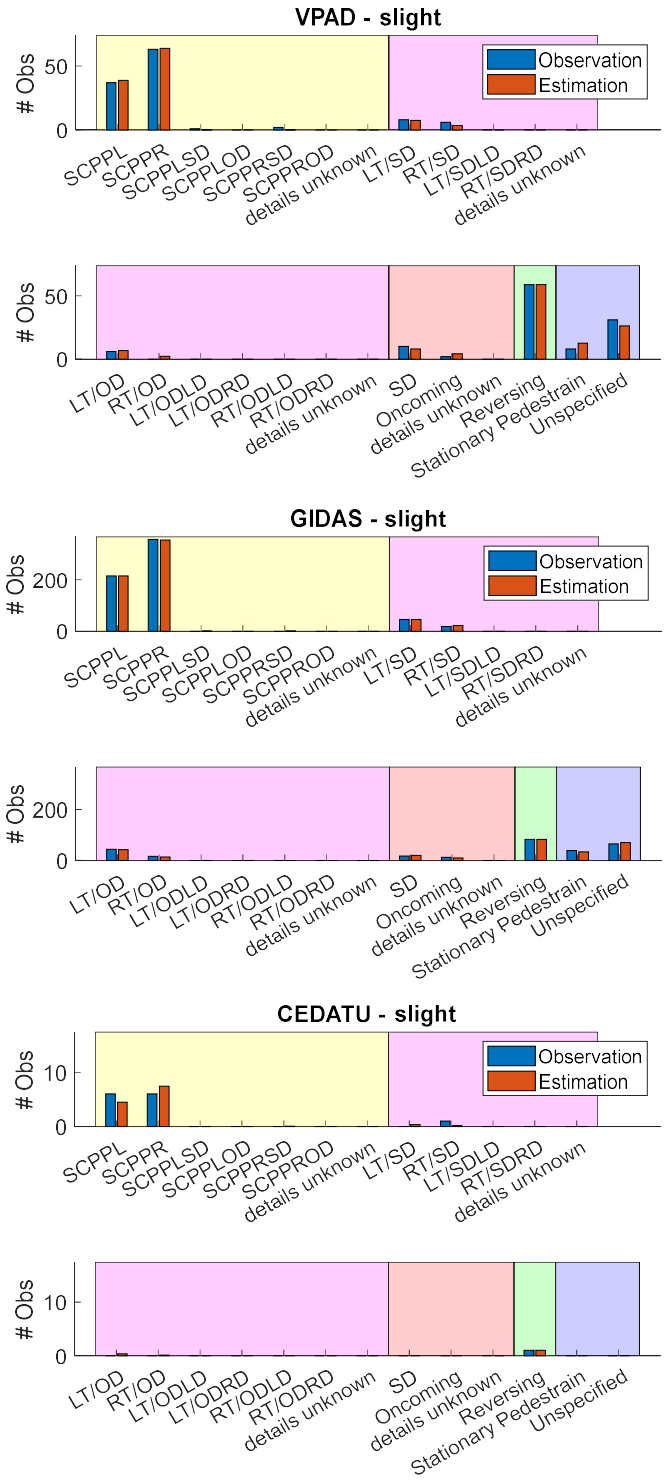

Figure A-9: Slight – observed and estimated accidents for investigated conflict situations. Clusters are colour coded as in CARE.

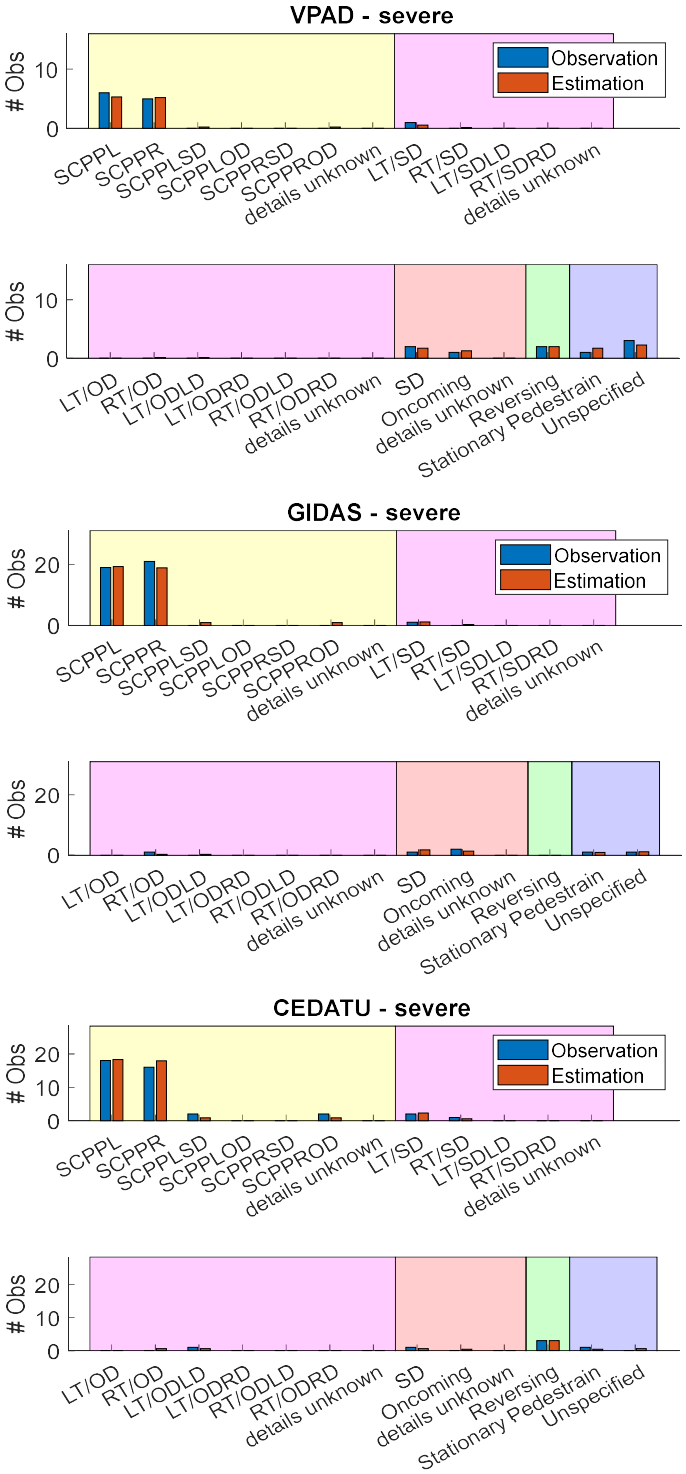

Figure A-10: Severe – observed and estimated accidents for investigated conflict situations. Clusters are colour coded as in CARE.

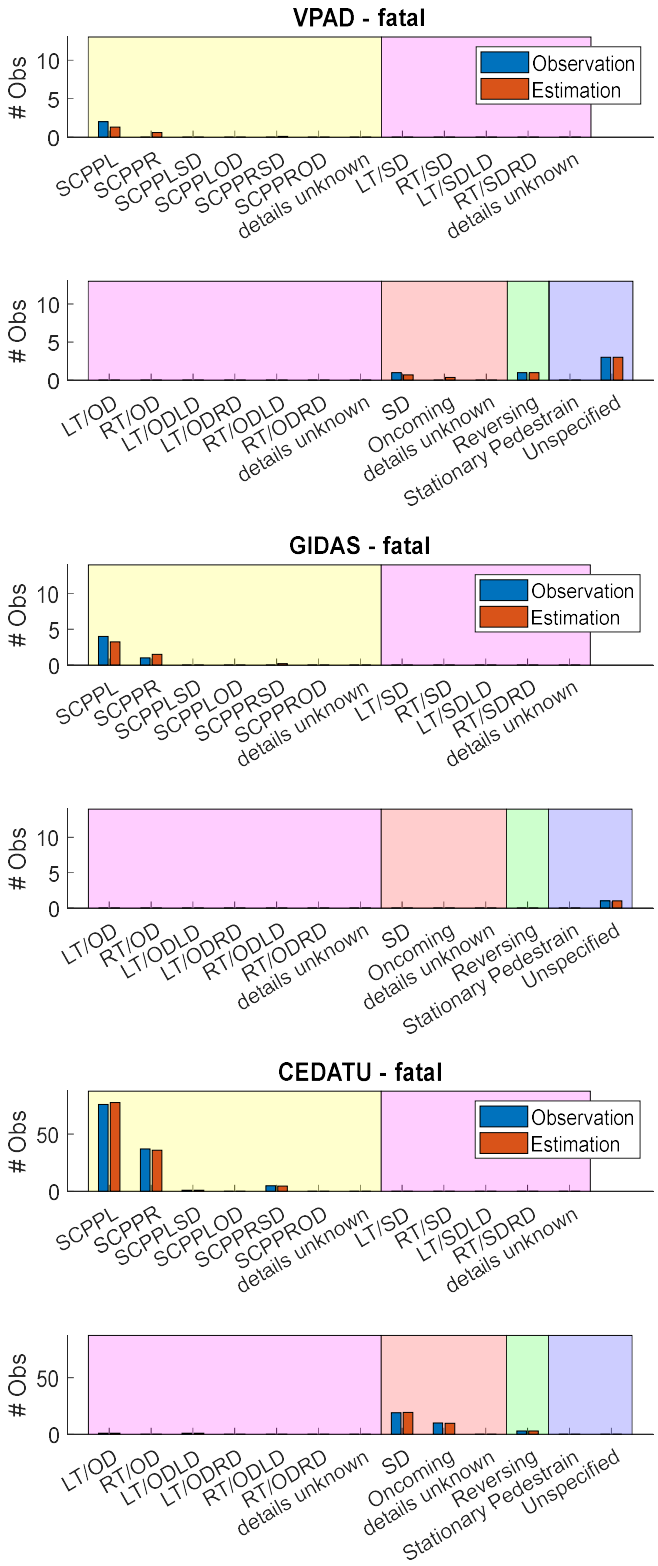

Figure A-11: Fatal – observed and estimated accidents for investigated conflict situations. Clusters are colour coded as in CARE.

A.4 Cyclists - Observed and Estimated Accidents per Conflict Situation

The observed and estimated accidents per conflict situation and different databases are shown below. Slight, severe and fatal injuries have been estimated and presented separately. The different clusters are colour coded according to STRADA in Figure Figure A-12 - Figure A-14and according to CARE in Figure A-15 - Figure A-17

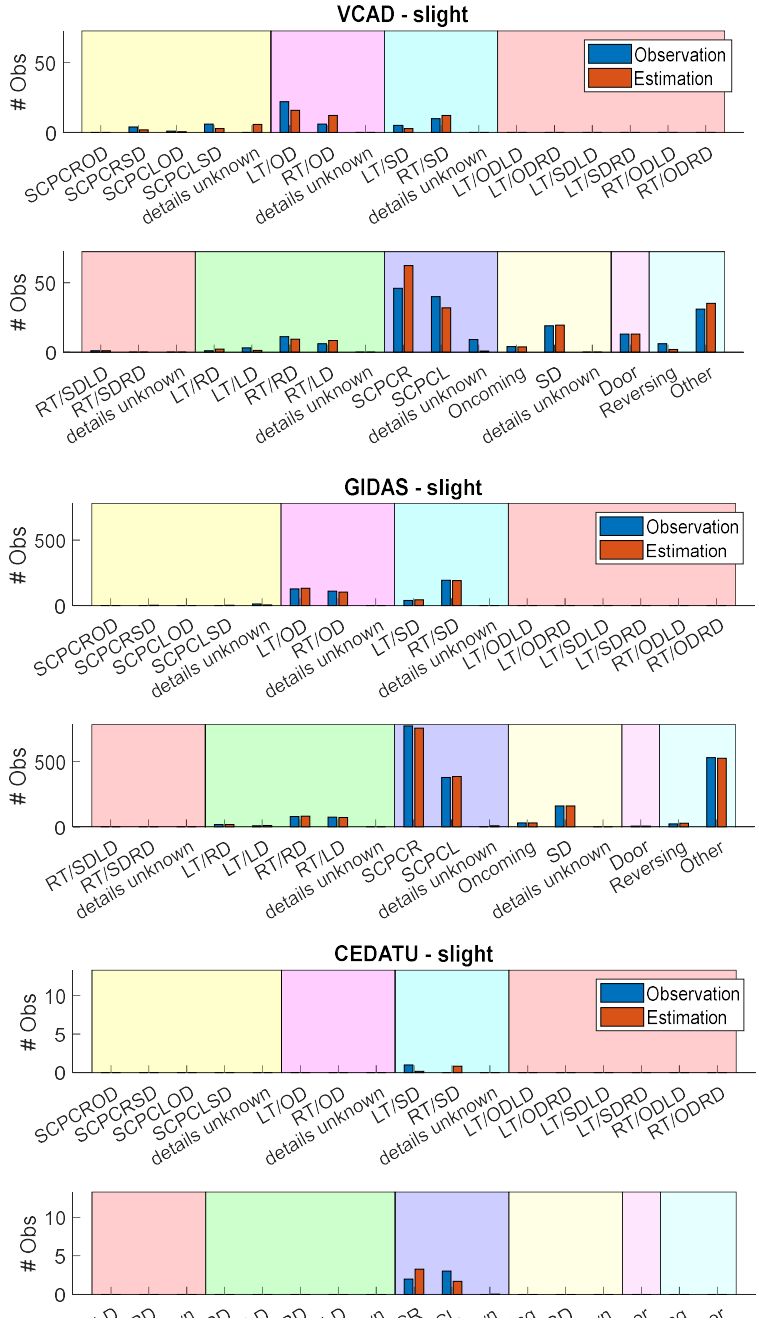

Figure A-12: Slight – observed and estimated accidents for investigated conflict situations. Cluster are colour coded as in STRADA.

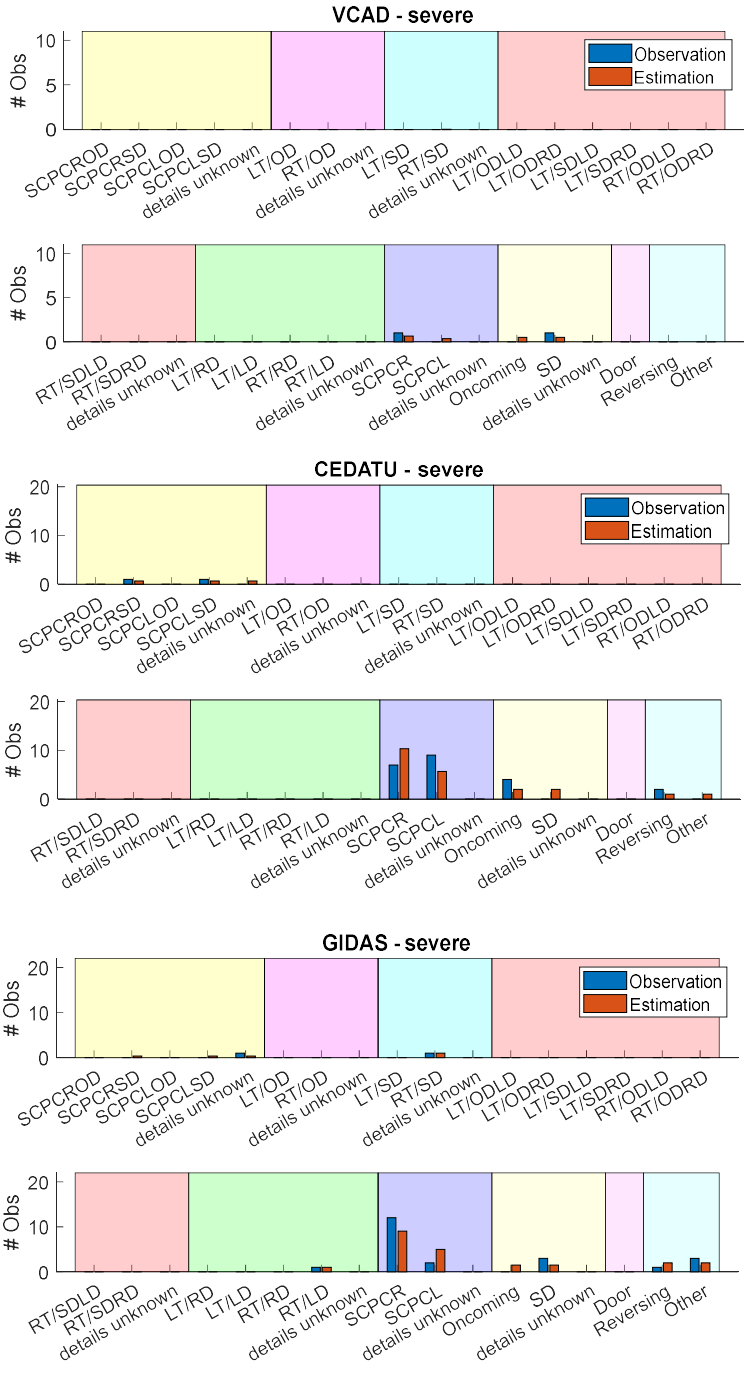

Figure A-13: Severe – observed and estimated accidents for investigated conflict situations. Clusters are colour coded as in STRADA.

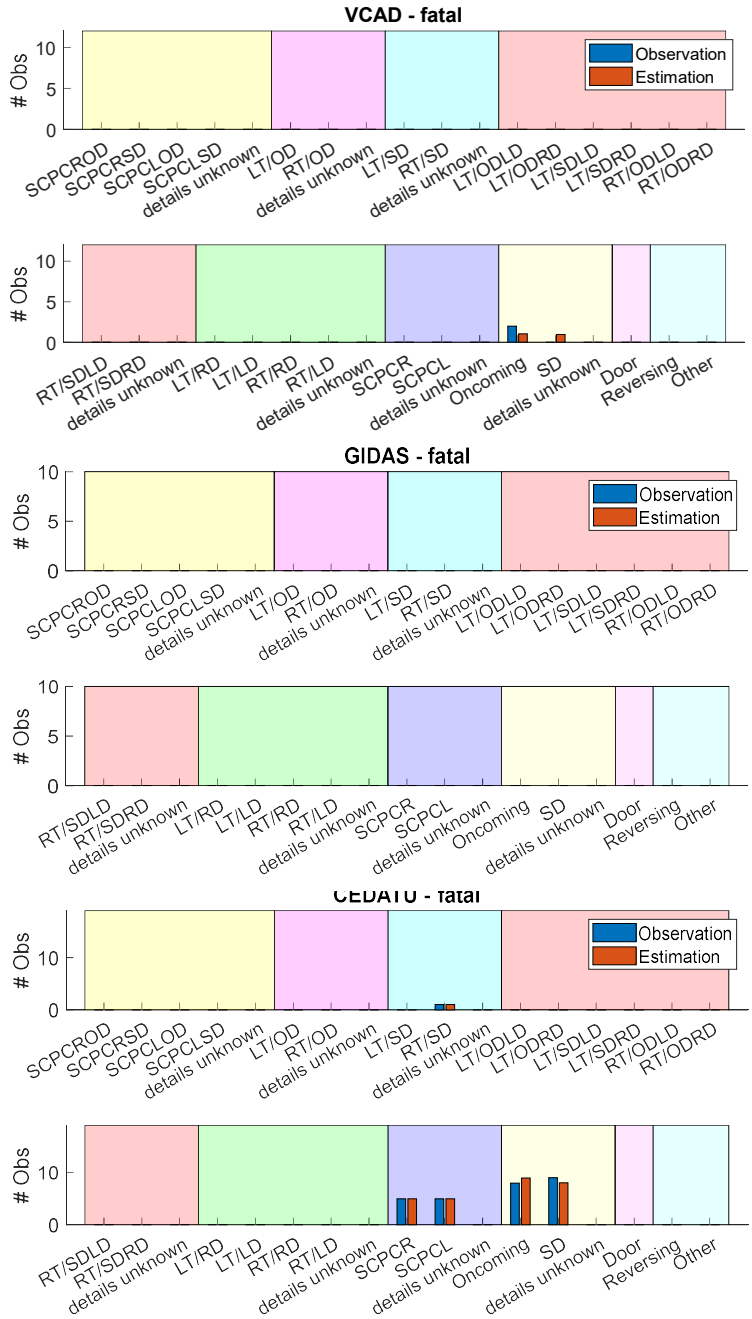

Figure A-14: Fatal – observed and estimated accidents for investigated conflict situations. Clusters are colour coded as in STRADA.

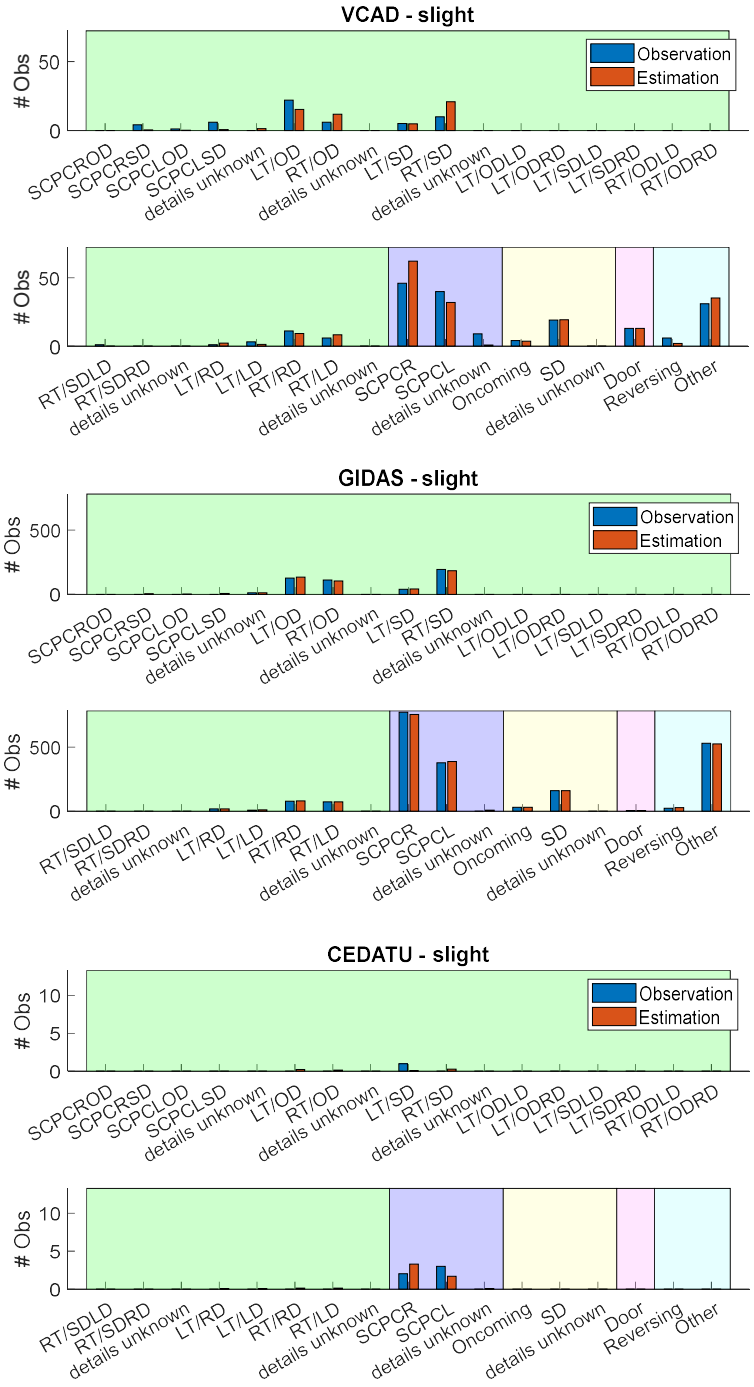

Figure A-15: Slight – observed and estimated accidents for investigated conflict situations. Clusters are colour coded as in CARE.

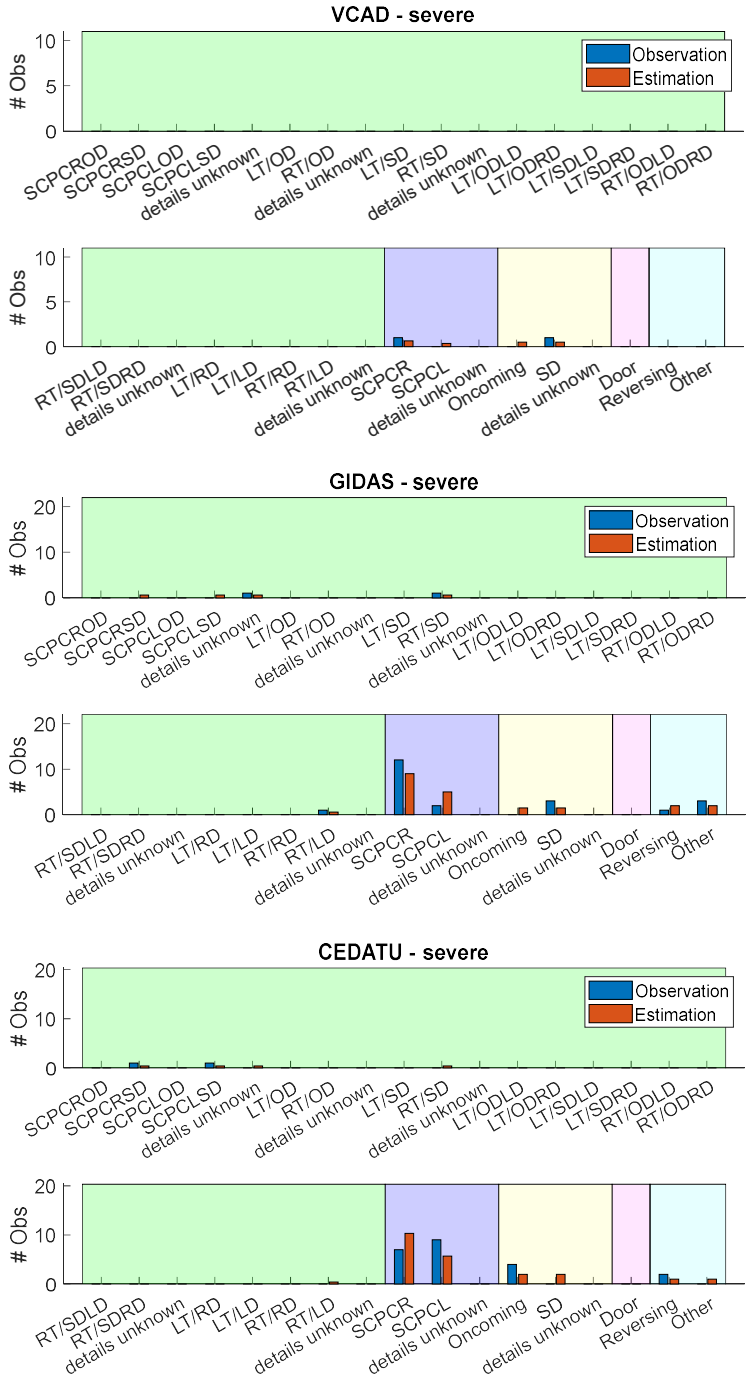

Figure A-16: Severe – observed and estimated accidents for investigated conflict situations. Clusters are colour coded as in CARE.

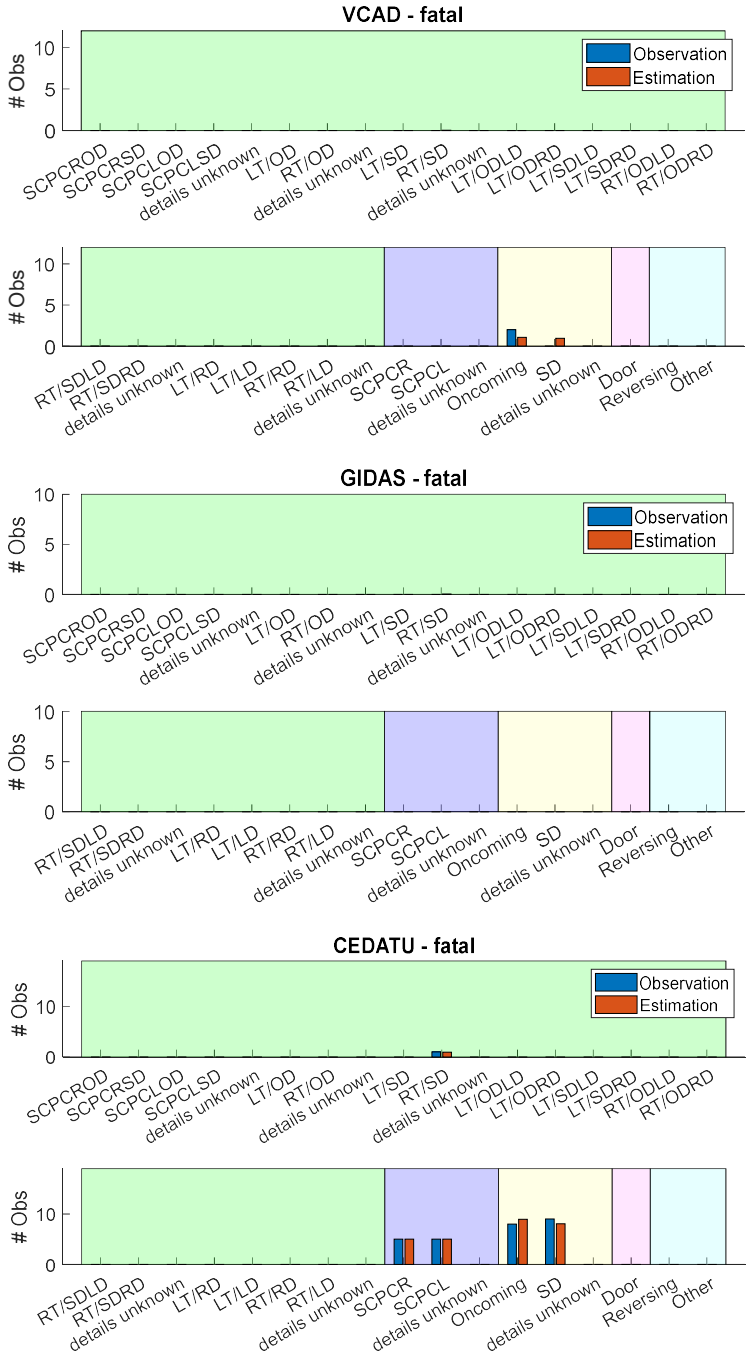

Figure A-17: Fatal – observed and estimated accidents for investigated conflict situations. Clusters are colour coded as in CARE.

A.5 Conflict Situation Probabilities

The conflict situation probabilities have been calculated per cluster. In the figures below, the clusters are colour coded according to the STRADA and CARE categorisation of clustering of conflict situations.

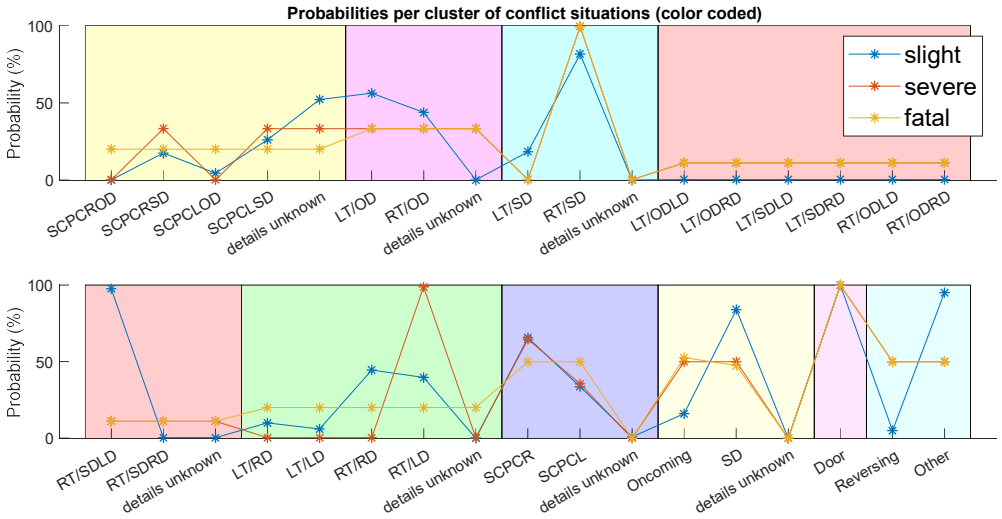

Figure A-18: Conflict situation probabilities for cyclists according to cluster of conflict situations as in STRADA.

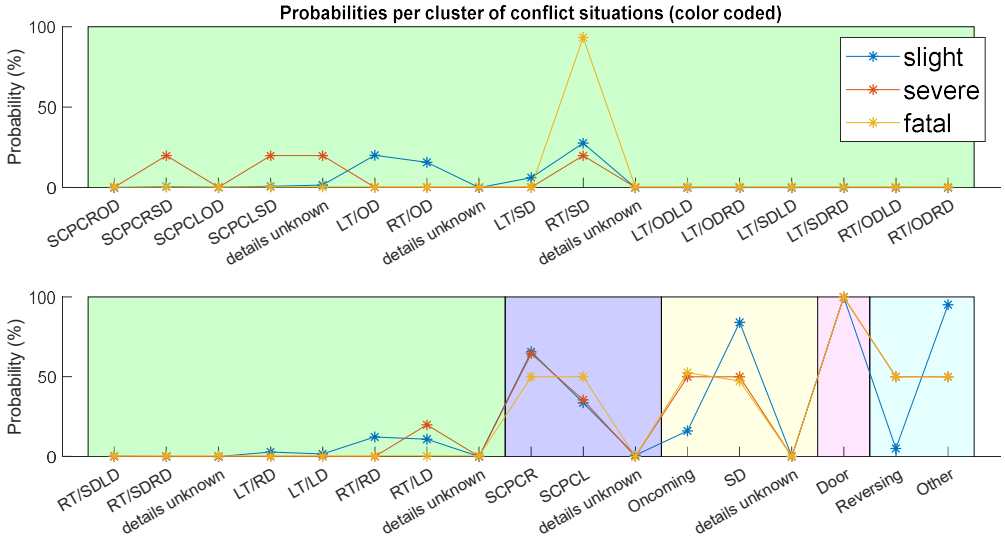

Figure A-19: Conflict situation probabilities for cyclists according to cluster of conflict situations as in CARE.

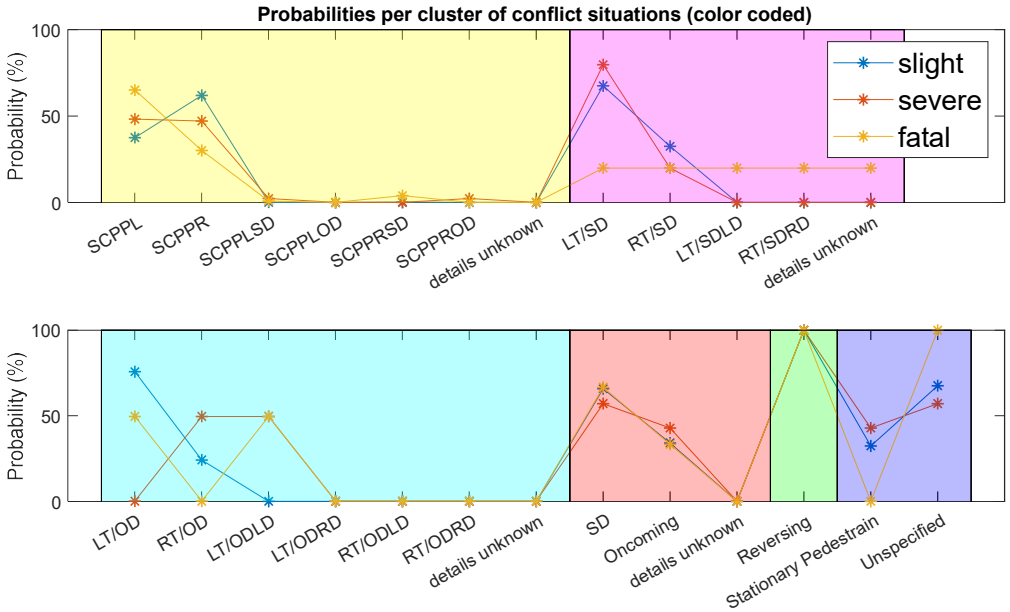

Figure A-20: Conflict situation probabilities for pedestrians according to cluster of conflict situations as in STRADA.

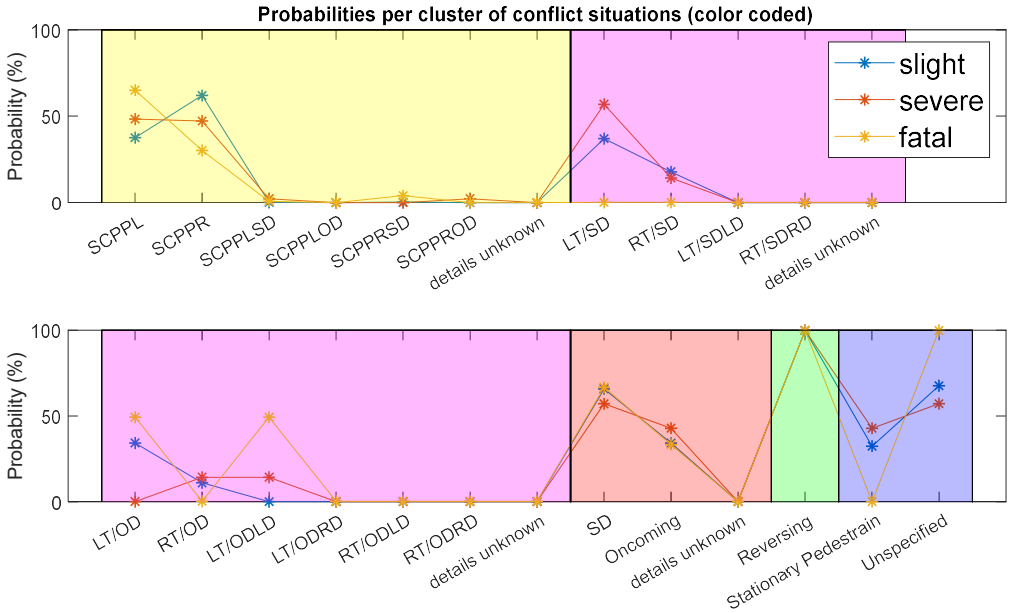

Figure A-21: Conflict situation probabilities for pedestrians according to cluster of conflict situations as in CARE.

A.6 Pedestrians – Verification with IGLAD

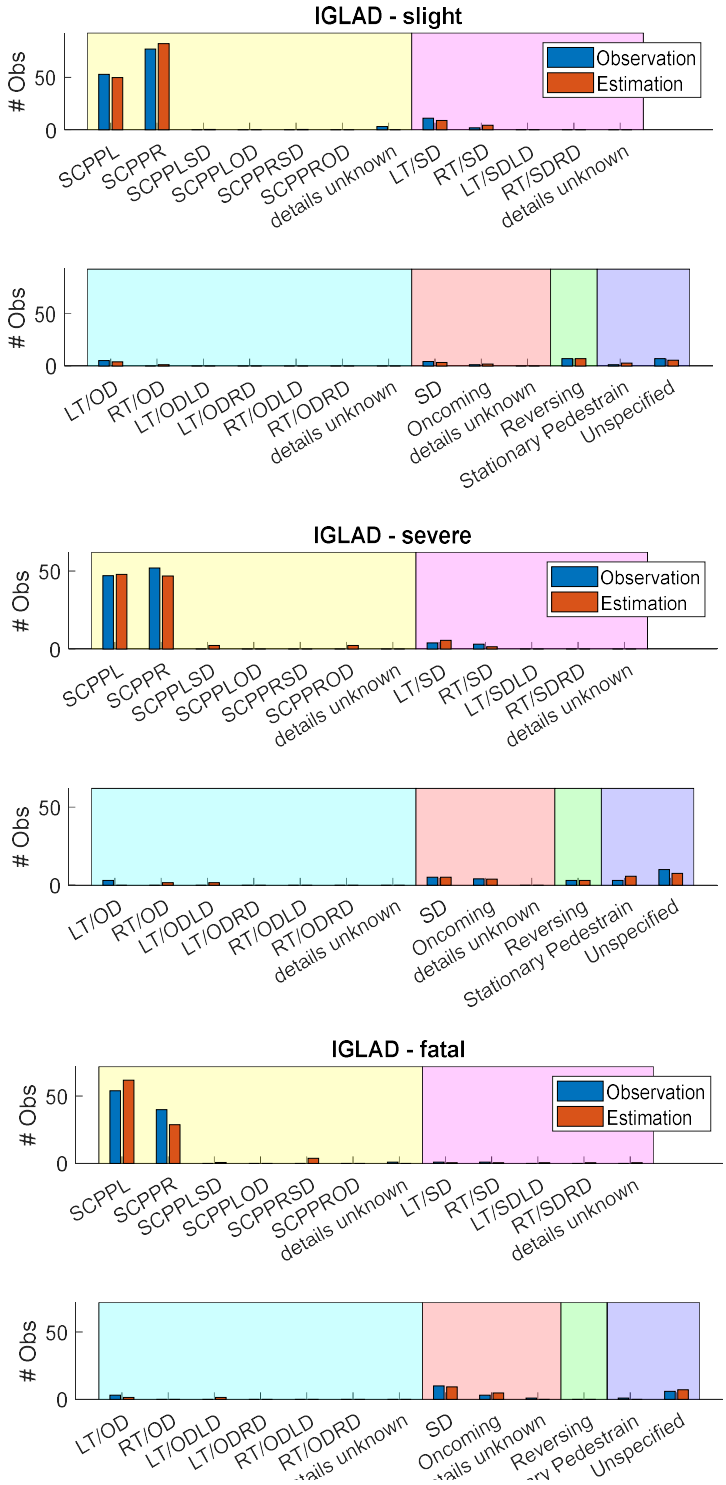

Figure A-22: Observed accidents per conflict situation and the number of accidents per conflict situation using estimated probabilities. Clusters are colour coded as in STRADA.

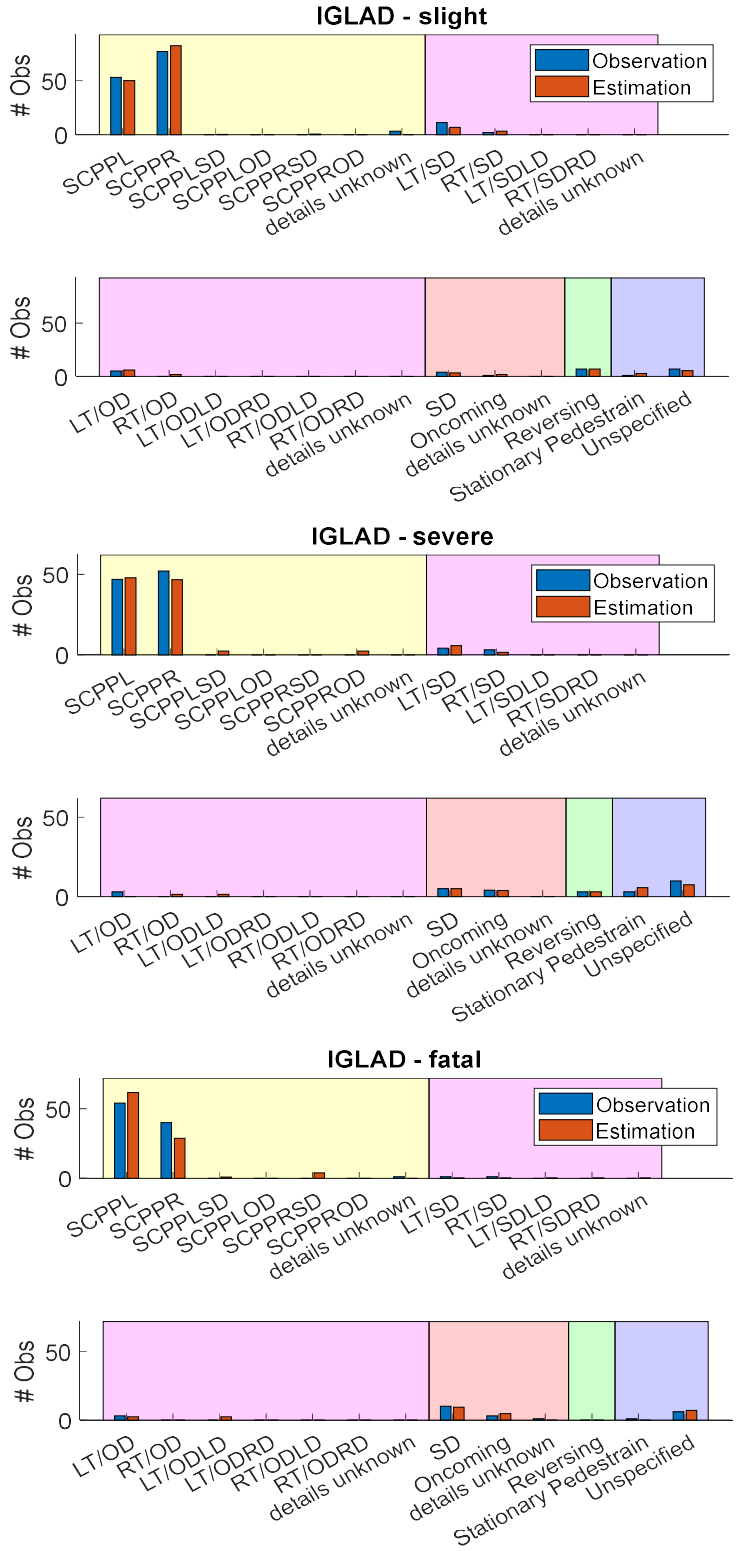

Figure A-23: Observed accidents per conflict situation and the number of accidents per conflict situation using estimated probabilities. Clusters are colour coded as in CARE.

A.7 Cyclists – Verification with IGLAD

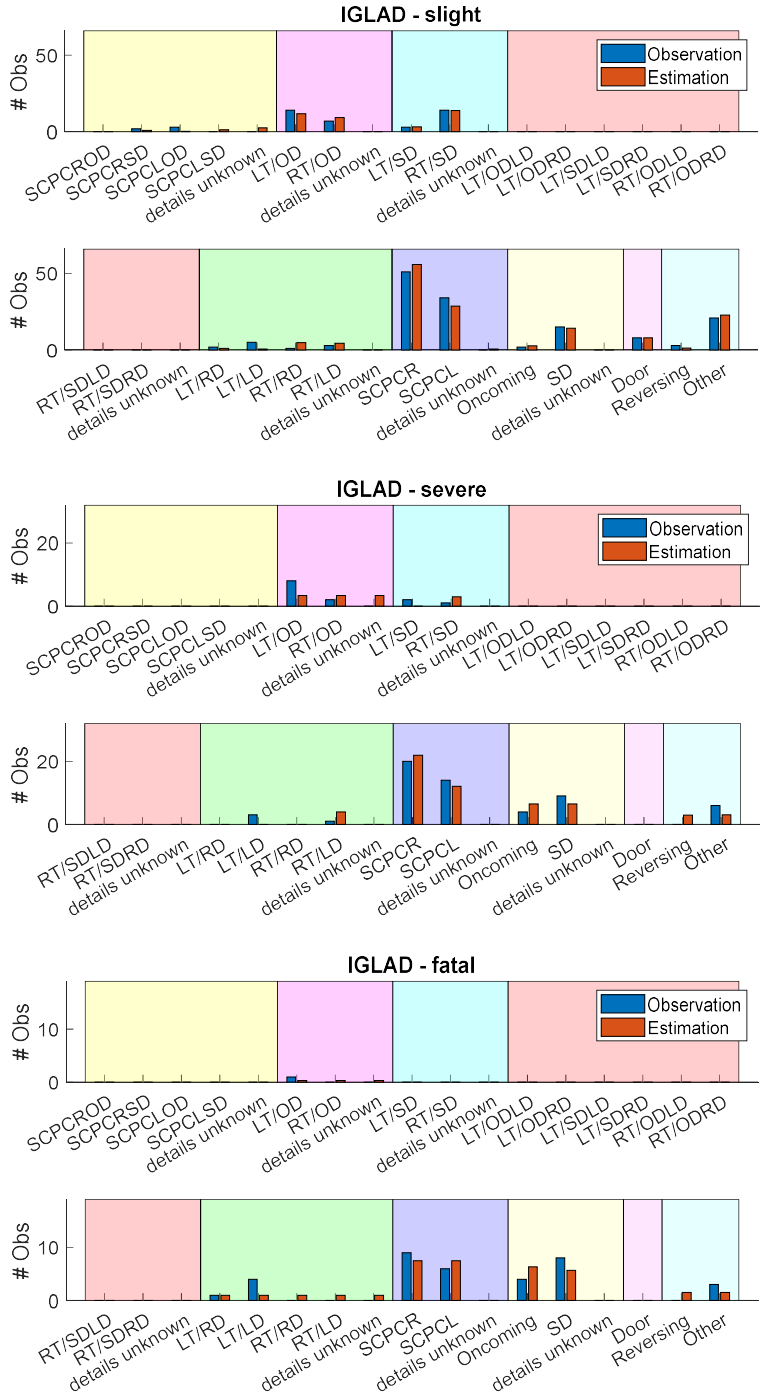

Figure A-24: Observed accidents per conflict situation and the number of accidents per conflict situation using estimated probabilities. Clusters are colour coded as in STRADA.

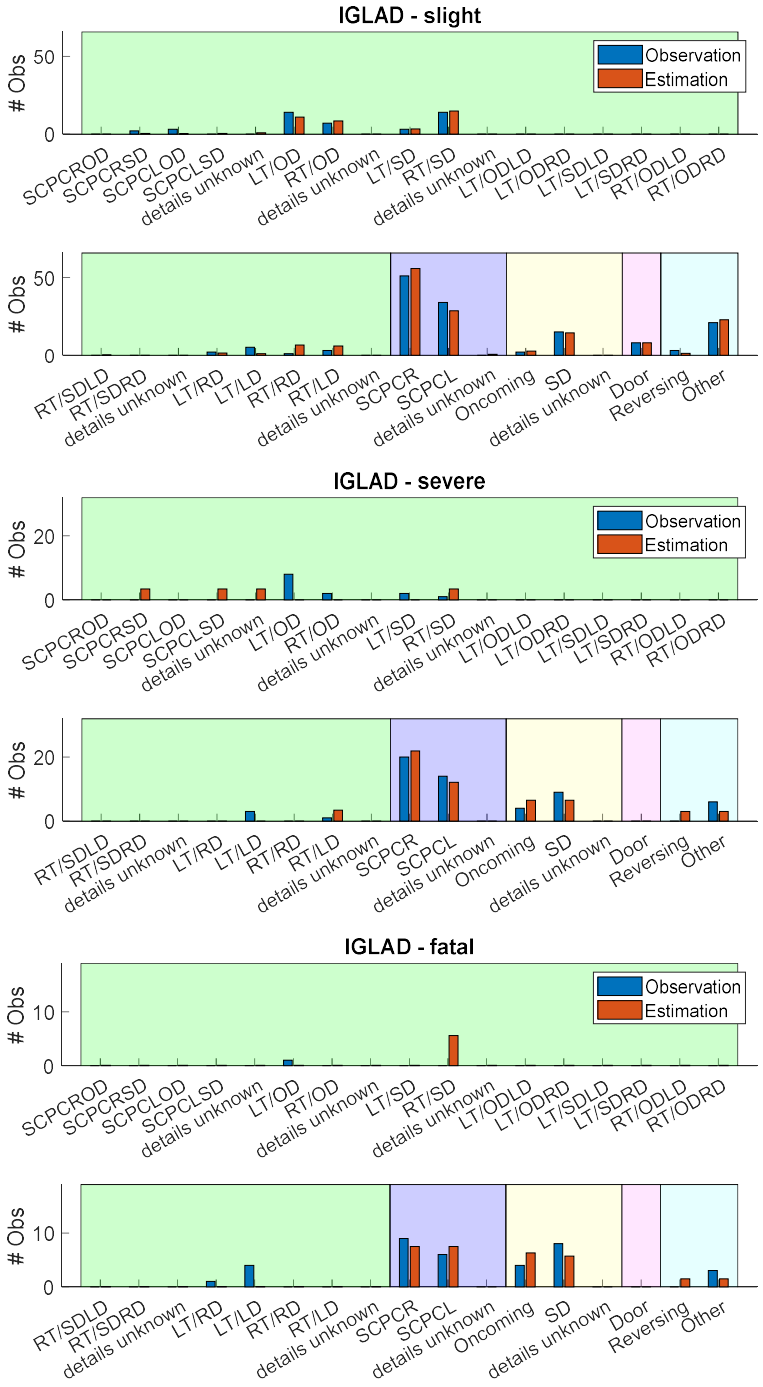

Figure A-25: Observed accidents per conflict situation and the number of accidents per conflict situation using estimated probabilities. Clusters are colour coded as in CARE.

A.8 Pedestrian – Comparison with Single Datasets

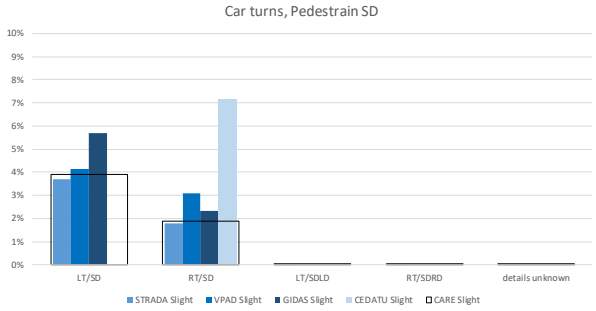

Figure A-26: Probability of conflict situations within the cluster "car turns, pedestrian same direction crossing" based on slight accidents.

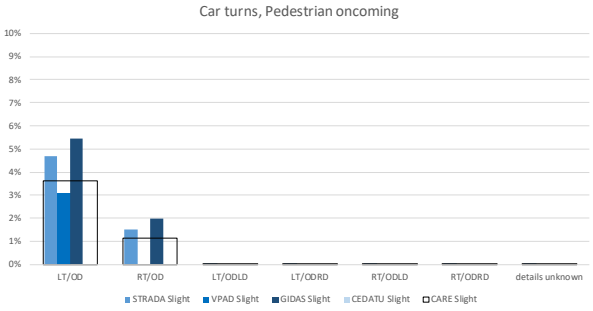

Figure A-27: Probability of conflict situations within the cluster "car turns, pedestrian oncoming" based on slight accidents.

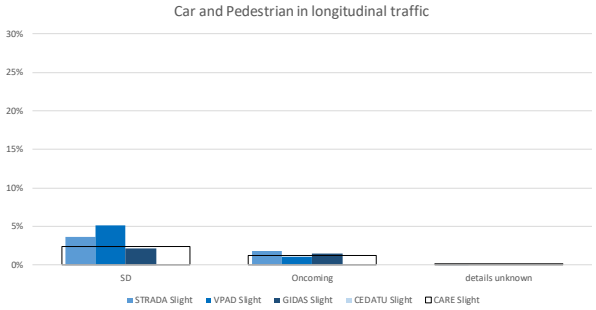

Figure A-28: Probability of conflict situations within the cluster "car and pedestrian in longitudinal traffic" based on slight accidents.

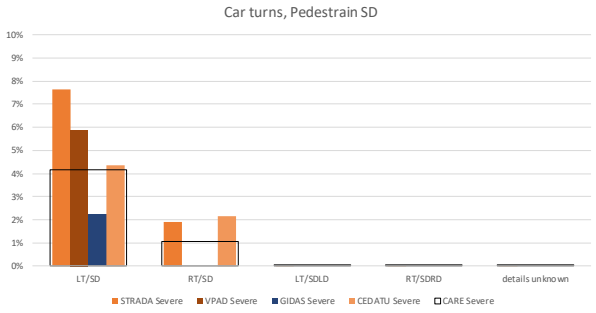

Figure A-29: Probability of conflict situations within the cluster "car turns, pedestrian same direction crossing" based on severe accidents.

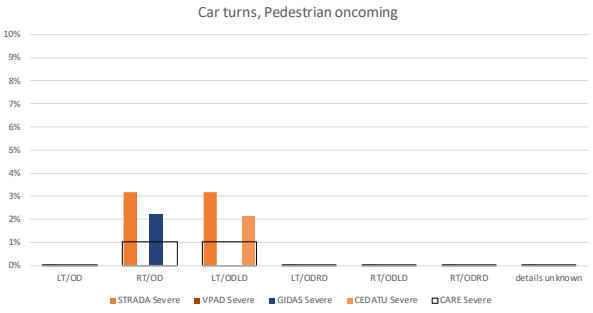

Figure A-30: Probability of conflict situations within the cluster "car turns, pedestrian oncoming" based on severe accidents.

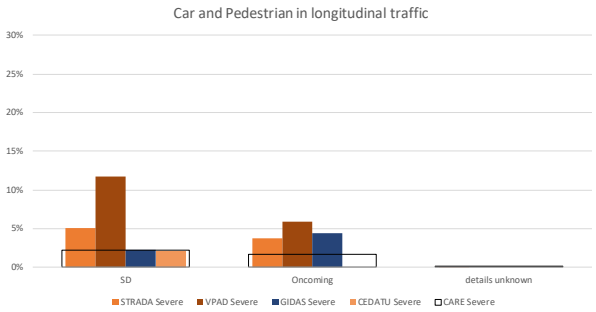

Figure A-31: Probability of conflict situations within the cluster "car and pedestrian in longitudinal traffic" based on slight accidents.

No data available

Figure A-32: Probability of conflict situations within the cluster "car turns, pedestrian same direction crossing" based on fatal accidents.

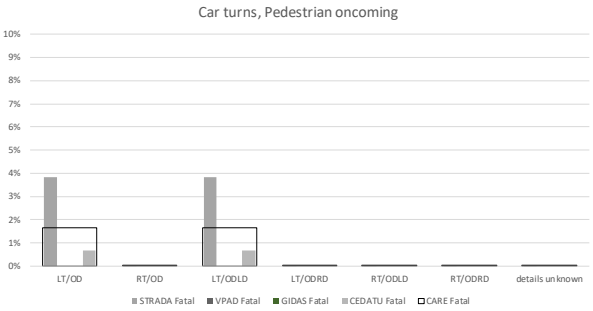

Figure A-33: Probability of conflict situations within the cluster "car turns, pedestrian oncoming" based on fatal accidents.

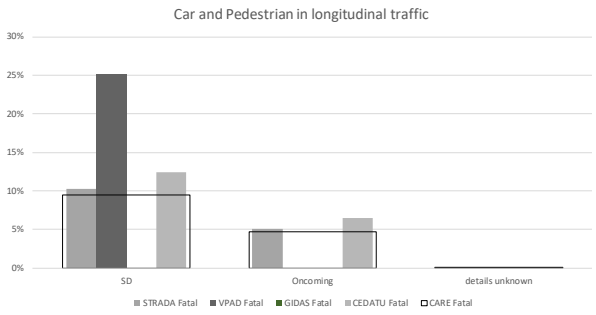

Figure A-34: Probability of conflict situations within the cluster "car and pedestrian in longitudinal traffic" based on fatal accidents.

A.9 Cyclist – Comparison with Single Datasets

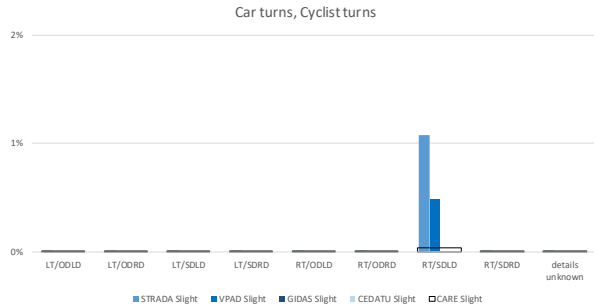

Figure A-35: Probability of conflict situations within the cluster "car turns, cyclist turns" based on slight accidents.

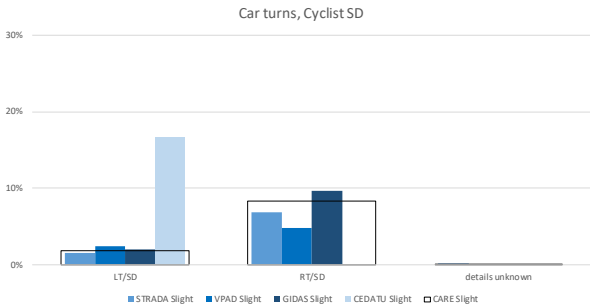

Figure A-36: Probability of conflict situations within the cluster "car turns, cyclist same direction" based on slight accidents.

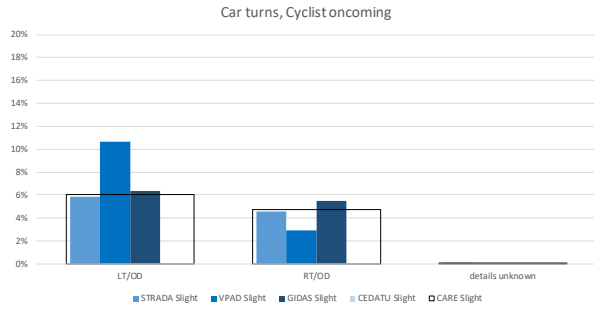

Figure A-37: Probability of conflict situations within the cluster "car turns, cyclist oncoming" based on slight accidents.

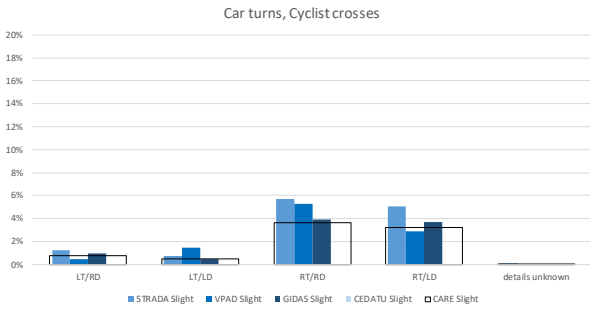

Figure A-38: Probability of conflict situations within the cluster "car turns, cyclist crossing" based on slight accidents.

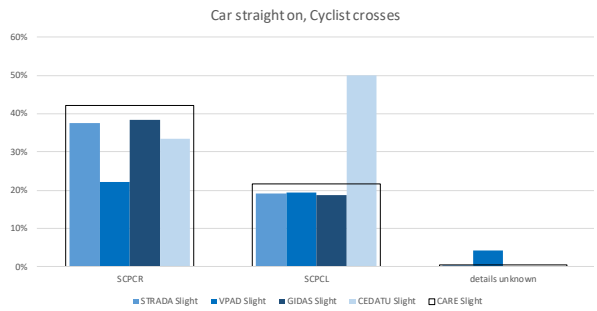

Figure A-39: Probability of conflict situations within the cluster "car straight on, cyclist crosses" based on slight accidents.

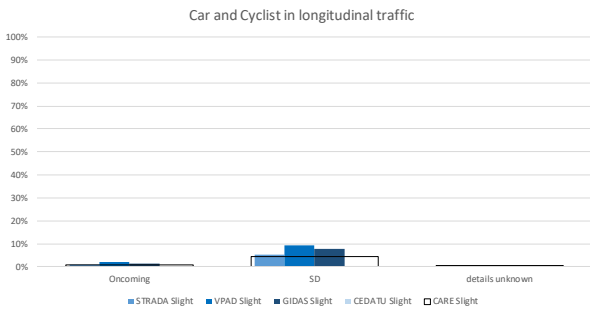

Figure A-40: Probability of conflict situations within the cluster "car and cyclist in longitudinal traffic" based on slight accidents.

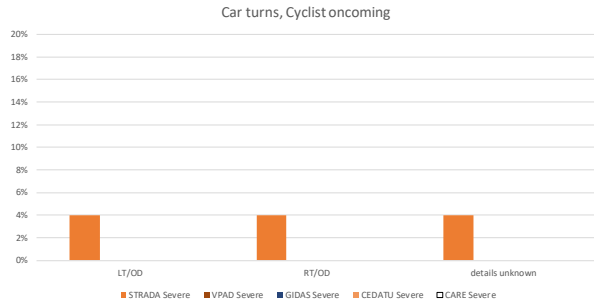

Figure A-41: Probability of conflict situations within the cluster "car turns, cyclist turning" based on severe accidents.

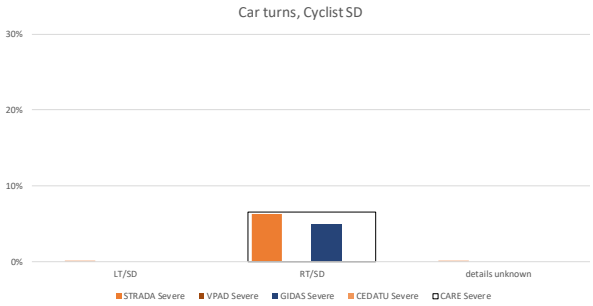

Figure A-42: Probability of conflict situations within the cluster "car turns, cyclist same direction" based on severe accidents.

No data available

Figure A-43: Probability of conflict situations within the cluster "car turns, cyclist oncoming" based on severe accidents.

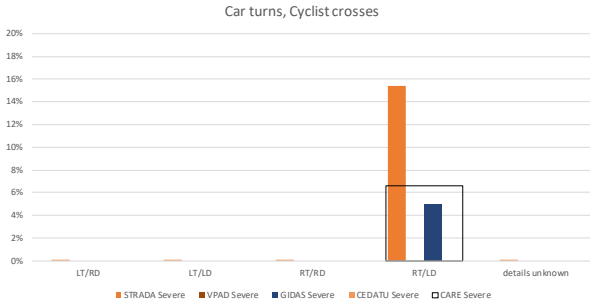

Figure A-44: Probability of conflict situations within the cluster "car turns, cyclist crossing" based on severe accidents.

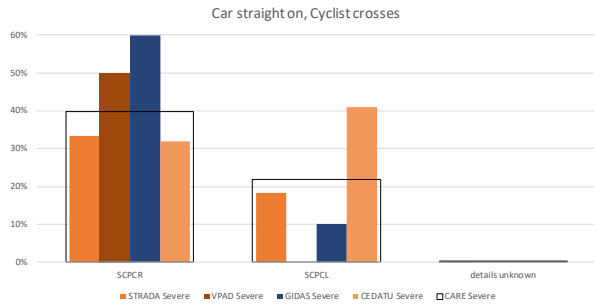

Figure A-45: Probability of conflict situations within the cluster "car straight on, cyclist crossing" based on severe accidents.

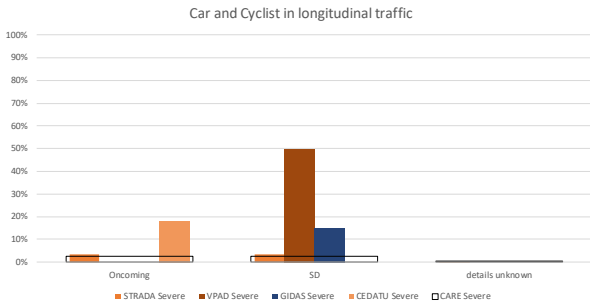

Figure A-46: Probability of conflict situations within the cluster "car and cyclist in longitudinal traffic" based on severe accidents.

No data available

Figure A-47: Probability of conflict situations within the cluster "car turns, cyclist turning" based on fatal accidents.

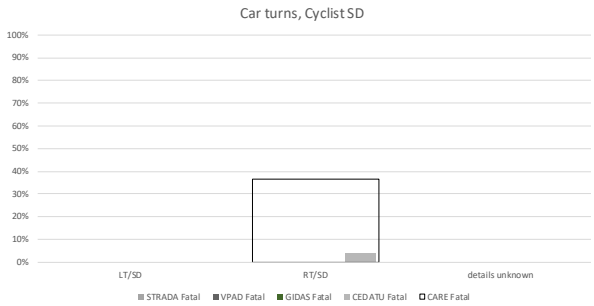

Figure A-48: Probability of conflict situations within the cluster "car turns, cyclist same direction" based on fatal accidents.

No data available

Figure A-49: Probability of conflict situations within the cluster "car turns, cyclist oncoming" based on fatal accidents.

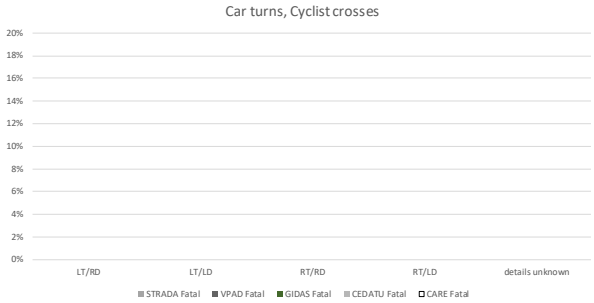

Figure A-50: Probability of conflict situations within the cluster "car turns, cyclist crossing" based on fatal accidents.

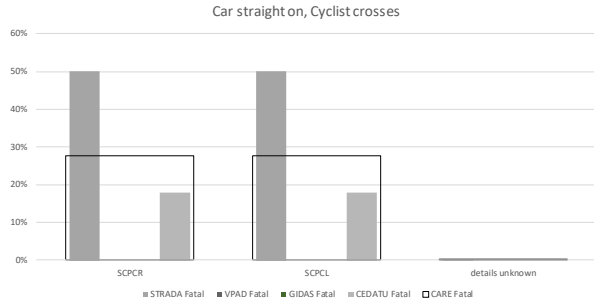

Figure A-51: Probability of conflict situations within the cluster "car straight on, cyclist crossing" based on fatal accidents.

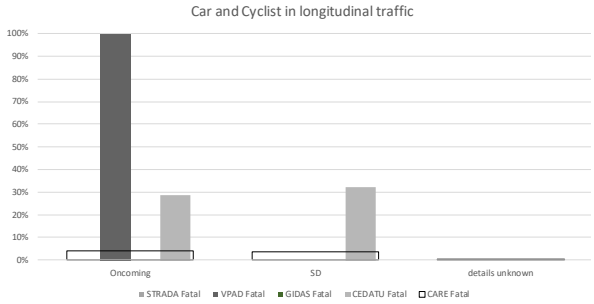

Figure A-52: Probability of conflict situations within the cluster "car and cyclist in longitudinal traffic" based on fatal accidents.

B. Probability of Accident Parameters

B.1 Initial Vehicle Speeds for Pedestrian - Car Accidents

	Slight	Severe	Fatal
SCPPL	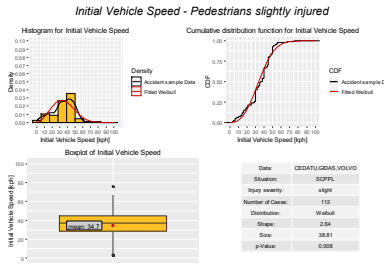	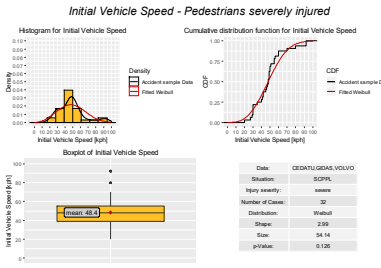	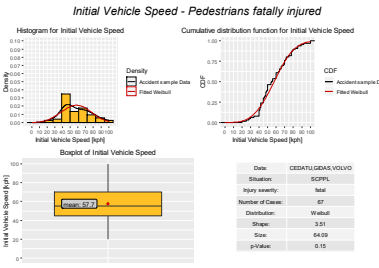
SCPPR	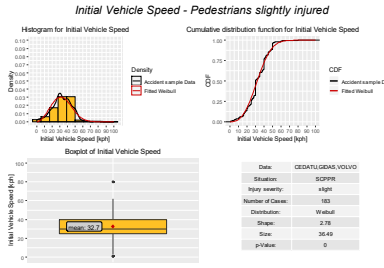	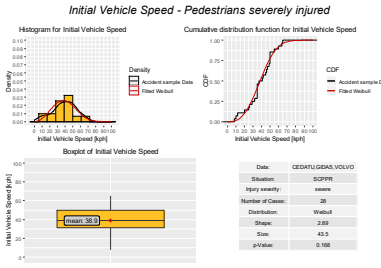	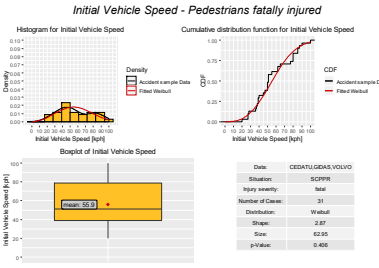
LT/SD	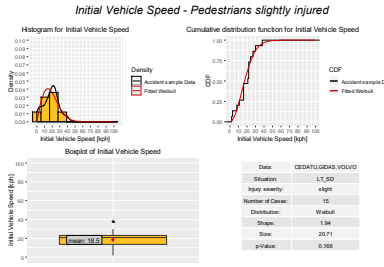	Not enough data	Not enough data
LT/OD	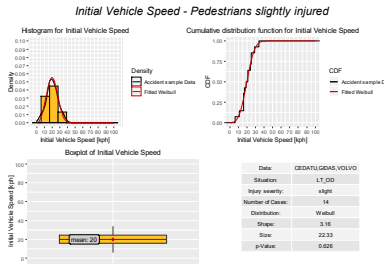	Not enough data	Not enough data

	Slight	Severe	Fatal
Reversing	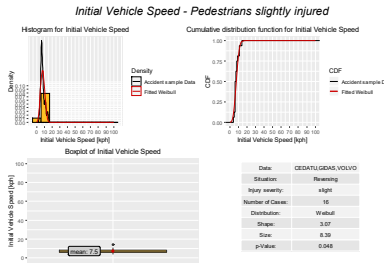	Not enough data	Not enough data
Unspecified	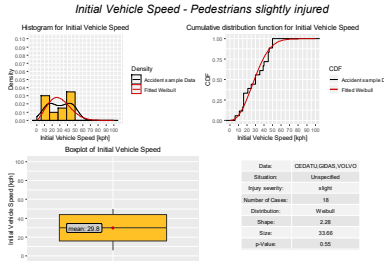	Not enough data	Not enough data
Overall	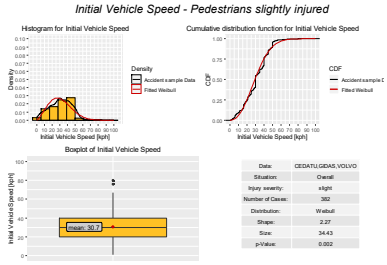	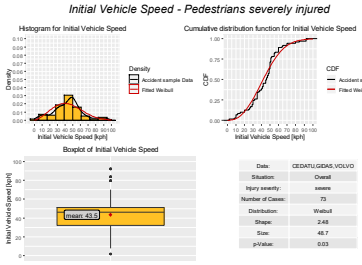	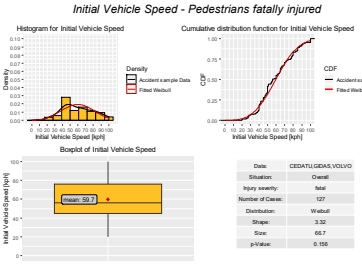

B.2 Initial Pedestrian Speeds for Pedestrian – Car Accidents

	Slight	Severe	Fatal
SCPPL	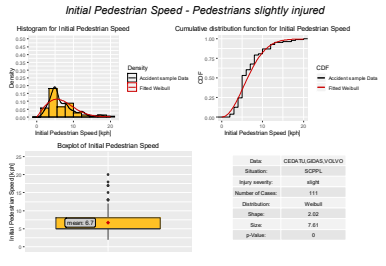	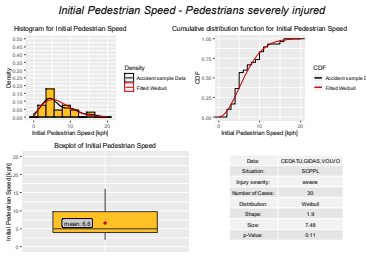	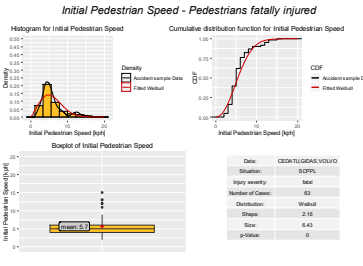

	Slight	Severe	Fatal
SCPPR	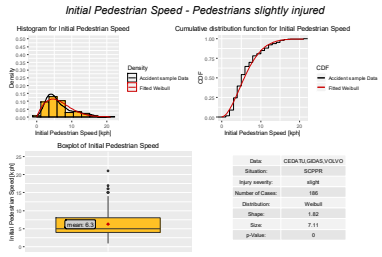	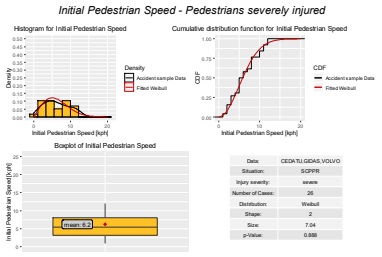	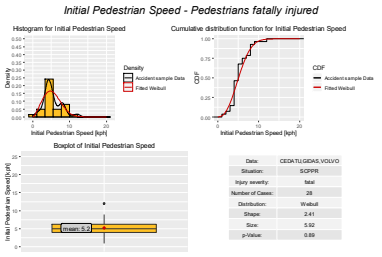
LT/SD	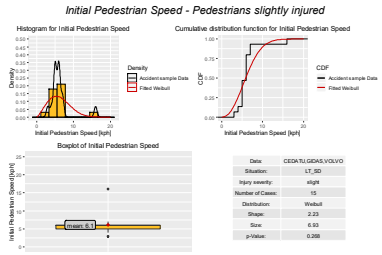	Not enough data	Not enough data
LT/OD	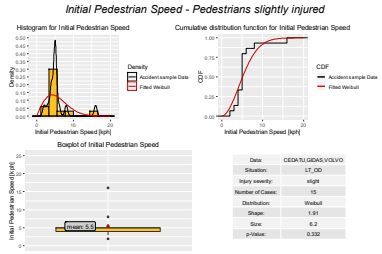	Not enough data	Not enough data
Reversing	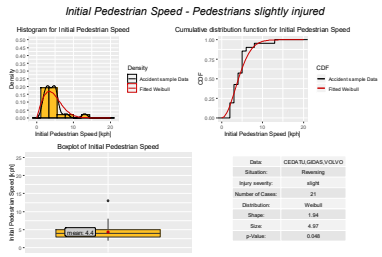	Not enough data	Not enough data
Unspecified	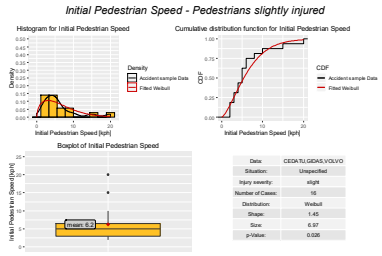	Not enough data	Not enough data

	Slight	Severe	Fatal
Overall	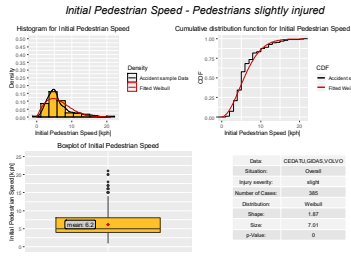 *Initial Pedestrian Speed - Pedestrians slightly injured*	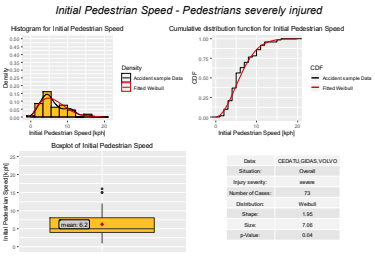 *Initial Pedestrian Speed - Pedestrians severely injured*	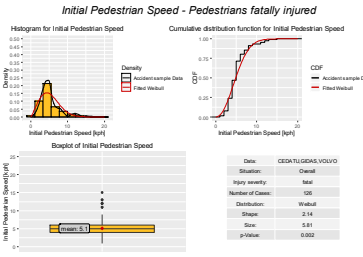 *Initial Pedestrian Speed - Pedestrians fatally injured*

B.3 Initial Vehicle Speeds for Cyclist - Car Accidents

	Slight	Severe	Fatal
SCPCR	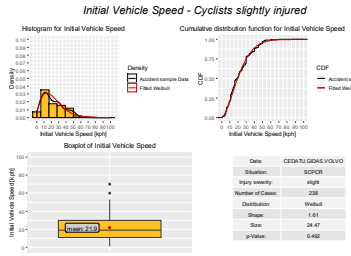 *Initial Vehicle Speed - Cyclists slightly injured*	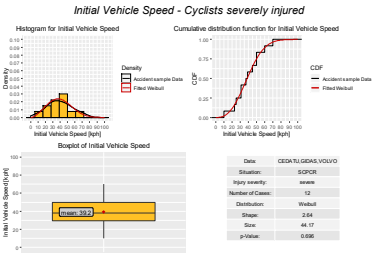 *Initial Vehicle Speed - Cyclists severely injured*	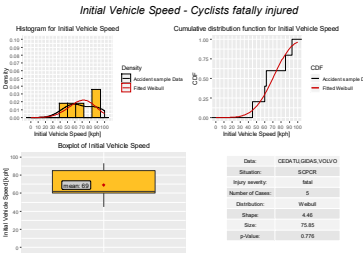 *Initial Vehicle Speed - Cyclists fatally injured*
SCPCL	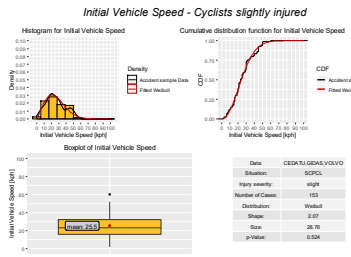 *Initial Vehicle Speed - Cyclists slightly injured*	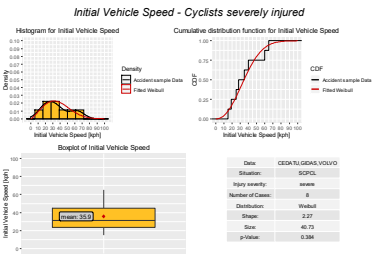 *Initial Vehicle Speed - Cyclists severely injured*	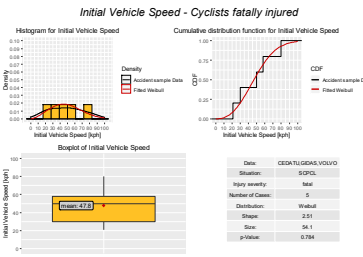 *Initial Vehicle Speed - Cyclists fatally injured*
LD/OD	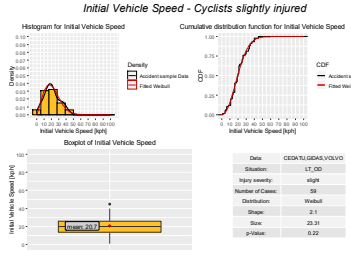 *Initial Vehicle Speed - Cyclists slightly injured*	Not enough data	Not enough data
RT/OD	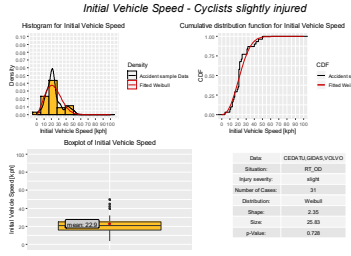 *Initial Vehicle Speed - Cyclists slightly injured*	Not enough data	Not enough data

	Slight	Severe	Fatal
LD/SD	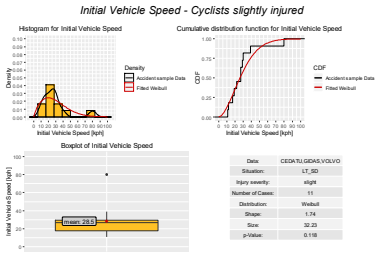	Not enough data	Not enough data
RT/SD	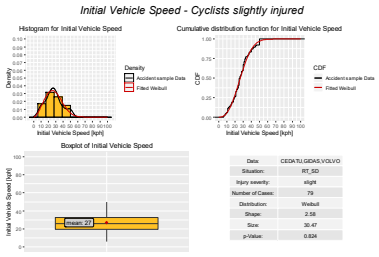	Not enough data	Not enough data
RT/RD	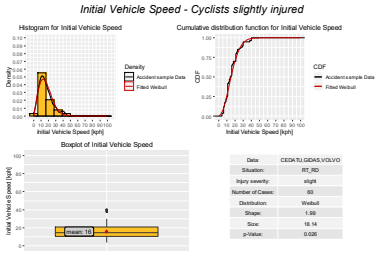	Not enough data	Not enough data
RT/LD	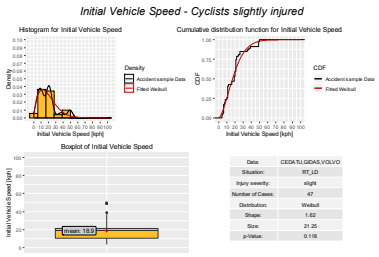	Not enough data	Not enough data
Oncoming	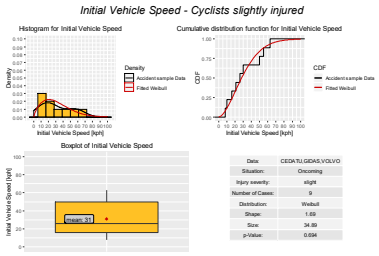	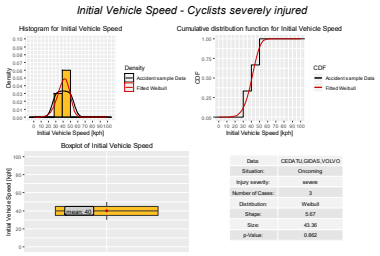	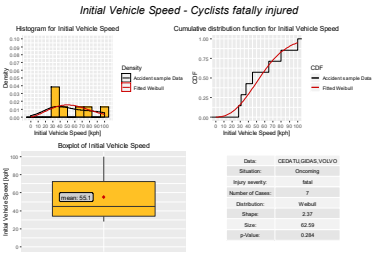

	Slight	Severe	Fatal
SD	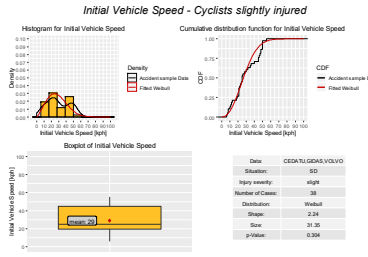	Not enough data	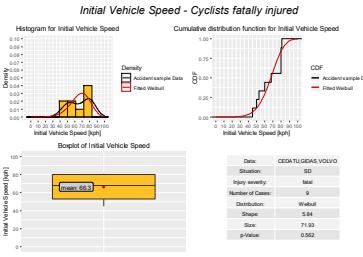
Other	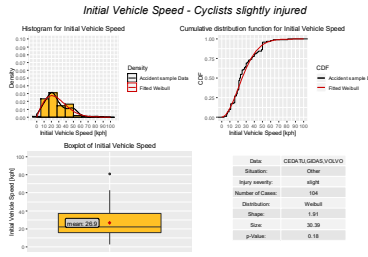	Not enough data	Not enough data
Overall	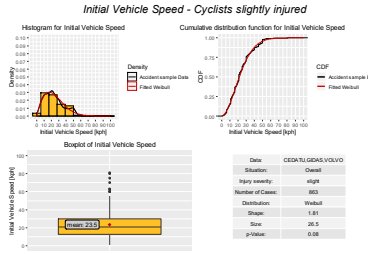	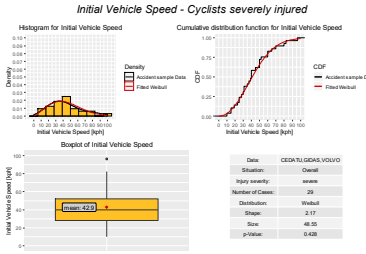	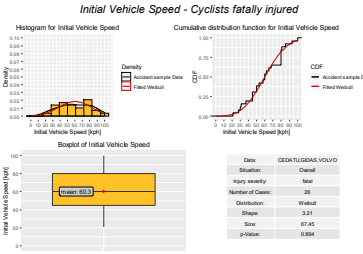

B.4 Initial Cyclist Speeds for Cyclist - Car Accidents

	Slight	Severe	Fatal
SCPCR	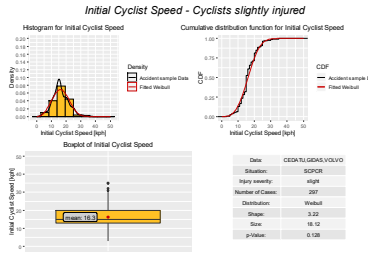	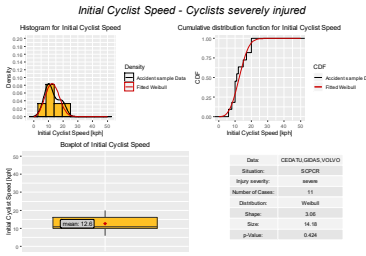	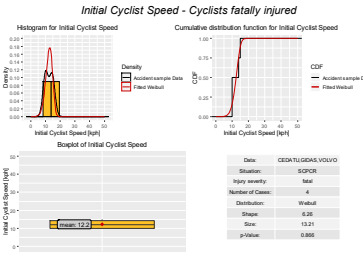
SCPCL	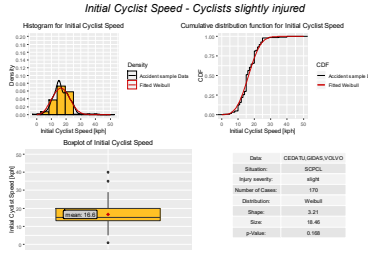	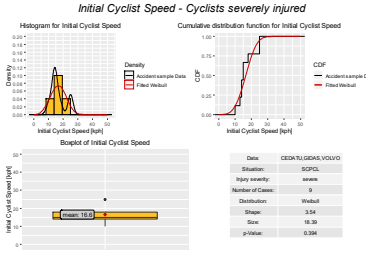	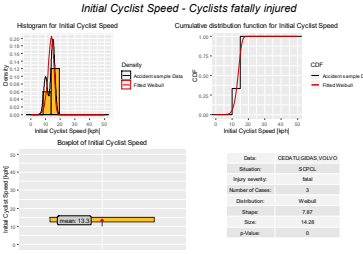

	Slight	Severe	Fatal
LD/OD	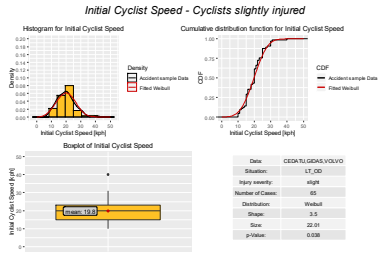	Not enough data	Not enough data
RT/OD	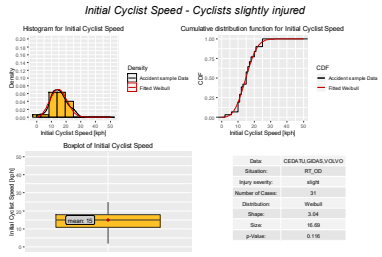	Not enough data	Not enough data
LD/SD	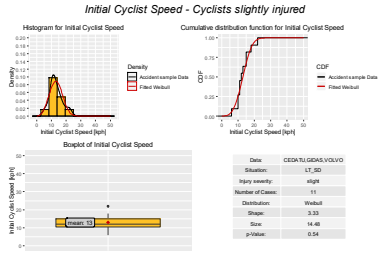	Not enough data	Not enough data
RT/SD	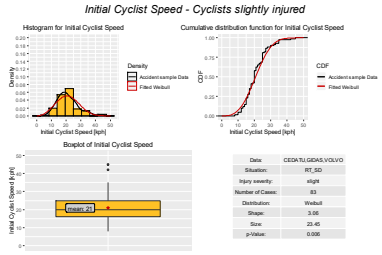	Not enough data	Not enough data
RT/RD	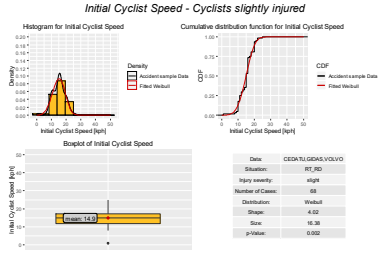	Not enough data	Not enough data

	Slight	Severe	Fatal
RT/LD	*Initial Cyclist Speed - Cyclists slightly injured* 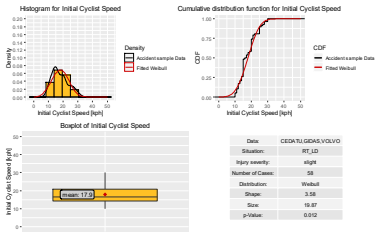	Not enough data	Not enough data
Oncoming	*Initial Cyclist Speed - Cyclists slightly injured* 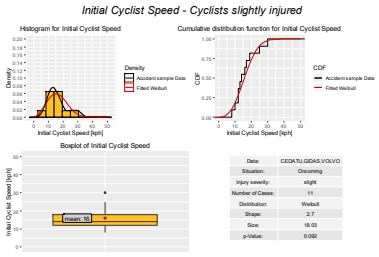	*Initial Cyclist Speed - Cyclists severely injured* 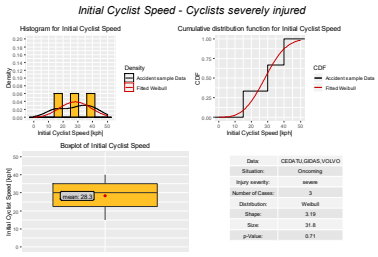	*Initial Cyclist Speed - Cyclists fatally injured* 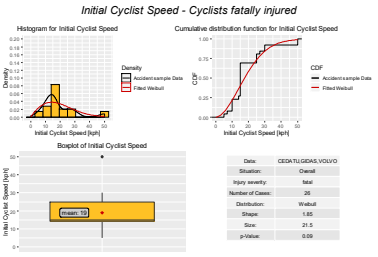
SD	*Initial Cyclist Speed - Cyclists slightly injured* 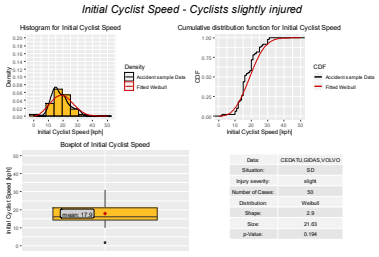	Not enough data	*Initial Cyclist Speed - Cyclists fatally injured* 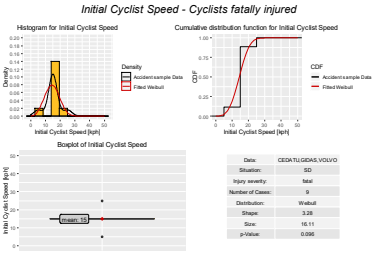
Other	*Initial Cyclist Speed - Cyclists slightly injured* 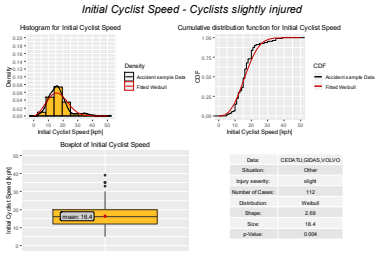	Not enough data	Not enough data
Overall	*Initial Cyclist Speed - Cyclists slightly injured* 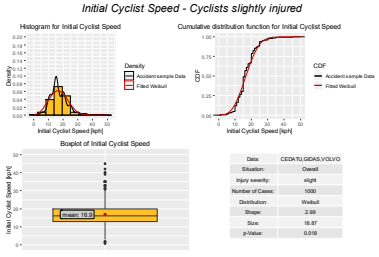	*Initial Cyclist Speed - Cyclists severely injured* 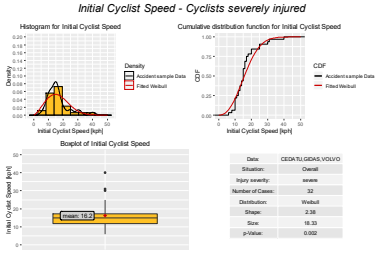	*Initial Cyclist Speed - Cyclists fatally injured* 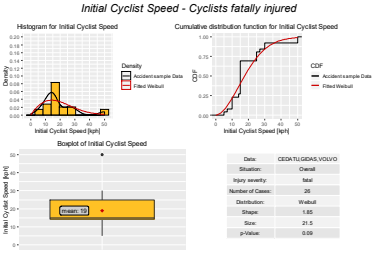

C. Pre-crash Tool

C.1 Input Files for the Simulation Platform

C.1.1 Example of a sceneryConfiguration.xml

```
<?xml version="1.0" encoding="UTF-8"?>
<PCM>
  <global_data>
    <OffsetX>5.834024911e+195</OffsetX>
    <OffsetY>2.128697896e-314</OffsetY>
    <Participants>30342724</Participants>
    <SimulationVersion>24023176</SimulationVersion>
  </global_data>
  <Marks>
    <marks_continuous/>
    <marks_interrupted_long/>
    <marks_interrupted_short/>
    <roadside/>
  </Marks>
  <Objects>
    <objects>
      <line id="0">
        <point id="0">
          <x>0</x>
          <y>0</y>
          <z>0</z>
        </point>
      </line>
      <ObjectType>0</ObjectType>
    </objects>
  </Objects>
  <ViewObjects>
    <view_object/>
  </ViewObjects>
  <intended_course/>
  <Trajectories>
   <Trajectory id="0">
    <Time>0, 10, 20, 30, 40, 50, 60<Time>
    <XPos>60.0032, 59.8782, 59.7532, 59.6283, 59.5033, 59.3783<XPos>
    <YPos>0.819, 0.8173, 0.8156, 0.8139, 0.8122, 0.8105, 0.8088,
    <VelocityX>12.5, 12.4992, 12.4985, 12.4977, 12.4969, 12.4962,
    <VelocityY>0, 0, 0, 0, 0, 0, 0, 0, 0,
    <Angle>-3.1279, -3.1279, -3.1279, -3.1279, -3.1279, -3.1279
   </Trajectory>
  <Trajectory id="1">
  ...
  </Trajectory>
</PCM>
```

C.1.2 Example of a runConfiguration.xml

```
<?xml version="1.0" encoding="UTF-8"?>
<RunConfiguration>
  <StartTime>0</StartTime>
  <EndTime>9820</EndTime>
  <NumberInvocations>1</NumberInvocations>
  <Weekday>undefined</Weekday>
  <TimeOfDay>-1</TimeOfDay>
  <WorldLibrary>World_PCM</WorldLibrary>
  <Stochastics>Stochastics</Stochastics>
  <CollisionDetection>CollisionDetection_Impact</CollisionDetection>
  <RandomSeed>0</RandomSeed>
  <SpawnPoints>
    <SpawnPoint id="0" library="SpawnPoint_PCM">
      <AgentRefs>
        <AgentRef>0</AgentRef>
      </AgentRefs>
      <SpawnPointParameters>
        <Double id="0" name="PositionX" value="60.0032"/>
        <Double id="1" name="PositionY" value="0.81899999999999995"/>
        <Double id="2" name="VelocityX" value="12.5"/>
        <Double id="3" name="VelocityY" value="0"/>
        <Double id="4" name="AccelerationX" value="-0.043299999999999998"/>
        <Double id="5" name="AccelerationY" value="0"/>
        <Double id="6" name="YawAngle" value="-3.1278999999999999"/>
      </SpawnPointParameters>
    </SpawnPoint>
    <SpawnPoint id="1" library="SpawnPoint_PCM">
      <AgentRefs>
        <AgentRef>1</AgentRef>
      </AgentRefs>
      <SpawnPointParameters>
       …
      </SpawnPointParameters>
    </SpawnPoint>
  </SpawnPoints>
  <Agents>
    <Agent id="0">
      <AgentTypeRef>0</AgentTypeRef>
      <Type>Car</Type>
      <Width>1.8999999999999999</Width>
      <Length>4.8899999999999997</Length>
      <DistanceCOGtoFrontAxle>1.4199999999999999</DistanceCOGtoFrontAxle>
      <Weight>2250</Weight>
      <HeightCOG>0.78000000000000003</HeightCOG>
      <Wheelbase>2.8399999999999999</Wheelbase>
      <MomentInertiaRoll>1190</MomentInertiaRoll>
      <MomentInertiaPitch>3967</MomentInertiaPitch>
      <MomentInertiaYaw>3967</MomentInertiaYaw>
      <FrictionCoeff>0.80000000000000004</FrictionCoeff>
      <TrackWidth>1.6299999999999999</TrackWidth>
      <DistanceCOGtoLeadingEdge>2.4500000000000002</DistanceCOGtoLeadingEdge>
    </Agent>
    <Agent id="1">
     …
    </Agent>
  </Agents>
  <Observations>
    <Observation id="0" library="Evaluation_Pcm">
      <ObservationParameters>
        <Int id="0" name="Supposed collision time" value="4910"/>
      </ObservationParameters>
    </Observation>
  <Observations>
</RunConfiguration>
```

C.1.3 Example of an agentConfiguration.xml

```
<?xml version='1.0' encoding='UTF-8'?>
<systems>
  <system>
   <id>0</id>
   <title/>
   <priority>0</priority>
   <components>
     <component>
     <id>0</id>
     <library>EgoSensor</library>
     <title>EgoSensor</title>
     <schedule>
       <priority>201</priority>
       <offset>0</offset>
       <cycle>10</cycle>
       <response>0</response>
       </schedule>
```

C.2 Algorithm to Determine the Collision Point between VRU and Vehicle

```
P_isec_vru <- from function
P_isec_veh <- from function

function get_collision_config( VEH_conts, VRU_conts, d_front_center):

(1) idx_vru <- P_isec_vru
  idx_veh <- P_isec_veh
  do while(intersect(VEH_conts[idx_veh], VRU_conts[idx_vru]))
    idx_veh <- idx_veh - 1
  idx_veh <- idx_veh + 1


(2)
  P_target <- front_pt(VEH_conts[idx_veh], d_front_center)
  % current collision point
  P_coll <- get_coll_pt(VEH_cont[idx_veh], VRU_conts[idx_vru])

  % movement direction of the pedestrian along the path
(3) dir <- get_ped_shift_direct(target_pt, VRU_contours[idx_vru])


(4) do while(P_coll_last > P_coll)
    idx_vru <- idx_vru + dir
    % case if the contours are not intersecting any longer
    while not intersect(VEH_conts[idx_veh], VRU_conts[idx_vru])
        idx_veh <- idx_veh + 1
        P_target <- front_pt(VEH_conts[idx_veh], d_front_center)
       P_coll <- get_coll_pt(VEH_cont[idx_veh], VRU_conts[idx_vru])

  P_coll_last <- P_coll


Return idx_veh, idx_vru
```

C.3 Example of an Agent Configuration List

```
agent_configs = [
 {'agent_type': 'Car',
  'start_road': 518
  'end_road':  520,
  'lane_type': driving,
  'sequence': [{'start':{'s':0.0,'v':80.0,'a':0.0}, 'end':{'ds': 100.0}}],
  'color': 'red',
  'system': {"sys_file": "/file/to/agent_2T-C_aeb_ideal.xml",
             "parms_var": {
           "IdealObjectDetector": {
            "AzimuthalResolution": 0.1,
            "FieldofViewHorizontal": 60,
            "SensorLocationX": 1.2,
            "SensorLocationY": 0.0,
```

```
            "MaxRange": 20
          }
        }
  },
  {'agent_type': 'Pedestrian',
   'start_road': 572,
   'end_road':  572,
   'lane_type': sidewalk,
   'sequence': [{'start': {'s':0.0,'v': 8.0, 'a': 0.0}, 'end': {'ds': 20.0}}],
   'color':   'blue',
   'system': {"sys_file": "/file/to/agent_pedestrian.xml"}
  }
]
```

D. Agent Paths of Conflict Situations

D.1 Car - Pedestrian Conflicts

Conflict Situation	**Pictogram** (Lindman *et al.*, 2011)	**ID Start-End Road**	**Derived paths**
Left Turn, pedestrian from Opposite Direction (LTOD)	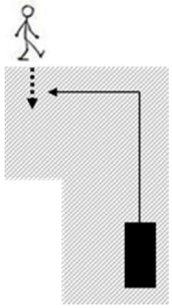	Vehicle: 518 – 521 Pedestrian: 573 - 573	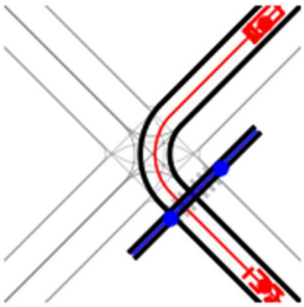
Left Turn, pedestrian from Opposite Direction, initially from Left Direction (LTODLD)	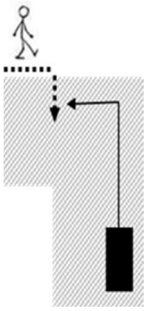	Vehicle: 518 – 521 Pedestrian: 575 – 575	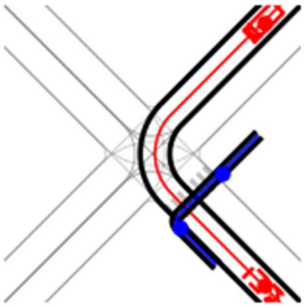
Left Turn, pedestrian from Opposite Direction, initially from Right Direction (LTODRD)	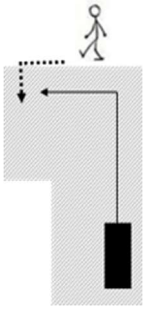	Vehicle: 518 – 521 Pedestrian: 576 – 576	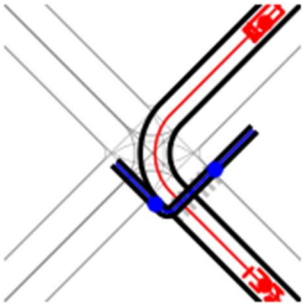

Left Turn, pedestrian from Same Direction (LTSD)	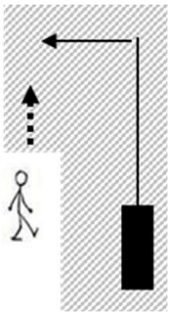	Vehicle: 518 – 521 Pedestrian: 572 – 572	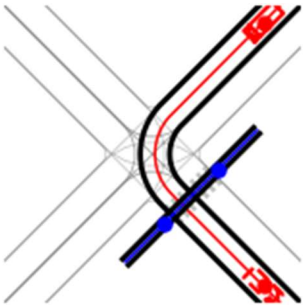
Left Turn, pedestrian from Same Direction, initially from Left Direction (LTSDLD)	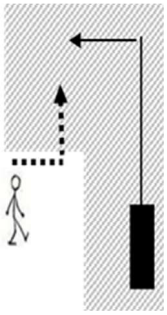	Vehicle: 518 – 521 Pedestrian: 571 – 571	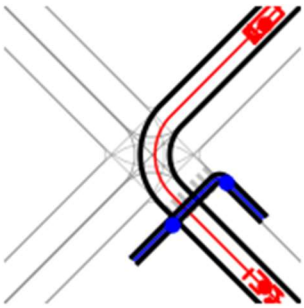
Straight, pedestrian Oncoming (oncoming)	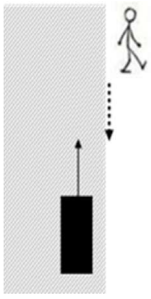	Vehicle: 521 – 519 Pedestrian: 578 - 578	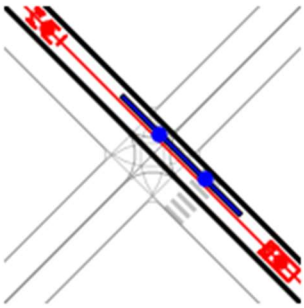
Car Reversing accident (reversing)	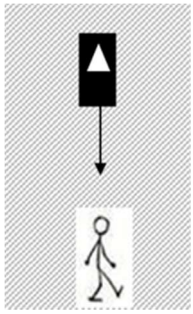	Not considered for current analysis of P-AEB	
Right Turn, pedestrian from Opposite Direction (RTOD)	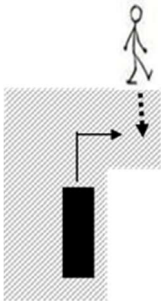	Vehicle: 520 – 521 Pedestrian: 572 – 572	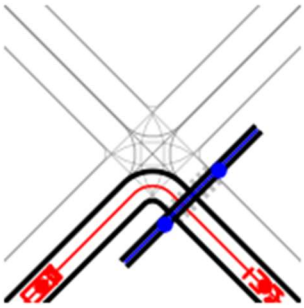

Right Turn, pedestrian from Opposite Direction, initially from Left Direction (RTODLD)	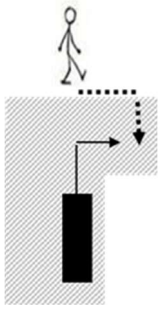	Vehicle: 520 – 521 Pedestrian: 574 – 574	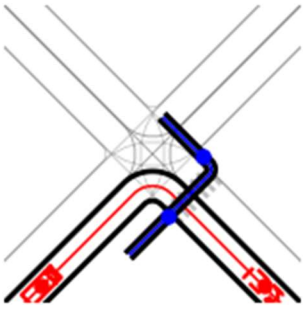
Right Turn, pedestrian from Opposite Direction, initially from Right Direction (RTODRD)	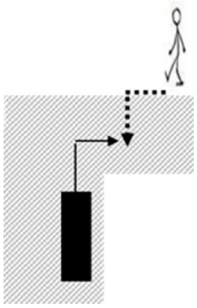	Vehicle: 520 – 521 Pedestrian: 571 – 571	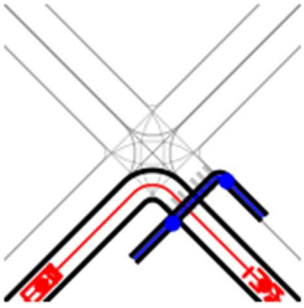
Right Turn, pedestrian from Same Direction (RTSD)	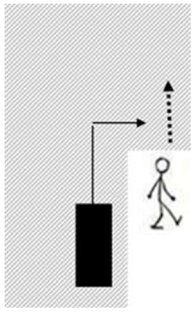	Vehicle: 520 – 521 Pedestrian: 573 - 573	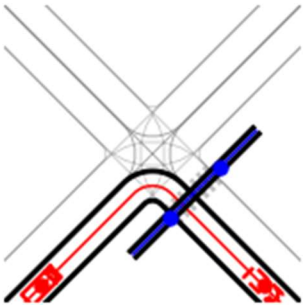
Right Turn, pedestrian from Same Direction, initially from Right Direction (RTSDRD)	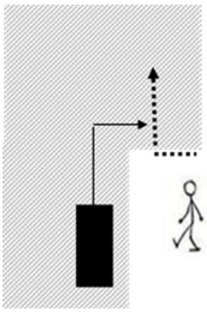	Vehicle: 520 – 521 Pedestrian: 575 – 575	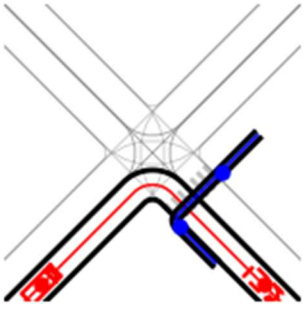
Straight Crossing Path, pedestrian from Left (SCPPL)	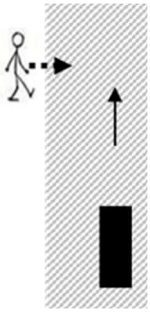	Vehicle: 521 – 519 Pedestrian: 573 – 573	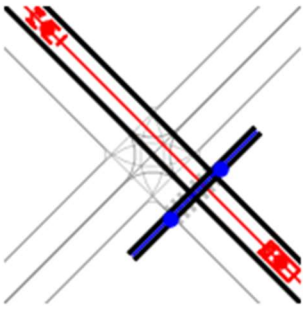

Straight Crossing Path, pedestrian from Left, initially from Opposite Direction (SCPPLOD)	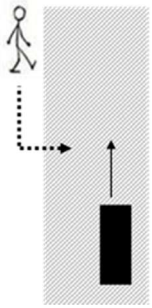	Vehicle: 521 – 519 Pedestrian: 576 - 576	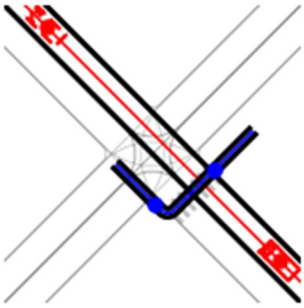
Straight Crossing Path, pedestrian from Left, initially from Same Direction (SCPPLSD)	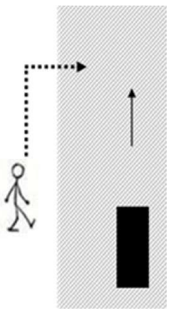	Vehicle: 521 – 519 Pedestrian: 575 - 575	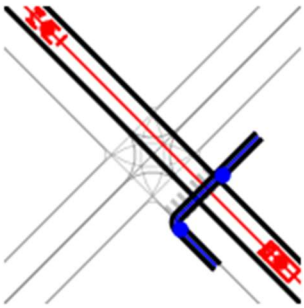
Straight Crossing Path, pedestrian from Right (SCPPR)	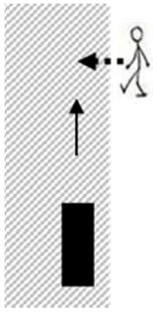	Vehicle: 521 – 519 Pedestrian: 572 - 572	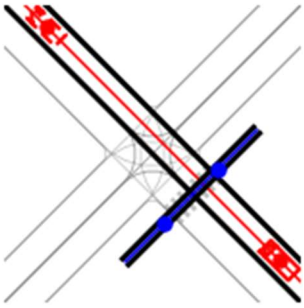
Straight Crossing Path, pedestrian from right, initially from Opposite Direction (SCPPROD)	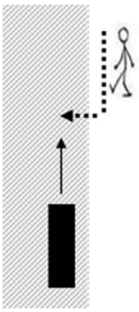	Vehicle: 521 – 519 Pedestrian: 574 - 574	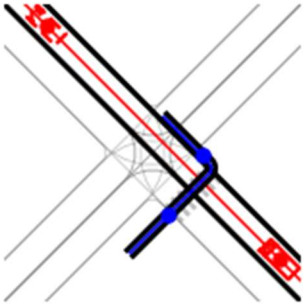
Straight Crossing Path, pedestrian from Right, initially from Same Direction (SCPRSD)	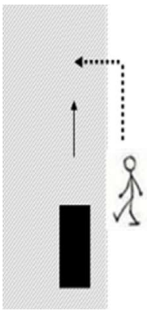	Vehicle: 521 – 519 Pedestrian: 571 - 571	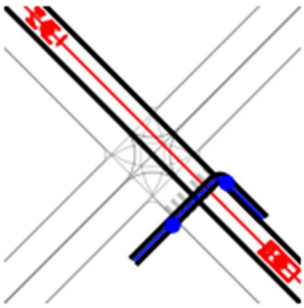

Straight, pedestrian Same Direction (SD)	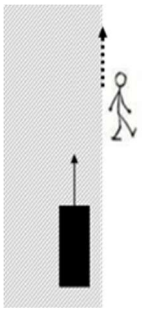	Vehicle: 521 – 519 Pedestrian: 577 - 577	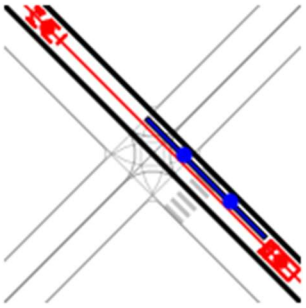

D.2 Car - Cyclist Conflicts

Conflict Situation	Pictogram (Lindman *et al.*, 2011)	ID Start-End Road	Derived paths
Straight Crossing Path, pedestrian from Right, initially from Opposite Direction (SCPCROD)	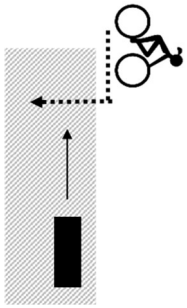	Vehicle: 1 – 0 Cyclist: 3 - 6	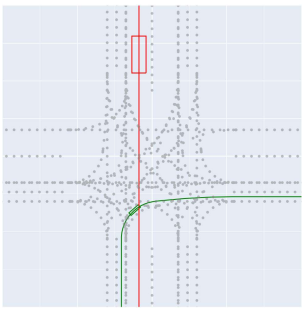
Straight Crossing Path, cyclist from Right, initially from Same Direction (SCPCRSD)	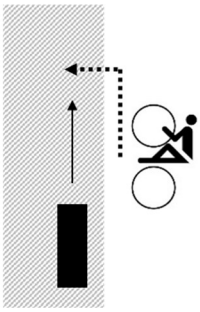	Vehicle: 0 – 1 Cyclist: 4 – 2	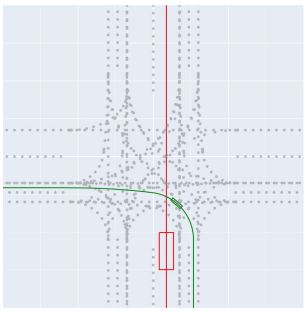
Straight Crossing Path, cyclist from Left, initially from Opposite Direction (SCPCLOD)	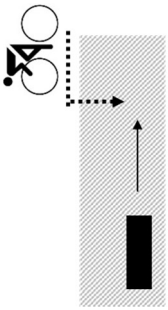	Vehicle: 1 – 0 Cyclist: 4 – 2	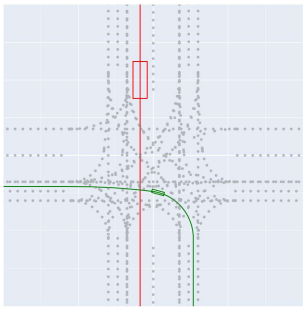

Straight Crossing Path, cyclist from Left, initially from Same Direction (SCPCLSD)	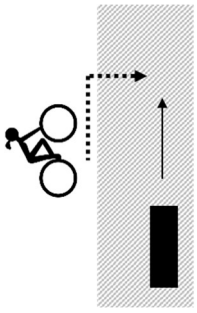	Vehicle: 0 – 1 Cyclist: 3 – 6	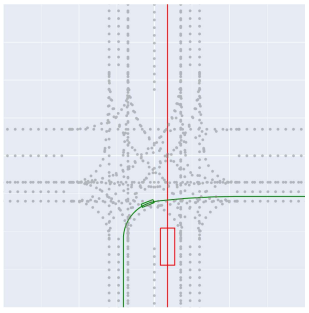
Straight Crossing Path, cyclist from Right (SCPCR)	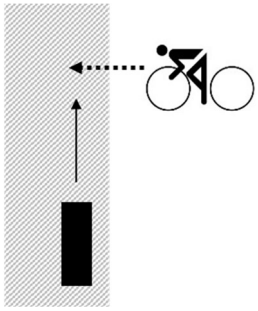	Vehicle: 0 – 1 Cyclist: 6 – 2	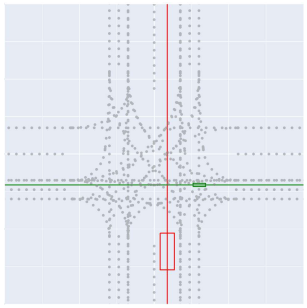
Straight Crossing Path, cyclist from Left (SCPCL)	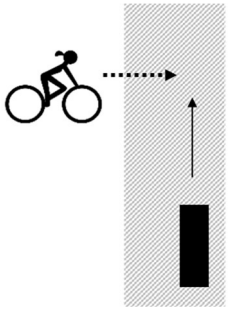	Vehicle: 0 – 1 Cyclist: 2 – 6	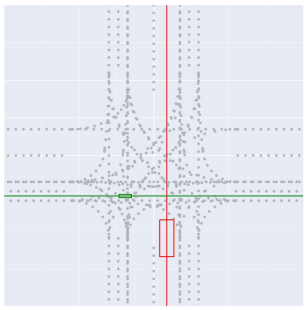
Left Turn, cyclist from Opposite Direction (LTOD)	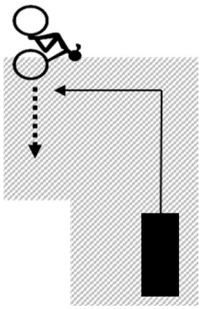	Vehicle: 8 – 0 Cyclist: 2 – 6	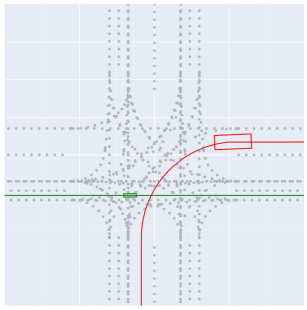
Right Turn, cyclist from Opposite Direction (RTOD)	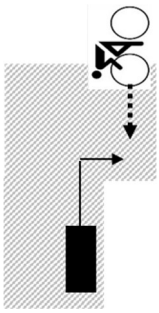	Vehicle: 7 – 0 Cyclist: 6 – 2	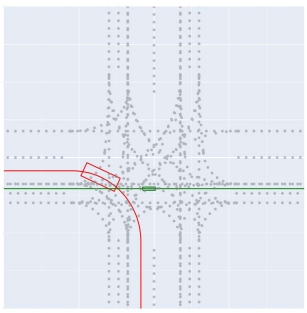

Left Turn, cyclist from Same Direction (LTSD)	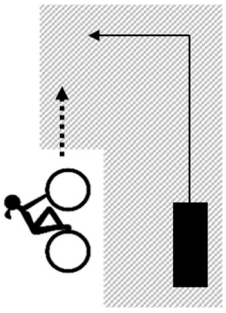	Vehicle: 8 – 0 Cyclist: 6 – 2	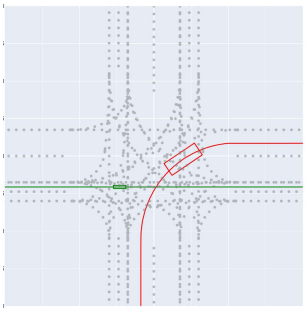
Right Turn, cyclist from Same Direction (RTSD)	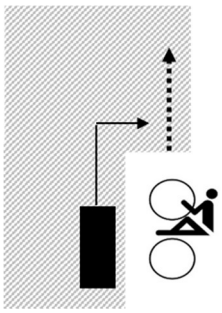	Vehicle: 7 – 0 Cyclist: 2 – 6	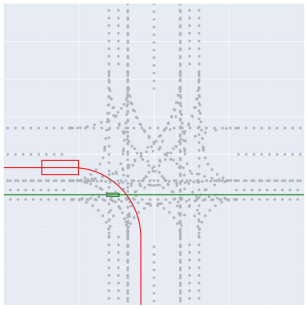
Left Turn, cyclist from Opposite Direction, initially from Left Direction (LTODLD)	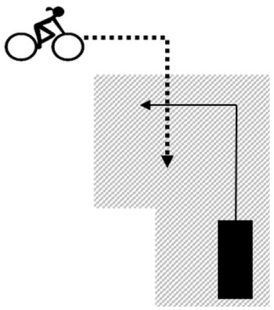	Vehicle: 8 – 0 Cyclist: 3 – 6	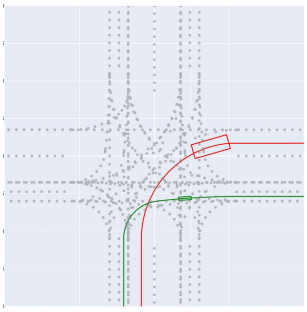
Left Turn, cyclist from Opposite Direction, initially from Right Direction (LTODRD)	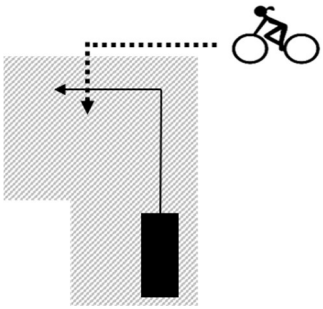	Vehicle: 8 – 0 Cyclist: 5 – 6	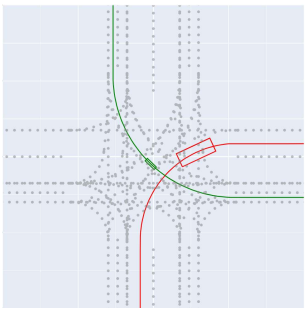
Left Turn, cyclist from Same Direction, initially from Left Direction (LTSDLD)	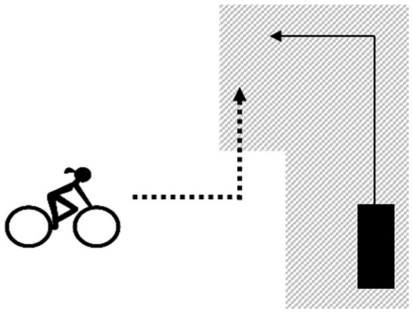	Vehicle: 8 – 0 Cyclist: 4 – 2	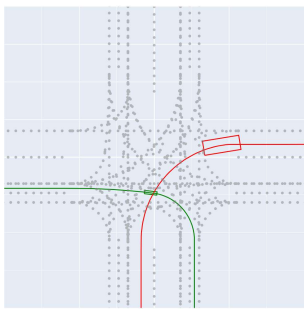

Left Turn, cyclist from Same Direction, initially Right Direction (LTSDRD)	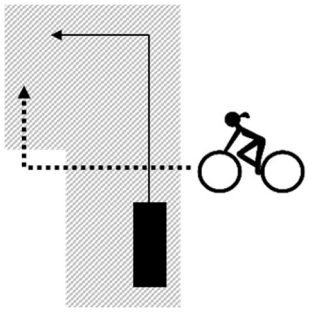	Vehicle: 8 – 0 Cyclist: 9 – 2	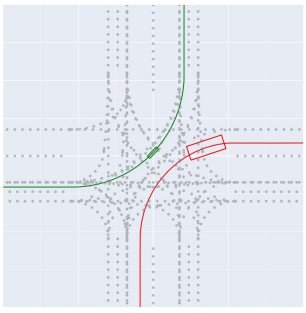
Right Turn, cyclist from Opposite Direction, initially from Left Direction (RTODLD)	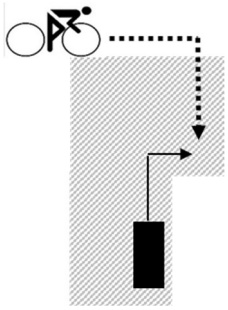	Vehicle: 7 – 0 Cyclist: 9 – 2	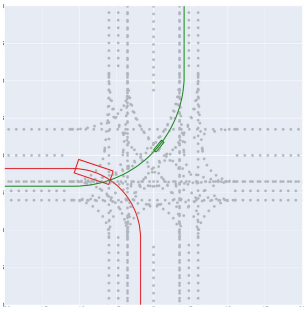
Right Turn, cyclist from Opposite Direction, initially from Right Direction (RTODRD)	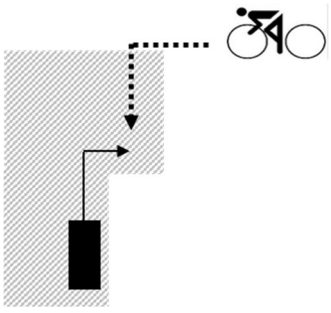	Vehicle: 7 – 0 Cyclist: 4 – 2	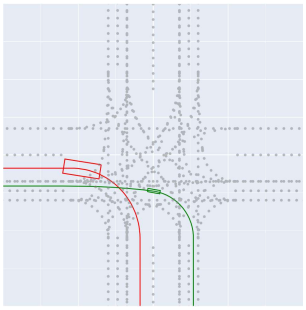
Right Turn, cyclist from Same Direction, initially Left Direction (RTSDLD)	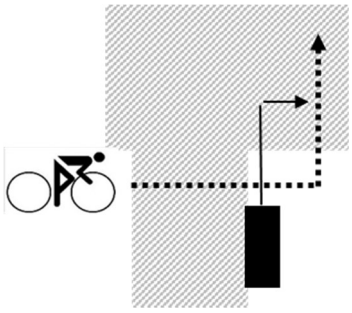	Vehicle: 7 – 0 Cyclist: 5 – 6	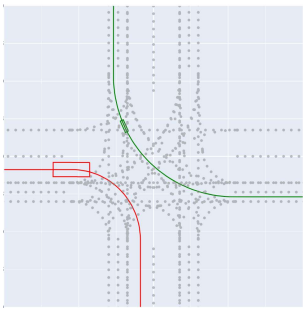
Right Turn, cyclist from Same Direction, initially from Right Direction (RTSDRD)	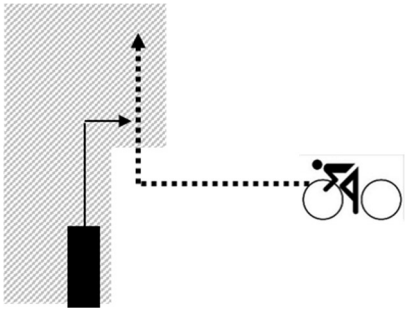	Vehicle: 7 – 0 Cyclist: 3 – 6	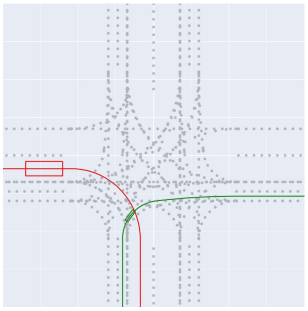

Left Turn, cyclist from Right Direction (LTRD)	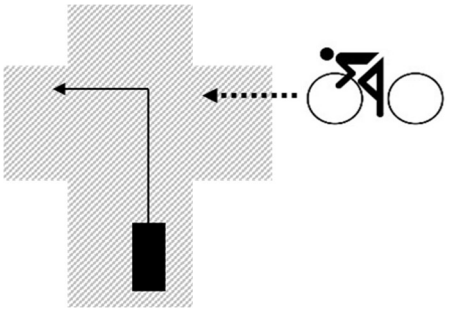	Vehicle: 8 – 0 Cyclist: 1 – 0	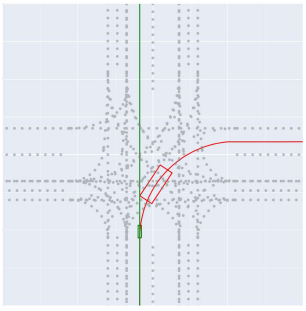
Left Turn, cyclist from Left Direction (LTLD)	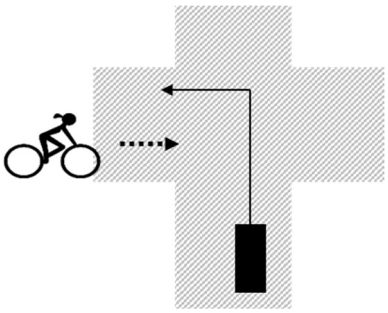	Vehicle: 8 – 0 Cyclist: 4 – 9	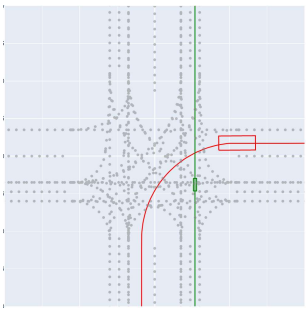
Right Turn, cyclist from Right Direction (RTRD)	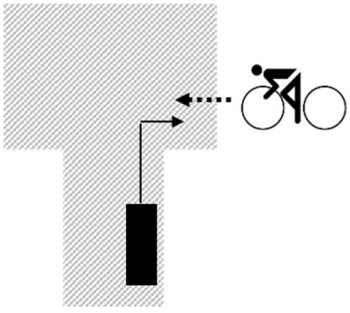	Vehicle: 7 – 0 Cyclist: 3 – 5	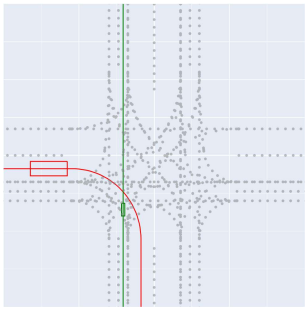
Right Turn, cyclist from Left Direction (RTLD)	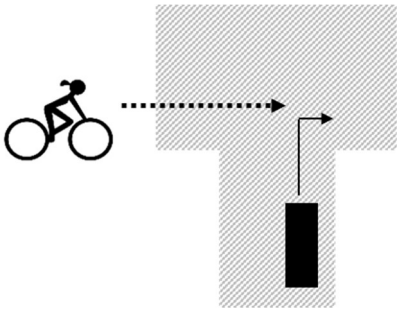	Vehicle: 7 – 0 Cyclist: 1 – 0	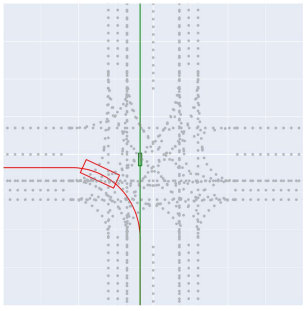
Straight, cyclist from Opposite direction (Oncoming)	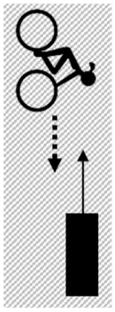	Vehicle: 0 – 1 Cyclist: 9 – 4	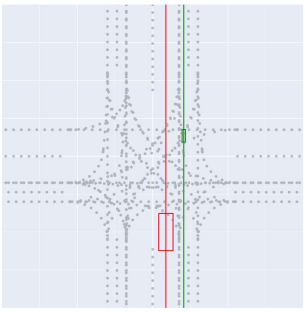

Straight, cyclist from Same Direction (SD)	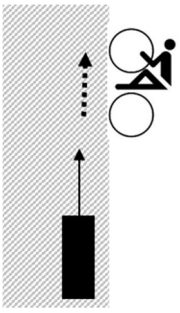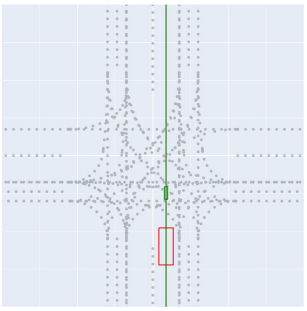	Vehicle: 0 – 1 Cyclist: 0 – 1